Transition metal complexes derived from ketone based N(4)-substituted thiosemicarbazones: Crystal structures and spectral studies

Thesis submitted to
Cochin University of Science and Technology
in partial fulfillment of the requirements
for the award of the degree of

DOCTOR OF PHILOSOPHY

in

CHEMISTRY

By

RENJUSHA S.

DEPARTMENT OF APPLIED CHEMISTRY
COCHIN UNIVERSITY OF SCIENCE AND TECHNOLOGY
KOCHI - 682 022

April 2012

Transition metal complexes derived from ketone based N(4)-substituted thiosemicarbazones: Crystal structures and spectral studies

Ph. D. Thesis under the Faculty of Science

Author:

Renjusha S.
Research Scholar, Department of Applied Chemistry
Cochin University of Science and Technology
Kochi, India 682 022
Email: renjushasathish@gmail.com

Research Advisor:

Dr. M. R. Prathapachandra Kurup
Professor
Department of Applied Chemistry
Cochin University of Science and Technology
Kochi, India 682 022
Email: mrp@cusat.ac.in

Department of Applied Chemistry
Cochin University of Science and Technology
Kochi, India 682 022

April 2012

Front cover: Crystal structure of [Zn(DpyMeTsc)(NO$_3$)]$_2$
Back Cover: The unit cell packing diagram of the compound [Zn(DpyMeTsc)(NO$_3$)]$_2$

to my very dearest Achan, Amma
&
Unnichettan

DEPARTMENT OF APPLIED CHEMISTRY
COCHIN UNIVERSITY OF SCIENCE AND TECHNOLOGY
KOCHI - 682 022, INDIA

Phone Off. :	0484-2575804
Phone Res. :	0484-2576904
Telex :	885-5019 CUIN
Fax :	0484-2577595
Email :	mrp@cusat.ac.in
	mrp_k@yahoo.com

Dr. M.R. Prathapachandra Kurup
Professor

18-04-2012

Certificate

This is to certify that the thesis entitled *"Transition metal complexes derived from ketone based N(4)-substituted thiosemicarbazones: Crystal structures and spectral studies"* submitted by Ms. Renjusha S., in partial fulfillment of the requirements for the degree of Doctor of Philosophy, to the Cochin University of Science and Technology, Kochi-22, is an authentic record of the original research work carried out by her under my guidance and supervision. The results embodied in this thesis, in full or in part, have not been submitted for the award of any other degree.

M.R. Prathapachandra Kurup

(Supervising guide)

Declaration

I hereby declare that the work presented in this thesis entitled **"Transition metal complexes derived from ketone based N(4)-substituted thiosemicarbazones: Crystal structures and spectral studies"** is entirely original and was carried out independently under the supervision of Professor M.R. Prathapachandra Kurup, Department of Applied Chemistry, Cochin University of Science and Technology and has not been included in any other thesis submitted previously for the award of any other degree.

Kochi-22   **Renjusha S.**

18-04-2012

Preface

Over the past few decades inorganic chemistry witnessed a great outflow of coordination compounds, with unique structural characteristics and diverse applications. The motive forces for the evolution have come from the versatile applications of coordination compounds in different areas such as catalysis, bioinorganic, biomimetic and medicinal chemistry. Coordination complexes can assume a wide variety of structures depending on the metal ion, its coordination number and the denticity of the ligands used. The ligands also range from monodentate to polydentate based on the potential donor sites available in their structural skeleton. The presence of more electronegative nitrogen and sulfur on the ligand is established to enhance the coordinating possibilities of ligands. In this aspect, a great deal of attention has been focused on the complexes formed by transition metal ions with thiosemicarbazones.

The work embodied in the thesis was carried out by the author in the Department of Applied Chemistry during the period 2007-2012. The present work deals with the syntheses and characterization of metal complexes of some heterocyclic thiosemicarbazones. Heterocyclic thiosemicarbazones have aroused considerable interest in chemistry due to their remarkable coordination properties and in biology owing to a wide spectrum of potential biological activities.

The work done is presented in seven chapters and Chapter 1 provides an introduction to thiosemicarbazones, their mode of bonding in complexes and applications in different areas. The objectives of the present work and the details of different analytical and spectroscopic techniques used for the characterization are also presented in this chapter. Chapter 2 deals with the syntheses and characterization of two different thiosemicarbazone ligands. Chapters 3-7 describe the syntheses and characterization of different metal complexes with the synthesized thiosemicarbazone ligands. The present study reveals that the

coordination modes of the ligands differ with different metal ions. We could isolate single crystals of some compounds and their structures have been established by single crystal X-ray diffraction studies. A brief summary and conclusion of the work is also included in the last part of the thesis.

Acknowledgement

During my research work I have been accompanied and supported by many people. It is a great pleasure to thank them all who helped me to bring this thesis a reality.

First of all, I bow before the God Almighty for His countless blessings showered on me and submit my thesis at his feet.

I express my profound gratitude to my supervising guide Prof. M.R. Prathapachandra Kurup, for his dynamic guidance, whole hearted support and personal attention at all stages of this research work. His patience, dedication, immense knowledge, positive attitude and encouragement act as motive forces behind this thesis. It has been an honour and pleasure to work with him and I shall always cherish this association.

I wish to express my heartiest thanks to Prof. K. Girish Kumar for his encouragement, timely suggestion and support as my doctoral committee member. I express my sincere gratitude to Prof. K. Sreekumar, Head, Department of Applied Chemistry, CUSAT for the support and co-operation during the period of this work. I am thankful for the support received from all the teaching and non-teaching staff of the Dept. of Applied Chemistry, CUSAT.

I would like to extend my gratitude to the Council of Scientific and Industrial Research (CSIR), New Delhi for the financial support offered. I thank heads of the institutions of SAIF Kochi, IISc Bangalore, IIT Roorkee, IIT Bombay and School of Chemistry, University of Hyderabad for the services and help they had given during my research studies.

I would like to extend my gratitude to my seniors Dr. E.B. Seena, Dr. P.F. Rapheal, Dr. Leji Latheef, Dr. Mini Kuriakose, Dr. Bessy Raj, Dr. Sreesha Sasi, Dr. E. Manoj, Dr. Binu Varghese, Dr. U.L. Kala, Dr. Suja Krishnan, Dr. S.R. Sheeja, Dr. Neema Ani Mangalam, Dr. T.R. Reena, Dr. Nancy Mathew and Dr. K. Laly for their help and cooperation.

I wish to express special thanks to all my labmates Jessy miss, Annie miss, Jayakumar sir, Ashokan sir, Roji, Jinsa, Bibitha, Nisha, Reshma, Ambily, Aiswarya, Sreejith and A.A. Ambily for providing a friendly working atmosphere. A special word of thanks to Easan sir for his timely help and suggestions. I would like to say thanks to all my friends in the Department of Applied Chemistry to make my research days memorable.

I am grateful to all my colleagues in the N.S.S. College, Nemmara for their support and help. I express my sincere thanks to all my teachers especially teachers of St. Gregorios college, Kottarakkara for their inspiring words and blessings. I would like to say special thanks to Dr. Thomas Mathew, Marthoma College, Thiruvalla for awakening my research interest. Starwin sir deserves a special mention; it was his excellent classes that boost up my interest in chemistry.

Words are insufficient to express the depth of my love and gratitude to my parents. The immense love, care, support and encouragement they showered on me throughout my life help a lot to reach me here. I put into words my sincere gratitude to my dearest sister, Rohini for her love and affection extended to me. I am grateful to my grandparents for their blessings. I express my extreme gratitude to my in-laws for the love and support showered at me. I would like to extend my gratitude to my uncles, aunts, and cousins for the love and support.

With great pleasure I would like to give special thanks to Unnichettan, my husband who is the driving force in bringing this thesis in the present form. His love, patience and encouragement have upheld me when I needed it the most. He has given me a hand of support, love and care in all my activities. I also express my deep sense of love to my kids, Niranjana and Neeraja, they missed a lot of my care and attention during these days.

Finally, I would like to thank everybody who was behind the fulfillment of my thesis.

Renjusha

Contents

Curriculum Vitae

RENJUSHA S.

Ravindra Vilas, Chathankery P.O.
Thiruvalla, Pathanamthitta
Kerala, India
Tel: 0469-2732354
E-mail: renjushasathish@gmail.com
          renjusathish@yahoo.co.in

Job Profile

- Working as Assistant Professor in Chemistry at N.S.S. College, Nemmara, Palakkad

Academic Profile

Pursuing Ph.D. (Inorganic Chemistry)

(2007 – present)
Area of research   :   Coordination Chemistry
Supervising guide :   Dr. M.R. Prathapachandra Kurup
                             Department of Applied Chemistry
                             Cochin University of Science & Technology, Kochi

M.Phil. Chemistry (66.6 %)

(2005 – 2006)
Department of Applied Chemistry, Cochin University of Science & Technology, Kochi

B.Ed. Physical science (69.8 %)

(2003 – 2004)
Mount Tabore Training College, Pathanapuram, Kerala University

Master of Science (Pure Chemistry) (76.7 %)

(2001 – 2003)
St. Gregorios College, Kottarakkara, Kerala University

Bachelor of Science (Chemistry) (92.1 %)

(1998 – 2001)
St. Gregorios College, Kottarakkara, Kerala University

Pre-Degree (Science) (70.2 %)

(1996 – 1998)
St. Gregorios College, Kottarakkara, Kerala University

S.S.L.C. (86.3 %)
     (1996)
     Govt. Higher Secondary School, Pattazhy

Additional Qualifications

- Qualified CSIR-JRF (NET) June 2005

Research Experience

- More than four years of research experience in the field of coordination chemistry

Teaching Experience

- Assistant Professor in Chemistry, N.S.S. College, Nemmara (06/10/2008 - present)
- Guest Lecturer in Chemistry, Marthoma College, Thiruvalla (09/08/2004 - 11/02/2005)

Professional Skills

- Familiar with MS Office
- Familiar with chemistry software packages like Chemsketch and Origin
- Familiar with crystallographic softwares
- Experienced in using instruments like UV-Vis spectrometer, FTIR spectrometer, Thermogravimetric analyzer etc.

Personal Profile

Father's name	:	S. Ramakrishna Pillai
Husband's name	:	Sathish Kumar R.
Date of Birth	:	22nd May 1981
Gender	:	Female
Marital Status	:	Married
Nationality	:	Indian

Paper published

- Structural and spectral studies on manganese(II) complexes of di-2-pyridyl ketone N(4)-methyl and N(4)-ethyl thiosemicarbazones, S. Renjusha, M.R.P. Kurup, Polyhedron 27 (2008) 3294.

Paper presented in symposia

- Participated and presented a poster in the National Seminar on "UPTRENDS IN CHEMICAL SCIENCES & TECHNOLOGY" held at N.S.S. Hindu College, Changanassery on 15th and 16th March 2012.

Chapter 1

A BRIEF INTRODUCTION TO THIOSEMICARBAZONES AND THEIR METAL COMPLEXES

1.1. Introduction

Coordination compounds have been known for well over a century and the scientific interest in these compounds increased dramatically. Coordination chemistry was pioneered by Nobel prize winner Alfred Werner [1]. He received the Nobel prize in 1913 for his coordination theory of transition metal-amine complexes. Inorganic chemistry was not a prominent field until Werner studied the metal-amine complexes such as $[Co(NH_3)_6Cl_3]$. Thereafter, inorganic chemistry witnessed a great outflow of coordination compounds, with unique structural characteristics and diverse applications. The recent surge in the popularity of coordination compounds is their perceived applications in many areas such as catalysis, analytical chemistry and medicine [2]. The importance of coordination complexes in our day to day life is increasing due to their complex structures and interesting magnetic, electronic and optical properties.

The stereochemistry of coordination compounds is one of the major interests of the coordination chemists. Coordination complexes show diversity in structures depending on the metal ion, its coordination number and the denticity of the ligands used. The presence of more electronegative nitrogen, oxygen or sulfur atoms on the ligand structure is established to enhance the coordinating possibilities of ligands. Hence there has been a continuous quest over the many years for nitrogen or sulfur donor ligands. In this aspect, a great deal of attention has been focused on the complexes formed by transition metal ions with thiosemicarbazones.

1.2. Thiosemicarbazones

Thiosemicarbazones are compounds obtained by the reaction of thiosemicarbazides or substituted thiosemicarbazides with aldehydes or ketones (Scheme **1**).
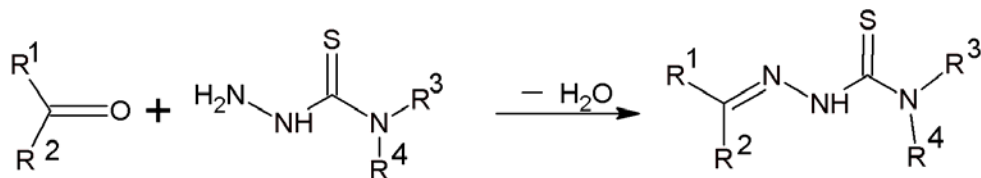
Scheme 1

The –C=S group provides the possibility for the electron delocalization within the thiosemicarbazone moiety and also, increases the denticity of these compounds. The thioamide sulfur and azomethine nitrogen are the available donor sites present in the thiosemicarbazone compounds. Further, the number of coordination sites can be increased by the suitable substitution on the thiosemicarbazone framework. If heterocyclic rings are attached to the thiosemicarbazone moiety, the hetero atoms can act as the donor sites.

An interesting attribute of the thiosemicarbazones is that in the solid state, they predominantly exist in the thioamido form, whereas in solution they exist both in thioamido and in thiol forms (Fig. 1.1). The thiol form predominates in the solution state and can effectively coordinate to a metal atom.
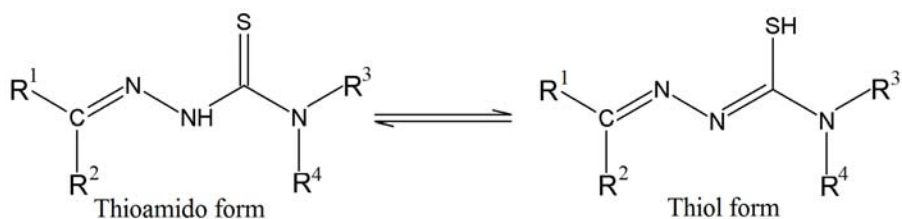
Fig. 1.1. Tautomerism in thiosemicarbazones

1.3. Importance of thiosemicarbazones

Thiosemicarbazones are a class of compounds with a wide range of analytical and pharmacological applications. Their metal complexes have also shown to possess interesting pharmacological properties as drug candidates or as the biological active form of the drug when coordination is part of the mechanism of action [3]. Thiosemicarbazones are compounds that have been studied for considerable period of time for their biological properties. Traces of interest date back to the beginning of the 20th century but the first reports on their medical applications began to appear in the fifties as drugs against tuberculosis and leprosy [4,5]. The antiviral activity of thiosemicarbazones was first reported in 1950 by Hamre *et al.*, who found that derivatives of benzaldehyde thiosemicarbazone were active against neurovaccinal infection in mice when given orally [6]. The first breakthrough in the comprehension of the antitumor effect of thiosemicarbazones was obtained in the sixties and deserves a brief resume. The anti-leukemic effect of 2-formylpyridine thiosemicarbazone was first reported by Brockman *et al.* [7] in 1956. Almost ten year later, in

1965, French *et al*. [8] formulated hypotheses about the mode of action of the α(N)-heterocyclic thiosemicarbazones: the active molecules shared a tridentate nature, that allows them to be effective chelators, and a better activity was obtained by modifying the aromatic system.

Metal complexes of thiosemicarbazones are of particular importance due to their potentially beneficial biological activities [9]. They have been extensively studied as they show a wide variety of biological applications: antitumoral, antiviral, antibacterial, antimalarial and antifungal [10,11]. Thiosemicarbazones and their metal complexes present a wide spectrum of antimicrobial activity. As early as in 1946, Domagk reported that some thiosemicarbazones of cyclic aldehydes and ketones possesses antitubercular activity *in vitro* [12]. Later, 2-formylpyridine thiosemicarbazones and their VO(IV) complexes exhibited powerful *in vitro* antibacterial activity towards *E. Coli* [13]. The antitumor activity of such thio compounds was revealed in their ability to inhibit ribonucleotide reductase (RR), a necessary enzyme for DNA synthesis [14]. Currently, 3-aminopyridine-2-carboxylaldehyde thiosemicarbazone, Triapine, is being evaluated in human phase II trials as a cancer chemotherapeutic agent [15]. The thiosemicarbazone side chain located at a position α to the heterocyclic nitrogen, through a conjugated N-N-S tridentate ligand system, is essential for anticancer activity [16]. Activities of a number of α-(N)-heterocyclic carboxaldehyde thiosemicarbazones were reported [17].

Thiosemicarbazone derivatives and their metal complexes are also reported to have diverse analytical applications [18]. Pavon *et al*. reported the 4-phenyl-3-thiosemicarbazone of biacetylmonoxime as an analytical reagent [19]. Some nickel complexes of thiosemicarbazones are reported to function as effective homogeneous catalysts for the alcoholysis of silanes [20] and for the reduction of imines to primary and secondary amines [21]. Thiosemicarbazones are also

reported to have corrosion inhibition properties [22]. Metal complexes of thiosemicarbazone ligands have shown variable bonding properties and structural diversity along with promising biological implications, and ion sensing abilities.

1.4. Bonding and coordination strategy of thiosemicarbazones

Thiosemicarbazones show a variety of coordination modes with transition metals. The coordination mode is influenced by the number and type of the substituents. This is because, the active donor sites of the ligand varies depending upon the substituents. The presence of di-2-pyridyl ketone at the ketonic part attributes many interesting coordination possibilities for the ligands under study. It can coordinate to the central metal by adopting an *NNS* coordination mode, either through neutral thioamido form (Structure **I**) or through the deprotonated thiolate form (Structure **II**) [23].
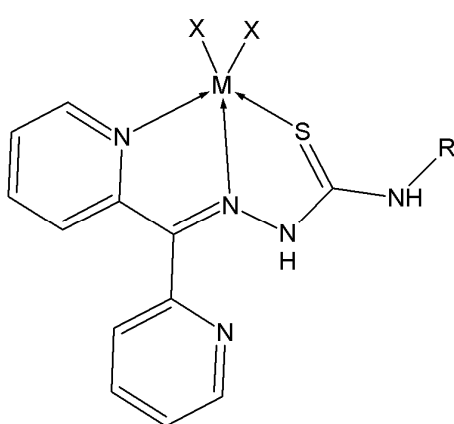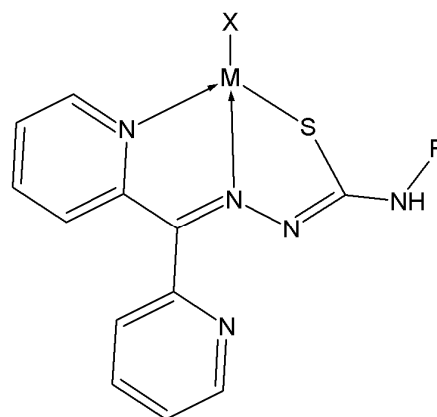
Structure I   **Structure II**

Sometimes, two ligands may coordinate to the same metal and six coordinate tetragonal geometry is expected (Structure **III**) [24].
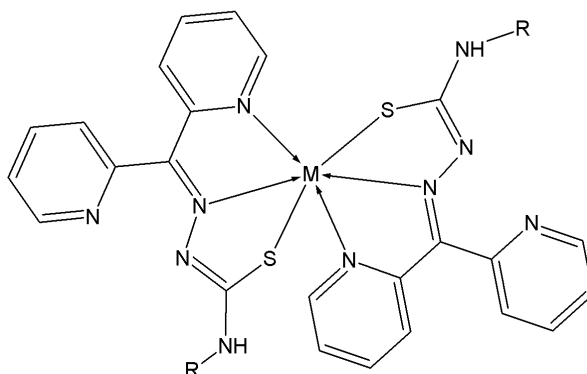
Structure III

However, in some cases thiosemicarbazone exhibits potential quadridentate attributes, when the second pyridyl nitrogen of a four-coordinated metal complex shows some tendency to form a coordinate bond with the metal centre of an adjacent metal complex in the lattice. This give rise to dimeric five-coordinated structures (Structure **IV**). Dimeric structures also result when two metal centers are bridged through anions such as chloride, bromide, azide etc (Structure **V**) [25]. There are also reports on the thiolate sulfur bridging in dimeric structures of thiosemicarbazones [26].
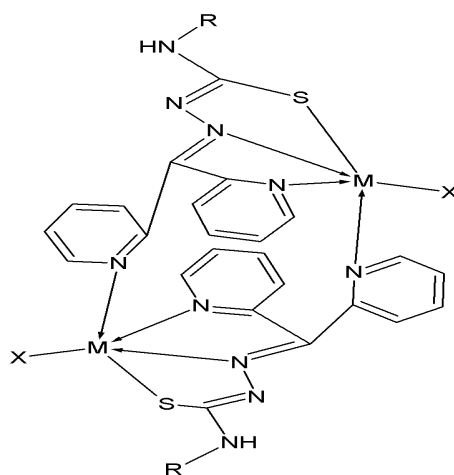
Structure IV
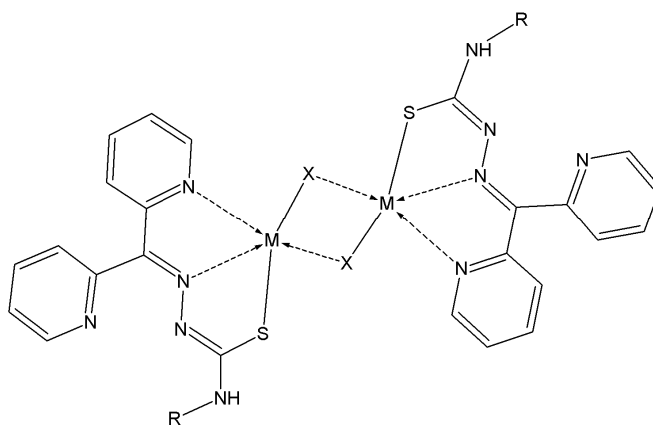
Structure V

1.5. Objectives of the present work

Thiosemicarbazones have recently attracted considerable attention due to their ability to form tridentate chelates with transition metal ions through either two nitrogen and sulfur atoms, N–N–S or oxygen, nitrogen and sulfur atoms, O–N–S. Considerable interest in thiosemicarbazones and their transition metal complexes has also grown in the areas of biology and chemistry due to biological activities such as antitumoral, fungicidal, bactericidal, antiviral and nonlinear optical properties. They have been used for metal analyses, for device applications related to telecommunications, optical computing, storage and information processing.

The versatile applications of metal complexes of thiosemicarbazones in various fields prompted us to synthesize the tridentate NNS-donor thiosemicarbazones and their metal complexes. As a part of our studies on transition metal complexes with these ligands, we undertook the current work with the following objectives.

1. To synthesize and physico-chemically characterize the following thiosemicarbazone ligands:

   a. Di-2-pyridyl ketone-*N*(4)-methyl thiosemicarbazone (HDpyMeTsc)

   b. Di-2-pyridyl ketone-*N*(4)-ethyl thiosemicarbazone (HDpyETsc)

2. To synthesize oxovanadium(IV), manganese(II), nickel(II), copper(II), zinc(II) and cadmium(II) complexes using the synthesized thiosemicarbazones as principal ligands and some anionic coligands.

3. To study the coordination modes of the ligands in metal complexes by using different physicochemical methods like partial elemental analysis, thermogravimetry and by different spectroscopic techniques.

4. To establish the structure of compounds by single crystal XRD studies.

This thesis is divided into seven chapters.

Chapter I, entitled 'a brief introduction to thiosemicarbazones and their metal complexes' describes importance of thiosemicarbazones, their mode of coordination and the relevance of present investigation. Brief introduction to the different analytical techniques for the characterization is also presented in this chapter.

Chapter II deals with the preparation of ligands and their physicochemical investigations.

Chapters III, IV, V, VI and VII discuss the procedure followed for the preparation of the complexes of oxovanadium(IV), manganese(II), nickel(II), copper(II), zinc(II) and cadmium(II) and their physicochemical investigations.

1.6. Physical measurements

The physicochemical methods adopted during the present study is discussed below.

1.6.1. Elemental analyses

Analyses for carbon, hydrogen and nitrogen in the synthesized thiosemicarbazones and in their metal complexes were carried out using Vario EL III CHNS analyzer at the Sophisticated Analytical Instrument Facility, Kochi.

1.6.2. Conductivity measurements

The molar conductivities of the complexes in dimethylformamide (DMF) solutions (10^{-3} M) at room temperature were measured using a Systronic model 303 direct-reading conductivity bridge at the Department of Applied Chemistry, CUSAT, Kochi, India.

1.6.3. Magnetic susceptibility measurements

The magnetic susceptibility measurements were done in the polycrystalline state at room temperature on a PAR model 155 Vibrating Sample Magnetometer at 5 kOe field strength at the Indian Institute of Technology, Roorkee, India.

1.6.4. Thermogravimetric analyses

TG-DTG analyses of the complexes were carried out in an atmosphere of nitrogen at a heating rate of 10 ºC per minute using a Perkin Elmer Pyris Diamond TG/DTA analyzer, at the Department of Applied Chemistry, CUSAT, Kochi, India.

1.6.5. Infrared spectroscopy

Infrared spectra of the compounds were recorded on a Thermo Nicolet AVATAR 370 DTGS model FT-IR Spectrometer in the range of 4000-400 cm^{-1} using KBr pellets and ATR technique at the Sophisticated Analytical Instrument Facility, Kochi, India.

1.6.6. Electronic spectroscopy

Electronic spectra of the compounds were taken on a Spectro UV-vis Double Beam UVD-3500 spectrometer in the 200-900 nm range at the Department of Applied Chemistry, CUSAT, Kochi, India.

1.6.7. NMR spectroscopy

^{1}H NMR spectra of thiosemicarbazone ligands were recorded using Bruker AMX 400 FT-NMR Spectrometer with CDCl$_3$ as the solvent and TMS as internal standard at the Sophisticated Analytical Instrument Facility, Indian Institute of Science, Bangalore, India.

1.6.8. EPR spectroscopy

The EPR spectra of the complexes in polycrystalline state at 298 K and in DMF at 77 K were recorded on a Varian E-112 spectrometer using TCNE as the standard, with 100 kHz modulation frequency at the SAIF, IIT Bombay, India.

1.6.9. Single crystal XRD

Single crystal X-ray diffraction data of two complexes were collected on a CrysAlis CCD, Oxford Diffraction Ltd. diffractometer, equipped with a graphite crystal, incident-beam monochromator, and a fine focus sealed tube, Mo Kα (λ = 0.71073 Å) X-ray source at the National Single Crystal X-ray diffraction Facility, IIT, Bombay, India. The trial structure was solved using

SHELXS-97 and refinement was carried out by full-matrix least squares on F^2 using SHELXL-97 [27], and all the hydrogen atoms were fixed in calculated positions.

X-ray crystal structure determination of another complex was performed with a Bruker SMART APEX CCD X-ray diffractometer at the University of Hyderabad, using graphite monochromated Mo Kα radiation (λ = 0.71073 Å). The Bruker SAINT software was used for data reduction and Bruker SMART for cell refinement. The structure was solved using SHELXS-97 and full-matrix least squares refinement against F^2 was carried out using SHELXL-97 in anisotropic approximation for non-hydrogen atoms. All hydrogen atoms were assigned on the basis of geometrical considerations and were allowed to ride upon the respective carbon atoms. Molecular graphics employed were MERCURY [28], PLATON [29] and DIAMOND [30].

References

[1]   J.E. Huheey, E.A. Keiter, R.L. Keiter, Inorganic Chemistry, Principles of Structure and Reactivity, 4th ed., Harper Collins College Publishers, New York, 1993.

[2]   J.C. Craliz, J.C. Rub, D. Willis, J. Edger, Nature 34 (1955) 176.

[3]   A.E. Graminha, A.A. Batista, I.C. Mendes, L.R. Teixeira, H. Beraldo, Spectrochim. Acta Part A 69 (2008) 1277.

[4]   E.M. Bavin, R.J.W. Rees, J.M. Robson, M. Seiler, D.E. Seymour, D. Suddaby, J. Pharm. Pharmacol (1950) 764.

[5]   O. Koch, G. Stuttgen, J. Pathol. Pharmacol (1950) 409.

[6]   D. Hamre, J. Bernstein, R. Donovick, Proc. Soc. Exp. Biol. Med. 73 (1950) 275.

[7]   R.W. Brockman, J.R. Thomson, M.J. Bell, H.E. Skipper, Cancer Res 16 (1956) 167.

[8]   F.A. French, E.J.J. Blanz, Cancer Res 25 (1965) 1454.

[9]   S. Halder, R.J. Butcher, S. Bhattacharya, Polyhedron 26 (2007) 2741.

[10]   R.A. Finch, M.C. Liu, A.H. Cory, J.G. Cory, A.C. Sartorelli, Adv. Enzyme Regul. 39 (1999) 393.

[11]   W. Antholine, J. Knight, H. Whelan, D.H. Petering, Pharmacol 13 (1977) 89.

[12]   G. Domagk, R. Behnish, F. Mietzch, H. Schimidt, Naturwissenschaften 33 (1946) 315.

[13]   A. Maiti, A.K. Guha, S. Ghosh, J. Inorg. Biochem. 33 (1988) 57.

[14] E.C. Moore, M.S. Zedeck, K.C. Agarwal, A.C. Sartorelli, Biochem. 9 (1970) 4492.

[15] Z.–G. Jiang, M.S. Lebowitz, H.A. Ghanbari, CNS Drug Rev. 12 (2006) 77.

[16] F.A. French, E.J. Blanz, J. Med. Chem. 9 (1966) 585.

[17] R. Pingaew, S. Prachayasittikul, S. Ruchirawat, Molecules 15 (2010) 988.

[18] R.B. Singh, B.S. Garg, R.P. Singh, Talanta 25 (1978) 619.

[19] J.N.C. Pavon, J.C.J. Sanchez, F. Pino, Anal. Chim. Acta 75 (1975) 335.

[20] D.E. Barber, Z. Lu, T. Richardson, R.H. Crabtree, Inorg. Chem. 31 (1992) 4709.

[21] A.H. Vetter, A. Berkessel, Synthesis (1995) 419.

[22] E.E. Ebenso, U.J Ekpe, B.I. Ita, O.E. Offiong, U.J. Ibok, Mat. Chem. Phy. 60 (1999) 79.

[23] V. Philip, V. Suni, M.R.P. Kurup, M. Nethaji, Polyhedron 23 (2004) 1225 .

[24] V. Philip, V. Suni, M.R.P. Kurup, M. Nethaji, Spectrochim. Acta Part A 64 (2006) 171.

[25] V. Philip, V. Suni, M.R.P. Kurup, M. Nethaji, Polyhedron 24 (2005) 1133.

[26] M. Joseph, V. Suni, M.R.P. Kurup, M. Nethaji, A. Kishore, S.G. Bhat, Polyhedron 23 (2004) 3069.

[27] G.M. Sheldrick, Acta Cryst. A 64 (2008) 112.

[28] C.F. Macrae, P.R. Edgington, P. McCabe, E. Pidcock, G.P. Shields, R. Taylor, M. Towler, J. Van de Streek, J. Appl. Cryst. 39 (2006) 453.

[29] A.L. Spek, J. Appl. Cryst. 36 (2003) 7.

[30] K. Brandenburg, Diamond Version 3.1f, Crystal Impact GbR, Bonn, Germany, 2008.

........................✑✑✑........................

SYNTHESES AND CHARACTERIZATION OF KETONE BASED N(4)-SUBSTITUTED THIOSEMICARBAZONES

2.1. Introduction

Thiosemicarbazone is an important class of compound containing both hard (N) and soft (S) donor atoms. Thiosemicarbazones are formed by the condenzation of thiosemicarbazides with aldehydes or ketones. Heterocyclic thiosemicarbazones have aroused considerable interest in chemistry due to their remarkable coordination properties and in biology owing to a wide spectrum of potential biological activities [1]. The biological activities of thiosemicarbazones are considered to be due to their ability to form chelates with heavy metals [2-5]. Thiosemicarbazones and their metal complexes find applications in areas as diverse as nuclear medicine, pharmacology and analytical chemistry. Heterocyclic thiosemicarbazones, a class of compounds posessing a wide spectrum of medicinal properties have been studied for activity against bacterial and viral infections, tuberculosis, leprosy, coccidiosis and malaria [6-10]. The present level of interest in metal complexes of thiosemicarbazones stems from the fact that the biological activity of the organic compound is enhanced by coordination to a transition metal [11].

In the laboratory, the interest in thiosemicarbazone complexes relates to their applications in chemical analysis. In inorganic analysis, thiosemicarbazones have been used as reagents for the quantitative determination of a variety of metal ions, and in organic analysis for identification of aldehydes and ketones [12,13].

The coordinating ability of thiosemicarbazones to both transition and main group metallic cations is attributed to the extended delocalization of electron density over the –NH–C(S)–NH–N= system, which is enhanced by substitution at the N(4) position. Condenzation of thiosemicarbazides with aromatic aldehydes or ketones extend the electron delocalization along the azomethine bond. Presence of additional donor sites in the ketonic part as in the case of di-2-pyridyl ketone, offer much more coordination possibilities for the thiosemicarbazone ligand [14].

This chapter describes the syntheses and characterization of thiosemicarbazone ligands. We synthesized two *N*(4)-substituted thiosemicarbazones using di-2-pyridyl ketone.
They are,

    a. Di-2-pyridyl ketone-*N*(4)-methyl thiosemicarbazone (HDpyMeTsc)

    b. Di-2-pyridyl ketone-*N*(4)-ethyl thiosemicarbazone (HDpyETsc)

The ligands were characterized by IR, electronic and NMR spectroscopy.

2.2. Experimental

2.2.1. Materials

All the chemicals and solvents used for the syntheses were of analytical grade. Di-2-pyridyl ketone (Aldrich), *N*(4)-methyl thiosemicarbazide (Aldrich), *N*(4)-ethyl thiosemicarbazide (Aldrich) and methanol were used as received.

2.2.2. Syntheses of ligands

2.2.2a. Di-2-pyridyl ketone-N(4)-methyl thiosemicarbazone (HDpyMeTsc)

N(4)-methyl thiosemicarbazide (0.105 g, 1 mmol) dissolved in methanol was added to a hot solution of di-2-pyridyl ketone (0.184 g, 1 mmol) in the same solvent. Two drops of glacial acetic acid was added to the reaction mixture. Then the above mixture was refluxed for 4 hours and cooled to room temperature. The pale yellow product formed was filtered off, washed with methanol and dried over P_4O_{10} *in vacuo*.

Elemental Anal. Found (Calcd.) (%): C: 57.76 (57.54); H: 5.03 (4.83); N: 25.26 (25.81).

The reaction scheme is depicted in the Scheme 2.1.
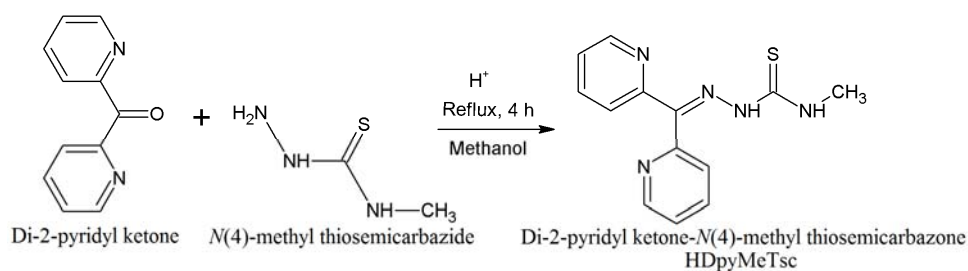
Scheme 2.1

2.2.2b. Di-2-pyridyl ketone-N(4)-ethyl thiosemicarbazone (HDpyETsc)

A solution of *N*(4)-ethyl thiosemicarbazide (0.119 g, 1 mmol) in methanol was mixed with a methanolic solution of di-2-pyridyl ketone (0.184 g, 1 mmol) and three drops of glacial acetic acid was added to this. The reaction mixture was refluxed for 4 hours and cooled to room temperature. The colorless crystalline product formed was filtered, washed with methanol and dried over P_4O_{10} *in vacuo*.

Elemental Anal. Found (Calcd.) (%): C: 58.80 (58.92); H: 5.17 (5.30); N: 24.72 (24.54).

The reaction scheme is depicted in the Scheme 2.2.
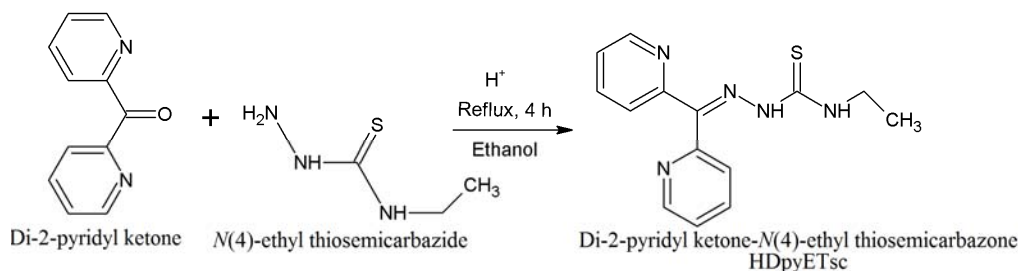
Scheme 2.2

2.3. Results and discussion

The ligands were synthesized in a very facile fashion by refluxing equimolar solutions of the corresponding thiosemicarbazides with the ketone.

2.3.1. Infrared spectral studies

IR spectral data provides significant information regarding the presence of characteristic groups in the compound. Infrared spectra were recorded on Thermo Nicolet AVATAR 370 DTGS FT-IR spectrophotometer using KBr pellets in the region 4000-400 cm^{-1}. The characteristic IR bands observed for the ligands along with their relative assignments are presented in the Table 2.1.

The ν(N–H) bands appear at *ca.* 3263 and 3199 cm^{-1} respectively for the ligands. The azomethine stretching vibrations, characteristic of a Schiff base, are observed at *ca.* 1585 cm^{-1} [15]. Absence of any bands in the 2800-2550 cm^{-1} region points towards the lack of –SH stretching vibrations in the molecule. It reveals the presence of only the thioamido form in the solid state [16]. IR spectra of compounds in which C=S group is attached to nitrogen atom contain several bands in the region 1560-700 cm^{-1} due to vibrations involving interactions between C=S and C–N stretching. The bands observed at 1431 and 800 cm^{-1} for HDpyMeTsc and at 1431 and 799 cm^{-1} for HDpyETsc are assigned to ν/δ(C–S) [17]. The hydrazinic N–N bands are observed at 1110 and 1109 cm^{-1} respectively for the ligands [18]. The 1600-1400 cm^{-1} region of the spectra is complicated by the presence of thioamide bands and ring breathing vibrations of the pyridyl rings. However, in-plane deformation vibrations characteristic of pyridyl rings are observed at 618 cm^{-1} for HDpyMeTsc and at 615 cm^{-1} for HDpyETsc [19]. IR spectra of the ligands, HDpyMeTsc and HDpyETsc are presented in Figs. 2.1 and 2.2 respectively.

Table 2.1. IR spectral data (cm^{-1}) of thiosemicarbazones

Compound	ν(C=N)	ν/δ(C–S)	ν(N–N)	py(ip)
HDpyMeTsc	1588	1431, 800	1110	618
HDpyETsc	1585	1431, 799	1109	615
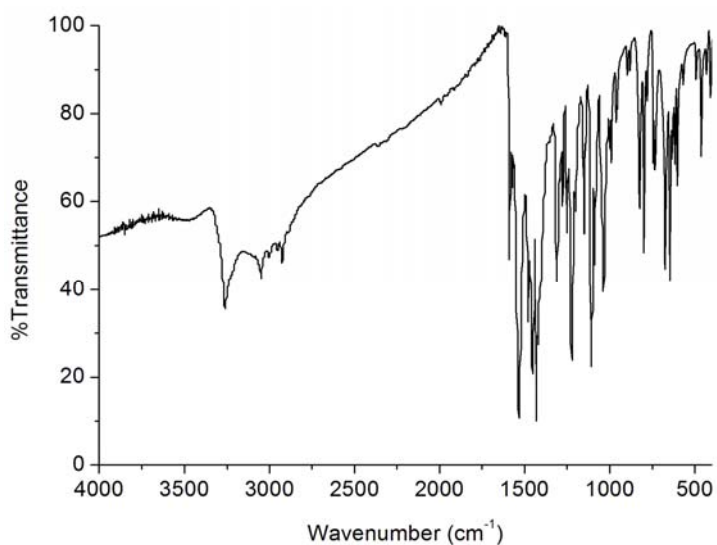
Fig. 2.1. IR spectrum of HDpyMeTsc
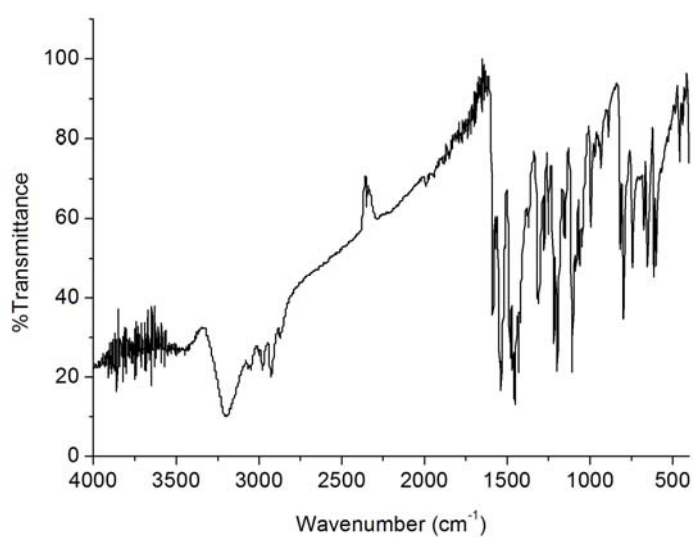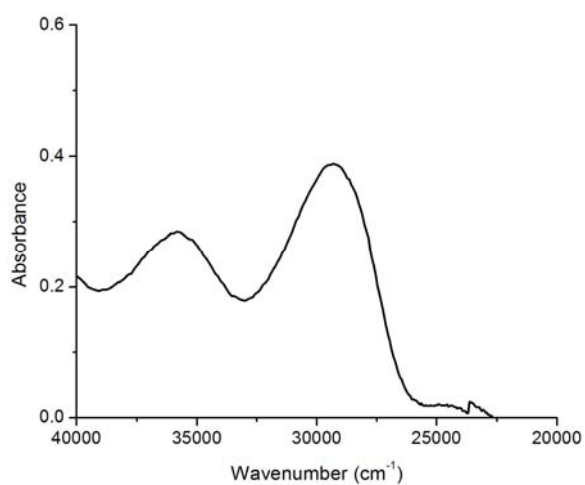

Fig. 2.2. IR spectrum of HDpyETsc

2.3.2. Electronic spectral studies

The UV-visible spectra of organic compounds are associated with the electronic transitions between energy levels, and at wavelengths above 200 nm, excitation of electrons from the π-orbitals usually occurs giving rise to
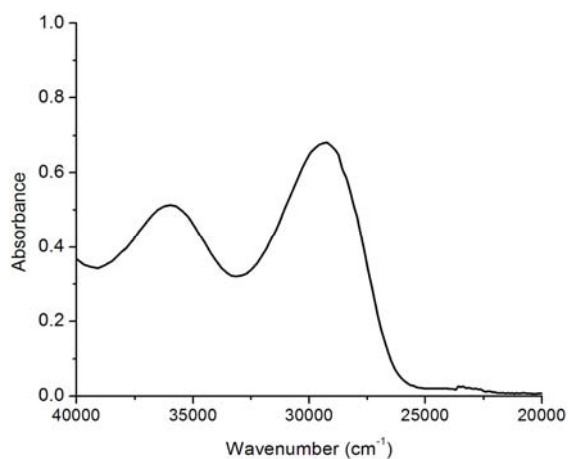
informative spectra [20]. The electronic spectra of HDpyMeTsc and HDpyETsc in acetonitrile show bands in the region 29280 - 35890 cm^{-1} due to π-π* transitions as summarized in Table 2.2. With increasing solvent polarity these bands showed a red shift in wavelengths [22] as shown in Table 2.3. The energy necessary for the π-π* transition is less in the more polar solvent due to stabilization of the excited state more than that of the ground state by interaction with the solvent. No bands which could be assigned to an n-π* type were observed in the spectra, since they are merged with the more intense π-π* bands [21]. The n-π* band often disappears in acidic media owing to protonation or upon formation of an adduct that ties up the lone pair. But here, there is no disappearance of any peak in acidic medium confirming the above. Figs. 2.3 and 2.4 represent the electronic spectra of ligands in acetonitrile and Figs. 2.5 and 2.6 represent the spectra of HDpyMeTsc and HDpyETsc in various solvents.

Table 2.2. Electronic spectral data (cm^{-1}) of thiosemicarbazones in acetonitrile

Compound	UV absorption bands λ_{max} cm^{-1} (ε M^{-1} cm^{-1})	
HDpyMeTsc	35890 (2.8x 10^4)	29280 (3.9 x 10^4)
HDpyETsc	35860 (5.1 x 10^4)	29360 (6.8 x 10^4)

Fig. 2.3. Electronic spectrum of HDpyMeTsc

Fig. 2.4. Electronic spectrum of HDpyETsc

Table 2.3. Electronic spectral data (cm^{-1}) of ligands in various solvents

Solvents	HDpyMeTsc	HDpyETsc
Ethanol	36030, 29550	36060, 29650
Methanol	36020, 29350	35960, 29560
Acetonitrile	35890, 29280	35860, 29360
DMF	35190, 27840	35580, 28890
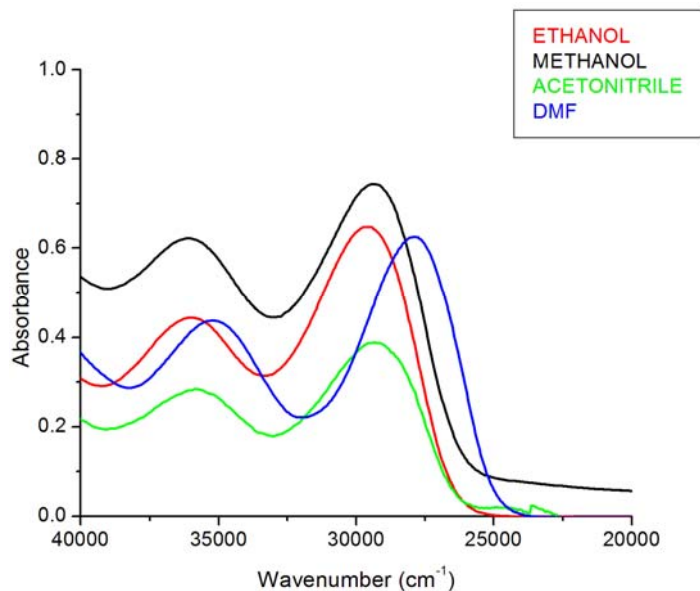
Fig. 2.5. Electronic spectra of HDpyMeTsc in different solvents
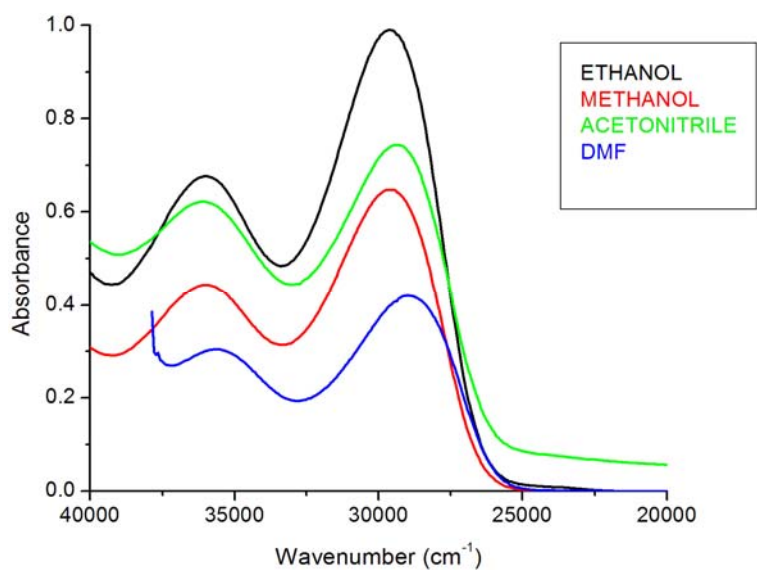
Fig. 2.6. Electronic spectra of HDpyETsc in different solvents

2.3.3. NMR spectral studies

Proton Nuclear Magnetic Resonance spectroscopy is a helpful tool for the identification of organic compounds in conjugation with other spectrometric information. The ^{1}H NMR spectra of HDpyMeTsc and HDpyETsc were recorded with CDCl$_3$ as solvent and TMS as the internal standard and are shown in Figs. 2.7 and 2.8 respectively.

A sharp singlet, which integrates as one hydrogen, at $\delta = 14.17$ ppm for HDpyMeTsc and at $\delta = 14.13$ ppm for HDpyETsc may be due to the existence of the compounds in thiol form. On D$_2$O exchange, the intensity of these peaks are found to be considerably decreased. Peaks at $\delta = 7.83$ ppm for HDpyMeTsc and $\delta = 7.74$ ppm for HDpyETsc, are assigned to the N(5) proton. This downfield shift is explained with the hydrogen bonding interaction with nitrogen atom N(3). Hydrogen bonding decreases the electron density around the protons and thus moves the proton absorption to a lower field [23].

Aromatic protons give peaks in the region of 7.3–8.8 ppm. For HDpyMeTsc, a peak at $\delta = 3.26$ ppm corresponds to C(13) proton. A multiplet at $\delta = 3.76$ ppm for C(13) and a triplet at $\delta = 1.30$ ppm for C(14) protons are obtained for HDpyETsc. All the assignments made above are observed to be in general agreement with previous reports on di-2-pyridyl ketone thiosemicarbazones [24,25].
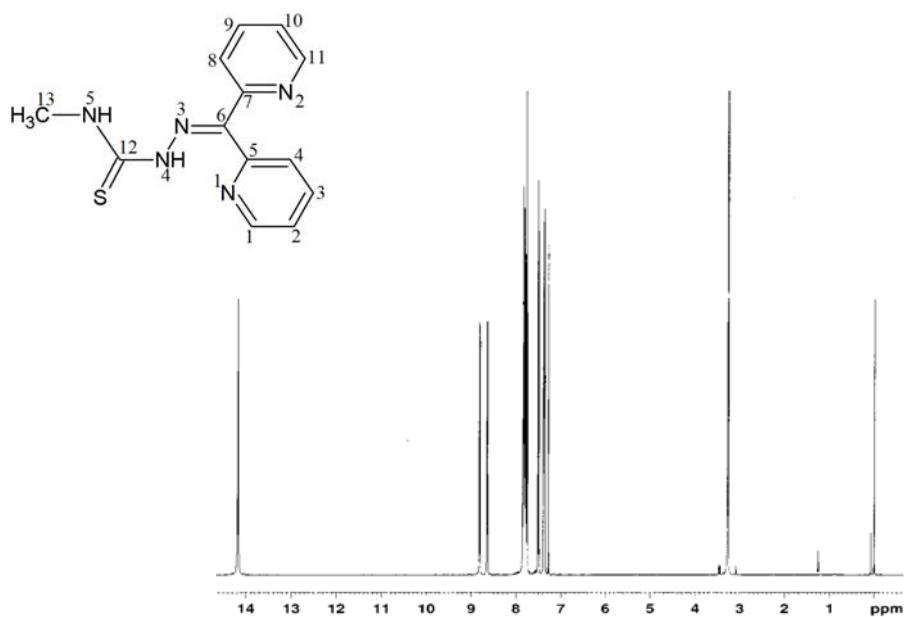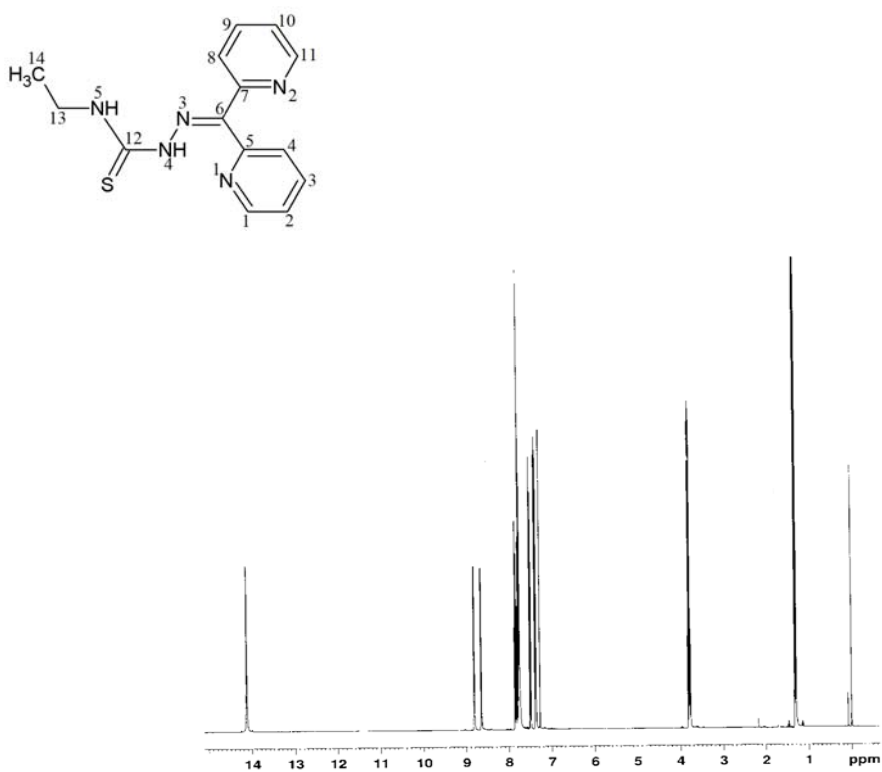
Fig. 2.7. ^{1}H NMR spectrum of HDpyMeTsc

Fig. 2.8. ^{1}H NMR spectrum of HDpyETsc

References

[1] E. Manoj, M.R.P. Kurup, Polyhedron 27 (2008) 275.

[2] U. Abram, K. Ortner, K. Sommer, J. Chem. Soc., Dalton Trans. (1999) 735.

[3] R. Dimmer, U. Dittes, B. Nuber, V. Sefried, W. Opferkuch, B.K. Keppler, Metal Based Drugs 2 (1995) 271.

[4] D.X. West, G.A. Bain, R.J. Butcher, J.P. Jasinski, Y. Li, R.Y. Pozdniakiv, J. Valdes-Martinez, R.A. Toscano, S. Hernandes-Ortega, Polyhedron 15 (1996) 665.

[5] D. Kovala-Demertzi, A. Domopoulou, M. Demertzis, C.P. Paptopoulou, A. Terzis, Polyhedron 13 (1994) 1917.

[6] J.P. Scovill, D.L. Klayman, C.F. Franchino, J. Med. Chem. 25 (1982) 1261.

[7] D.L. Klayman, J.P. Scovill, J.F. Bartosevich, C.J. Mason, J. Med. Chem. 22 (1979) 1367

[8] D.L. Klayman, J.F. Bartosevich, T.S. Griffin, C.J. Mason, J.P. Scovill, J. Med. Chem. 22 (1979) 855.

[9] I.H. Hall, K.G. Rajendran, D.X. West, A.E. Liberta, Anticancer Drugs 4 (1993) 251.

[10] P. Genova, T. Varadinova, A.I. Matesanz, D. Marinova, P. Souza, Toxicol. Appl. Pharmacol, 197 (2004) 107.

[11] A.J.M. Al-Karawi, W. Clegg, R.S. Harrington, R.A. Henderson, Dalton Trans. (2009) 564.

[12] S.E. Ghazy, M.A. Kabil, A.A. El-Asmy, Y.E. Sherif, Afinidad 52 (1995) 128.

[13] M.A. Kabil, S.A. Ghazy, A.A. El-Asmy, Y.E. Sherif, Anal. Sci. 12 (1996) 431.

[14] V. Suni, M.R.P. Kurup, M. Nethaji, Spectrochim. Acta A 63 (2006) 174.

[15] W. Kemp, Organic Spectroscopy, 3rd ed., Mcmillan, Hampshire, 1996.

[16] V. Suni, M.R.P. Kurup, J. Mol. Struct. 749 (2005) 177.

[17] D.X. West, A.M. Stark, G.A. Bain, A.E. Liberta, Trans. Met. Chem. 21 (1996) 289.

[18] M. Joseph, M. Kuriakose, M.R.P. Kurup, E. Suresh, A. Kishore, S.G. Bhat, Polyhedron 25 (2006) 61.

[19] E. Bermejo, A. Casteneiras, R. Dominguez, R. Carballo, C.M-Mossmer, J. Strahle, D.X. West, Z. Anorg, Allg. Chem. 625 (1999) 961.

[20] D.H. Williams, I. Fleming, Spectroscopic methods in Organic Chemistry, 4th ed., McGraw- Hill, London, 1989.

[21] S.S. Konstantinovic, B.C. Radovanovic, Z.B. Todorovic, S.B. Ilic, J. Serb. Chem. Soc. 72 (2007) 975.

[22] H. Kiliç, Spectrochim. Acta A 75 (2010) 728.

[23] R.M. Silverstein, G.C. Bassler, T.C. Morrill, Spectrometric Identification of Organic Compounds, 4th ed., John Wiley & Sons, New York, 1981.

[24] J.K. Swearingen, W. Kaminsky, D.X. West, Trans. Met. Chem. 27 (2002) 724.

[25] J.K. Swearingen, D.X. West, Trans. Met. Chem. 26 (2001) 252.

........................ঙঙঙ........................

SYNTHESES AND SPECTRAL CHARACTERIZATION OF VANADIUM(IV) COMPLEXES OF KETONE BASED N(4)-SUBSTITUTED THIOSEMICARBAZONES

3.1. Introduction

Vanadium is a widespread trace element distributed in nature. Vanadium is an essential trace element of plants and animals and has significant effect on normal growth [1]. In higher animals, once absorbed through the gastrointestinal tract, it is mainly accumulated in bone tissue. In the last decades, vanadium compounds have been widely studied because of their potential therapeutic applications. The pharmacological effects of vanadium include insulin mimetic actions, antineoplastic effects and osteogenic effects [2].

The coordination chemistry of vanadium, in view of the fact that its catalytic activity is of particular importance in the biosphere, has generated a considerable escalation of interest in related investigations in recent years. The broad range of ligands used to synthesize oxovanadium complexes include a wide range of Schiff base-type ligands, which can afford monomeric or dimeric compounds [3]. Oxovanadium(IV) and (V) complexes, especially with bi- and tridentate chelating ligands bound to the metal mainly *via* oxygen and nitrogen atoms, have being extensively investigated in recent years with respect to their remarkable efficiency as insulin mimetic compounds. Their use as orally active

medicaments would represent an important advance in the treatment of human diabetes mellitus. Other studies involving potential applications of oxovanadium complexes have been also performed, with emphasis, for example, in their antitumor and antibacterial activity [4].

The interaction of simple vanadium species (viz., VO^{2+} and VO^{3+}) with ligand groups having pharmacological activity is of growing interest. More detailed physico-chemical characterization of vanadium compounds with pharmacologically important ligands will help in further understanding of pharmacology of vanadium [5]. The discovery of the insulin-like *in vitro* and *in vivo* activity of oxovanadates(V) and oxovanadium(IV) complexes has stimulated research on vanadium compounds that may have important application in the treatment of type-1 and type-2 diabetes mellitus [6]. Organic ligands, complexed to vanadium in coordination compounds, provide way in tuning the effects of vanadium, thereby minimizing any adverse effects without sacrificing important benefits [7-9].

Vanadium forms a large number of compounds in which the most important oxidation states are +3, +4 and +5. Vanadium easily switches between the oxidation states +4 and +5. Complexes of vanadium usually adopt five-coordinate square pyramidal and six-coordinate distorted octahedral geometries.

3.2. Experimental

3.2.1. Materials

All the chemicals and solvents used for the syntheses were of analytical grade. Di-2-pyridyl ketone (Aldrich), *N*(4)-methyl thiosemicarbazide (Aldrich), vanadyl sulphate monohydrate (Aldrich), potassium thiocyanate (E-Merck), ethanol and methanol were used as supplied.

3.2.2. Synthesis of the ligand

The synthesis of the thiosemicarbazone ligand, HDpyMeTsc has been described already in Chapter 2.

3.2.3. Syntheses of oxovanadium(IV) complexes

3.2.3a. Synthesis of [VO(DpyMeTsc)(NCS)] (1)

HDpyMeTsc (0.271 g, 1 mmol) was dissolved in ethanol by heating. To this, an aqueous solution of KSCN (0.097 g, 1 mmol) and methanolic solution of vanadyl sulfate (0.163 g, 1 mmol) were added and refluxed for 4 hours. The resulting solution was allowed to stand at room temperature and after slow evaporation, the orange precipitate separated out was filtered, washed with ethanol followed by ether and dried over P_4O_{10} *in vacuo*.

λ_m (DMF): 31 ohm^{-1} cm^2 mol^{-1}, Elemental Anal. Found (Calcd.) (%): C: 42.60 (42.53); H: 3.25 (3.06); N: 20.90 (21.26).

3.2.3b. Synthesis of [VO(HDpyMeTsc)(SO$_4$)] (2)

To a solution of the ligand, HDpyMeTsc (0.271 g, 1 mmol) in hot ethanol, was added a methanolic solution of vanadyl sulfate (0.163 g, 1 mmol). The mixture was heated under reflux for 3 hours and cooled. The light green precipitate obtained was filtered, washed with ethanol and then with ether and dried over P_4O_{10} *in vacuo*.

λ_m (DMF): 16 ohm^{-1} cm^2 mol^{-1}, Elemental Anal. Found (Calcd.) (%): C: 34.76 (34.52); H: 2.93 (3.34); N: 15.39 (15.48).

3.3. Results and discussion

Based on the elemental analyses, conductivity measurements and spectral investigations, the complexes were formulated. Both the complexes

contain the VO^{2+} unit, in which vanadium is in +4 oxidation state (d^1). The molar conductivity measurements in 10^{-3} M DMF solution indicate that both complexes are non-electrolytic in nature [10]. In complex **1**, the thiosemicarbazone deprotonates and chelates in thiolate form as evidenced by the IR spectra, while in complex **2** the ligand coordinates in the thioamido form.

The magnetic moments of the complexes were calculated from the magnetic susceptibility measurements and the value for complex **1** at room temperature is 1.60 B.M. and that for **2** is 1.67 B.M. The values are found to be very close to the spin only value 1.73 B.M., which indicate the presence of one unpaired electron [11]. Both the complexes are EPR active due to this unpaired electron.

3.3.1. Infrared spectra

The characteristic IR bands of the complexes show significant changes when compared with that of the parent ligand and shift of some of characteristic vibrational frequency of the ligand upon complexation provides evidence for the mode of binding of the ligand to the metal ion. The significant bands observed in the IR spectrum of the ligand and its complexes along with their tentative assignments are summarized in Table 3.1.

Table 3.1 IR spectral data (cm^{-1}) of vanadium(IV) complexes

Compound	v(C=N)	v(C=N)^a	v/δ(C–S)	v(N–N)	py(ip)
HDpyMeTsc	1588	...	1431, 800	1110	618
[VO(DpyMeTsc)(NCS)] **(1)**	1513	1545	1390, 788	1168	649
[VO(HDpyMeTsc)(SO$_4$)] **(2)**	1580	...	1326, 793	1183	646

^{a} Newly formed C=N

The v(C=N) band of thiosemicarbazone is found to be shifted to lower frequencies in both complexes representing the coordination *via* the azomethine

nitrogen [12]. The increase for the ν(N–N) frequency in the spectra of the complexes is probably due to enhanced double bond character through chelation, thus offsetting the loss of electron density *via* donation to the metal atom, and is supportive of azomethine nitrogen coordination. For complex **1**, a new band at 1545 cm^{-1} due to the newly formed –C=N– moiety is observed. This indicates that the ligand enolizes and coordinates in the thiolate form [13]. Coordination *via* thiolate sulfur is also indicated by the downward shift of frequencies of ν/δ(C–S) bands found at 1431 and 800 cm^{-1} [14]. The in-plane bending vibrations of the pyridine ring in uncomplexed ligand at 618 cm^{-1} shift to higher frequencies on complexation, conforming the coordination of the ligand to the metal *via* the pyridine nitrogen.

Further, the intense bands observed at 974 cm^{-1} for complex **1** and 981 cm^{-1} for complex **2** correspond to the terminal V=O stretching band [15]. Thiocyanato complex **1** has a very strong and sharp band at 2084 cm^{-1} and a medium band at 740 cm^{-1} corresponding to ν(CN) and ν(CS) modes of the NCS group. The intensities and positions of these bands indicate the unidentate coordination of the thiocyanate group through the nitrogen atom [16].

It was found that the sulfato complex **2** exhibits four fundamental vibrations. Bands at ~980 cm^{-1} due to ν_1 and medium bands around 460 cm^{-1} due to ν_2, strong bands at 1278, 1191 and 1017 cm^{-1} corresponding to ν_3 and band at 727 cm^{-1} due to ν_4. These bands are attributed to a chelating bidentate sulfato group [17]. IR spectra of complexes are presented in Figs. 3.1 and 3.2.
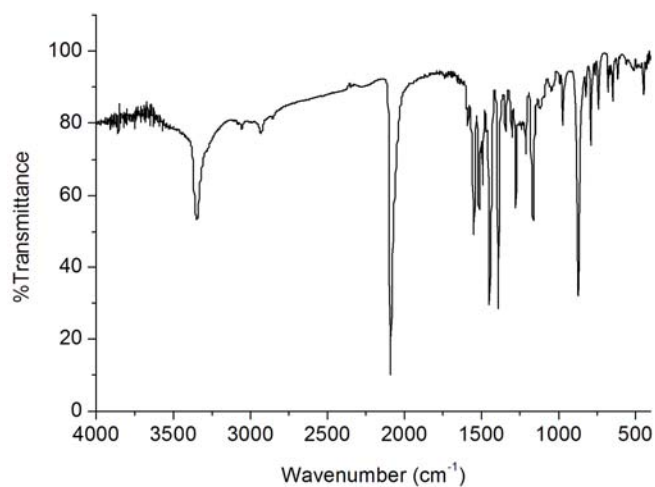
Fig. 3.1. IR spectrum of [VO(DpyMeTsc)(NCS)] (**1**)
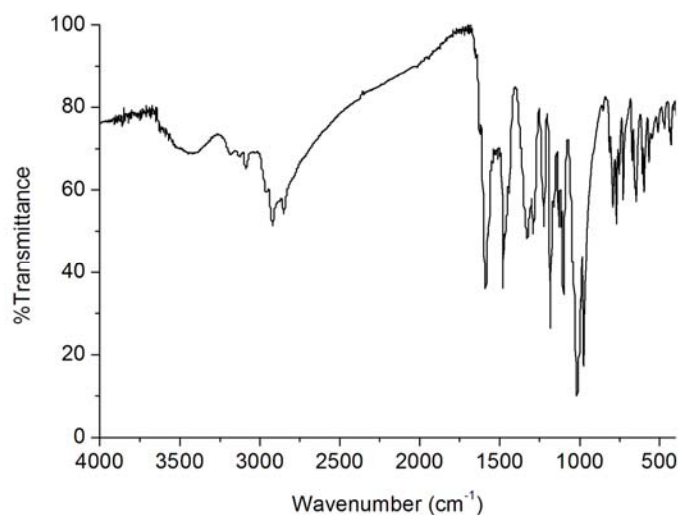
Fig. 3.2. IR spectrum of [VO(HDpyMeTsc)(SO$_4$)] (**2**)
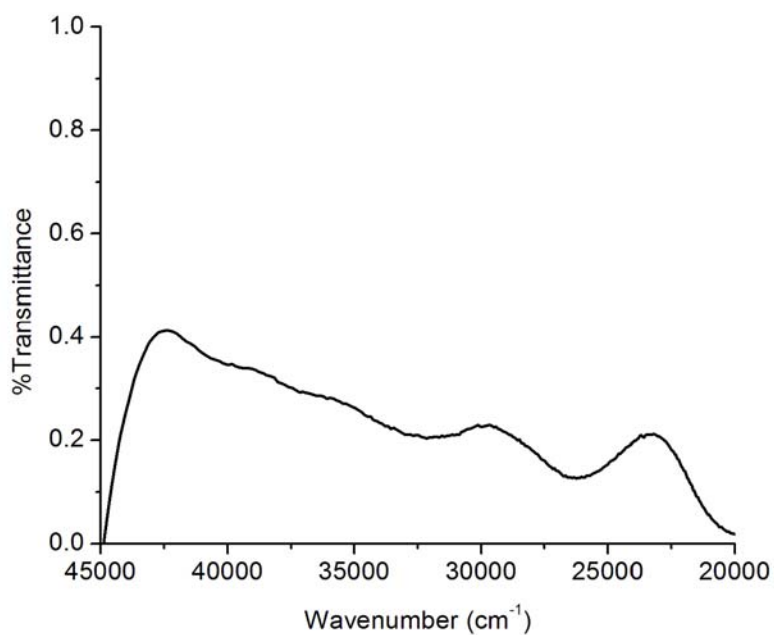
3.3.2. Electronic spectra

The electronic spectral assignments for the free ligand (HDpyMeTsc) and their V(IV) complexes are summarized in Table 3.2. The ligand exhibits intraligand transitions at 35890 and 29280 cm^{-1} assignable to $\pi \rightarrow \pi^*$ transitions of the pyridyl ring and thiosemicarbazone moiety [18]. These bands suffer considerable shifts on coordination. In addition to these intra-ligand bands,

new bands at 23340 cm^{-1} are observed in the spectra of complexes. This bands can safely be assigned to ligand→metal charge-transfer bands.

Table 3.2. Electronic spectral data (cm^{-1}) of vanadium(IV) complexes

| Compound	UV absorption bands (cm^{-1})				
HDpyMeTsc	35890	29280			
[VO(DpyMeTsc)(NCS)] **(1)**	35680	29750	23340	17270	14600
[VO(HDpyMeTsc)(SO$_4$)] **(2)**	37250	29560	23340	18450	

Interpretation of the electronic spectra of oxovanadium(IV) complexes is the subject of continuing investigation and discussion. Following the energy level scheme derived by Ballhausen and Gray for oxovanadium(IV) complexes, the energy of the molecular orbitals are ordered as B_2 (d_{xy}) < E (d_{xz}, d_{yz}) < B_1 ($d_{x^2-y^2}$) < A_1 (d_{z^2}). Thus the spectral bands at 13,000-14,000, 15,400-16,300 and 22,000-24,600 cm^{-1} can be assigned to $^2E \leftarrow {}^2B_2$ ($d_{xy} \rightarrow d_{xz}, d_{yz}$), $^2B_1 \leftarrow {}^2B_2$ ($d_{xy} \rightarrow d_{x^2-y^2}$) and $^2A_1 \leftarrow {}^2B_2$ ($d_{xy} \rightarrow d_{z^2}$) transitions [19]. Most of the oxovanadium complexes show three prominent bands in the electronic spectral region. However, we can locate only two weak bands for complex **1** and one band for complex **2**, probably due to the masking by high intensity charge transfer bands. The electronic spectra of complexes are given in Figs. 3.3–3.5.

Fig. 3.3. Electronic spectrum of [VO(DpyMeTsc)(NCS)] **(1)**
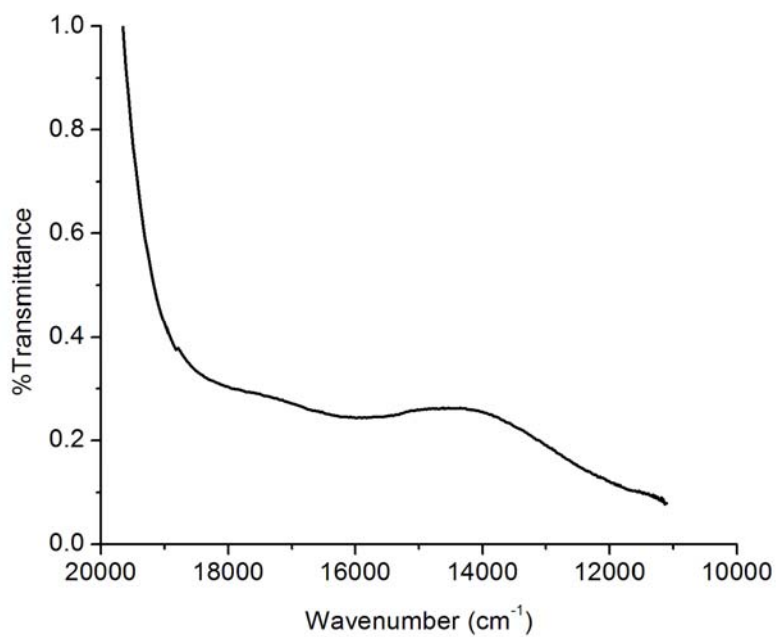
Fig. 3.4. Electronic spectrum of [VO(DpyMeTsc)(NCS)] **(1)** in the visible region
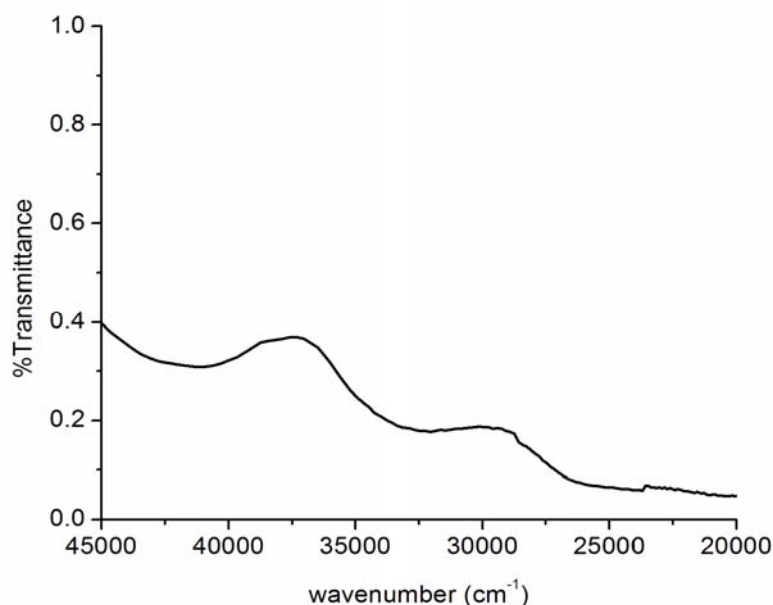
Fig.3.5. Electronic spectrum of [VO(HDpyMeTsc)(SO$_4$)] (**2**)

3.3.3. Electron paramagnetic resonance spectra

All the compounds are EPR active due to the presence of an unpaired electron. The oxidation state of the central vanadium atom in the complexes was confirmed by the measurements of EPR spectroscopy. EPR spectra of both the complexes were recorded in polycrystalline state at 298 K and in frozen DMF at 77 K. EPR spectral parameters of oxovanadium(IV) complexes are summarized in Table 3.3.

In polycrystalline state at 298 K, the two complexes are isotropic in nature with g_{iso} = 1.956 and 1.968 respectively (Figs. 3.6 & 3.7). In frozen DMF at 77 K both the complexes show well resolved axial anisotropy characterized by two sets of eight lines, which result from coupling of the electron spin to the spin of the ^{51}V nucleus (I = 7/2), characteristic of mononuclear oxovanadium complexes (Figs. 3.8 & 3.9). The anisotropic hyperfine parameters were also calculated. The $g_{\parallel} < g_{\perp}$ and $A_{\parallel} > A_{\perp}$

relationship, characteristic of an axially compressed system with unpaired electron in d_{xy} orbital [20]. The absence of superhyperfine splittings in the spectra also indicate the unpaired electron to be in d_{xy} orbital localized on metal, thus excluding the possibility of its direct interaction with the ligand [21,22].

The EPR parameters $g_\parallel$, $g_\perp$, $A_\parallel$ and $A_\perp$ and energies of *d-d* transitions were used to evaluate the molecular orbital coefficients α^2 and β^2 for the complexes by using the following equations [23]

$$\alpha^2 = \frac{(2.00277 - g_\parallel)E_{d-d}}{8\lambda\beta^2}$$

$$\beta^2 = \frac{7}{6}\left[\left(\frac{-A_\parallel}{P}\right) + \left(\frac{A_\perp}{P}\right) + \left(g_\parallel - \frac{5}{14}g_\perp\right) - \frac{9}{14}g_e\right]$$

Where $P = 128 \times 10^{-4}$ cm^{-1}, $\lambda = 135$ cm^{-1} and E_{d-d} is the energy of *d-d* transition. The lower values for α^2 compared to β^2 indicate that in-plane σ-bonding is more covalent than in-plane π-bonding.

Table 3.3. EPR spectral data of vanadium (IV) complexes in the polycrystalline state at 298 K and in frozen DMF at 77 K

Compound	Polycrystalline (298 K)	DMF Solution (77 K)					
	g_{iso}	$g_\parallel$	$g_\perp$	$A_\parallel{}^a$	$A_\perp{}^a$	α^2	β^2
[VO(DpyMeTsc)(NCS)] **(1)**	1.956	1.950	1.987	145	60	0.953	0.987
[VO(HDpyMeTsc)(SO$_4$)] **(2)**	1.968	1.964	1.992	167	75	0.976	0.994

^{a} values in 10^{-4} cm^{-1}
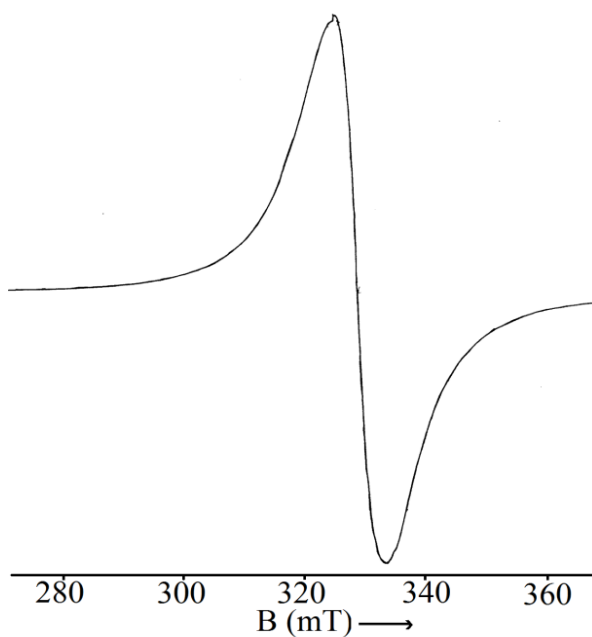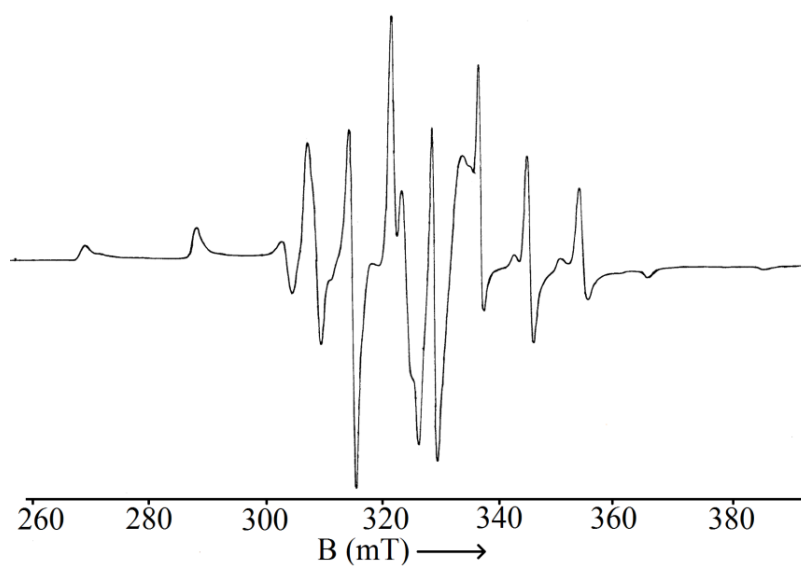
Fig. 3.6. EPR spectrum of [VO(DpyMeTsc)(NCS)] (**1**) in polycrystalline state at 298 K
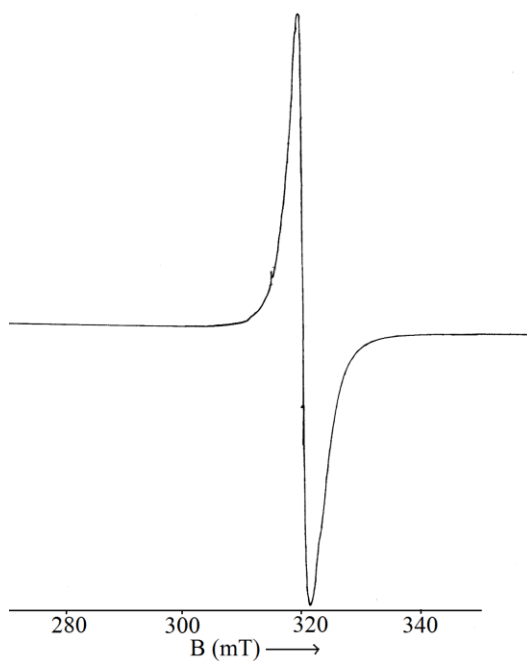
Fig. 3.7. EPR spectrum of [VO(HDpyMeTsc)(SO$_4$)] (**2**) in polycrystalline state at 298 K
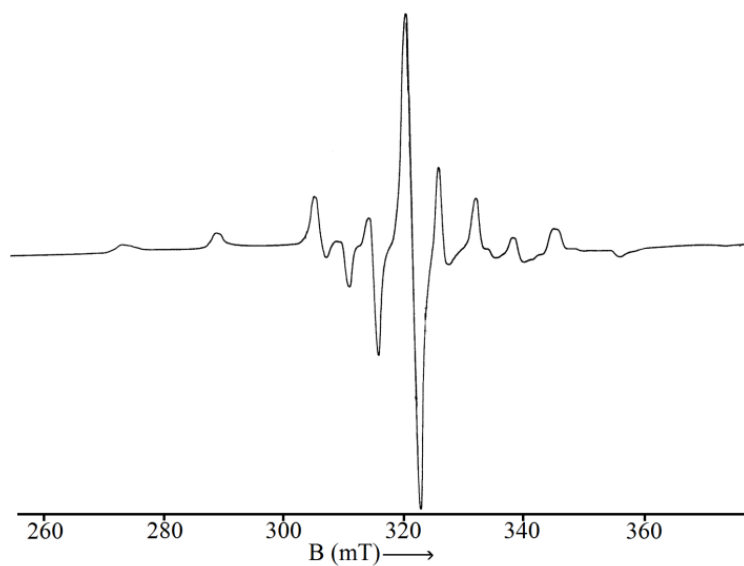
Fig. 3.8. EPR spectrum of [VO (DpyMeTsc)(NCS)] (**1**) in DMF at 77 K

Fig. 3.9. EPR spectrum of [VO(HDpyMeTsc)(SO_4)] (**2**) in DMF at 77 K

References

[1]   D. Rehder, Angew. Chem. Int. Ed. Engl. 30 (1991) 148.

[2]   J. Rivadeneira, D.A. Barrio, G. Arrambide, D. Gambino, L. Bruzzone, S.B. Etcheverry, J. Inorg. Biochem. 103 (2009) 633.

[3]   D. Charistos, B. Voulgaropoulose, G. Voutsas, Struct. Chem. 12 (2001) 1.

[4]   P.I.S. Maia, V.M. Deflon, E.J. de Souza, E. Garcia, G.F. de Sousa, A.A. Batista, A.T. de Figueiredo, E. Niquet, Trans. Met. Chem. 30 (2005) 404.

[5]   E.J. Baran, J. Inorg. Biochem. 80 (2000) 1.

[6]   T. Ghosh, S. Bhattacharya, A. Das, G. Mukherjee, M.G.B. Drew, Inorg. Chim. Acta 358 (2005) 989.

[7]   K.H. Thompson, V.G. Yuen, J.H. McNeill, C. Orvig, in: A.S. Tracey, D.C. Crans (Eds.), Vanadium Compounds: Chemistry, Biochemistry and Therapeutic Applications, Oxford University Press, New York, 1998.

[8]   K.H. Thompson, C. Orvig, J. Chem. Soc., Dalton Trans. (2000) 2885.

[9]   P. Noblia, E.J. Baran, L. Otero, P. Draper, H. Cerecetto, M. Gonzalez O.E. Piro, E. Castellano, T. Inohara, Y. Adachi, H. Sakurai, D. Gambino, Eur. J. Inorg. Chem. (2004) 322.

[10] W.J. Geary, Coord. Chem. Rev. 7 (1971) 81.

[11] R. l. Dutta, G.P. Senguptha, J. Ind. Chem. Soc. 49 (1972) 919.

[12] E.B. Seena, M.R.P. Kurup, Spectrochim. Acta A69 (2008) 726.

[13] E. Manoj, M.R.P. Kurup, Polyhedron 27 (2008) 275.

[14] L. Latheef, M.R.P. Kurup, Polyhedron 27 (2008)35.

[15] R.K. Agarwal, S. Prasad, N. Gahlot, Turk J. Chem. 28 (2004) 691.

[16] R.A. Bailey, S.L. Kozak, T.W. Michelson, W.N. Mills, Coord. Chem. Rev. 6 (1971) 407.

[17] K. Nakamoto, Infrared and Raman Spectra of Inorganic and Coordination Compounds, Part B, 5th edition, Wiley, New York, 1997.

[18] A. Castineiras, E. Bermejo, D.X. West, L.J. Ackerman, J.V. Martinez, S.H. Ortega, Polyhedron 18 (1999) 1469.

[19] B.J.A. Jeragh, A. El-Dissouky, Trans. Met. Chem. 29 (2004) 579.

[20] S. Bhattacharya, T. Ghosh, Indian J. Chem. A38 (1999) 601.

[21] H. Kon, E. Sharpless, J. Chem. Phys. 42 (1965) 906.

[22] D. Kivelson, S.K. Lee, J. Chem. Phys. 41 (1964) 1896.

[23] N.A. Mangalam, M.R.P. Kurup, Spectrochim. Acta A71 (2009) 2040.

........................🙠🙠🙠........................

SYNTHESES, SPECTRAL AND STRUCTURAL CHARACTERIZATION OF MANGANESE(II) COMPLEXES OF KETONE BASED N(4)-SUBSTITUTED THIOSEMICARBAZONES

4.1. Introduction

Manganese metal has a well established importance in the field of biology and medicine [1]. The element is a required trace mineral for all known living organisms. The most important natural role of manganese is in the oxidation of water in green plant photosynthesis where its presence in photosystem II is essential [2]. Manganese(II) ions function as cofactors for a number of enzymes in higher organisms, where they are essential in detoxification of superoxide free radicals. Particularly, over the past decade there has been a considerable interest in synthesizing biomimetic complexes that can act as manganoenzymes such as superoxide dismutase (SOD) [3]. Mn(II) ions also serve as a valuable probe of the Mg(II) binding sites in nucleic acids as well as catalytically relevant M^{2+} binding sites found in nucleic acids polymerases and nucleases. A particularly interesting case is the identification and study of Mg/Mn sites in ribozymes [4].

Manganese carbonyl compounds are of interest in part because of their rich physico-chemical properties, reactivity patterns and applications in many important chemical processes [5]. Manganese and its compounds are widely

used in analytical chemistry, metallurgical processes and paint and pigment industry. Manganese(II) complexes are well known for their excellent catalytic activity towards the disproportionation of hydrogen peroxide and a number of them have been shown to catalyze the low temperature peroxide bleaching of fabrics [6]. Manganese complexes exhibit interest due to their catalytic antioxidant activity, in blocking oxidant stress *in vitro* [7]. Moreover, the biomedical use of manganese(II) mononuclear complexes (ie, contrast agents for MRI) has been implied [8].

Manganese exhibits versatile coordination chemistry with diverse Mn(II/III/IV/V) oxidation states [9]. The chemistry of manganese, in various oxidation states of the metal and in various combinations of nitrogen and oxygen donor environment, is presently witnessing intense activity [10-12]. The coordination chemistry of manganese has received a great deal of attention because of the variable structures of manganese complexes and the possibility of magnetic coupling interaction [13-17]. This chapter focuses on the syntheses, structural and spectral characterization of manganese(II) complexes of the two thiosemicarbazone ligands, viz., di-2-pyridyl ketone-*N*(4)-methylthiosemicarbazone (HDpyMeTsc) and di-2-pyridyl ketone-*N*(4)-ethylthiosemicarbazone (HDpyETsc).

4.2. Experimental

4.2.1. Materials

All the chemicals and solvents used for the syntheses were of analytical grade. Di-2-pyridyl ketone (Aldrich), *N*(4)-methyl thiosemicarbazide (Aldrich), *N*(4)-ethylthiosemicarbazide (Aldrich), manganese(II) acetate tetrahydrate (E-Merck), manganese(II) chloride tetrahydrate (E-Merck), manganese(II)

perchlorate hexahydrate (E-Merck), ethanol and methanol were used as supplied.

4.2.2. Syntheses of ligands

The ligands HDpyMeTsc and HDpyETsc were prepared as described previously in Chapter 2.

4.2.3. Syntheses of manganese (II) complexes

4.2.3a. Synthesis of [Mn(DpyMeTsc)₂] (3)

To a solution of HDpyMeTsc (0.542 g, 2 mmol) in hot ethanol was added a methanolic solution of manganese(II) acetate tetrahydrate (0.245 g, 1 mmol). To this added 1 mmol of triethylamine and the resulting solution was stirred for 3 hours and then kept at room temperature. The reddish brown precipitate of **3** that separated out was filtered, washed with ether and dried over P_4O_{10} *in vacuo*.

λ_m (DMF): 8 ohm^{-1} cm^2 mol^{-1}, μ_{eff} *(B.M.)*: 5.78, Elemental Anal. Found (Calcd.) (%): C: 52.18 (52.43); H: 4.17 (4.06); N: 23.06 (22.83).

4.2.3b. Synthesis of [Mn(HDpyMeTsc)Cl₂] (4)

Manganese(II) chloride tetrahydrate (0.198 g, 1 mmol) in methanol was added to a solution of HDpyMeTsc (0.271 g, 1 mmol) in hot ethanol. The reaction mixture was refluxed for 3 hours, cooled and filtered. The orange red precipitate obtained was washed with ether and then dried over P_4O_{10} *in vacuo*.

λ_m (DMF): 48 ohm^{-1} cm^2 mol^{-1}, μ_{eff} *(B.M.)*: 5.63, Elemental Anal. Found (Calcd.) (%): C: 39.92 (39.31); H: 3.46 (3.30); N: 17.92 (17.63).

4.2.3c. Synthesis of [Mn(HDpyMeTsc)₂](ClO₄)₂ · H₂O (5)

HDpyMeTsc (0.271 g, 1 mmol) in hot ethanol and manganese(II) perchlorate hexahydrate (0.361 g, 1 mmol) in methanol were mixed and refluxed for 3 hours. Orange red precipitate was obtained. The reaction mixture was cooled and filtered. Then the precipitate was washed with ether and then dried over P_4O_{10} *in vacuo*.

λ_m (DMF): 182 ohm^{-1} cm^2 mol^{-1}, μ_{eff} *(B.M.)*: 5.85, Elemental Anal. Found (Calcd.) (%): C: 38.34 (38.34); H: 3.16 (3.46); N: 17.32 (17.20).

4.2.3d. Synthesis of [Mn(DpyETsc)₂] · 2H₂O (6)

Manganese(II) acetate tetrahydrate (0.245 g, 1 mmol) in methanol was added to the hot ethanolic solution of HDpyETsc (0.570 g, 2 mmol). To this added 1 mmol of triethylamine and the solution was refluxed for 3 hours and then kept at room temperature. The reddish brown precipitate obtained was filtered, washed with ether and then dried over P_4O_{10} *in vacuo*.

λ_m (DMF): 12 ohm^{-1} cm^2 mol^{-1}, μ_{eff} *(B.M.)*: 5.80, Elemental Anal. Found (Calcd.) (%): C: 50.38 (50.98); H: 4.31 (4.89); N: 21.15 (21.23).

Caution: Perchlorate complexes of metals with organic ligands are potentially explosive and should be handled with care.

4.3. Results and discussion

The four manganese complexes reported have been prepared using the two thiosemicarbazones, HDpyMeTsc and HDpyETsc. Equimolar ratio of the thiosemicarbazone and the metal salt yielded complexes **4** and **5**, whereas the reaction of the ligand and metal salt in ratio 2:1 yielded complexes **3** and **6**. Complexes were found to be reddish brown or yellowish orange in color. All

the four compounds are soluble in polar organic solvents like acetonitrile, DMF and DMSO, but only partially soluble in other organic solvents such as CHCl$_3$, ethanol, methanol etc.

Analytical data show that in complexes **3** and **6,** the thiosemicarbazones deprotonate and chelate in the thiolate form whereas in complexes **4** and **5**, the ligand moieties are in the thioamido form. The molar conductivity measurements in DMF (10^{-3} M) solution indicate that complexes **3**, **4** and **6** are non-electrolytes and complex **5** is probably 2:1 electrolyte [18]. The magnetic moments of the complexes are found to be in the range 5.6 – 5.9 *B.M.*, which are indicative of a high spin d^5 system [19]. The complexes are found to be EPR active.

4.3.1. Infrared spectra

To clarify the mode of bonding, the IR spectra of metal free ligands and manganese(II) complexes were studied and assigned on the basis of a careful comparison of the latter with the free ligands. It revealed that there is significant variations in the characteristic bands due to coordination with the central metal ion. The tentative IR spectral assignments are listed in Table 4.1.

The ν(C=N) bands of thiosemicarbazones are found to be shifted to lower frequencies in all the complexes indicating coordination *via* the azomethine nitrogen (Figs. 4.1–4.4). The shifting of the azomethine (C=N) band to a lower frequency is attributed to the conjugation of the *p*-orbital on the double bond with the *d*-orbital on the metal ion with reduction of the force constant. The involvement of this nitrogen in bonding is also supported by a

shift in ν(N–N) band to higher frequencies [20]. Coordination *via* thiolate sulfur is indicated by the negative shift of the two bands assigned to ν(C=S) and δ(C=S) vibrations. The appearance of new bands at 1510 and 1484 cm^{-1} in the IR spectra of complexes **3** and **6** due to the newly formed –C=N– moiety, support the above observation. The in-plane bending vibrations of the pyridine ring in uncomplexed ligands shift to higher frequencies on complexation, confirming the coordination of ligands to the metal *via* the pyridine nitrogen [21].

Table 4.1. IR spectral data (cm^{-1}) of manganese(II) complexes

| Compound	ν(C=N)	ν(C=N)^a	ν/δ(C–S)	ν(N–N)	py(ip)
HDpyMeTsc	1588	...	1431, 800	1110	618
[Mn(DpyMeTsc)$_2$](**3**)	1560	1510	1329, 786	1151	634
[Mn(HDpyMeTsc)Cl$_2$] (**4**)	1533	...	1328, 741	1175	650
[Mn(HDpyMeTsc)$_2$](ClO$_4$)$_2$ · H$_2$O (**5**)	1555	...	1332, 747	1168	623
HDpyETsc	1585	...	1431, 799	1109	615
[Mn(DpyETsc)$_2$] · 2H$_2$O (**6**)	1518	1484	1325, 742	1147	635

^{a} Newly formed C=N
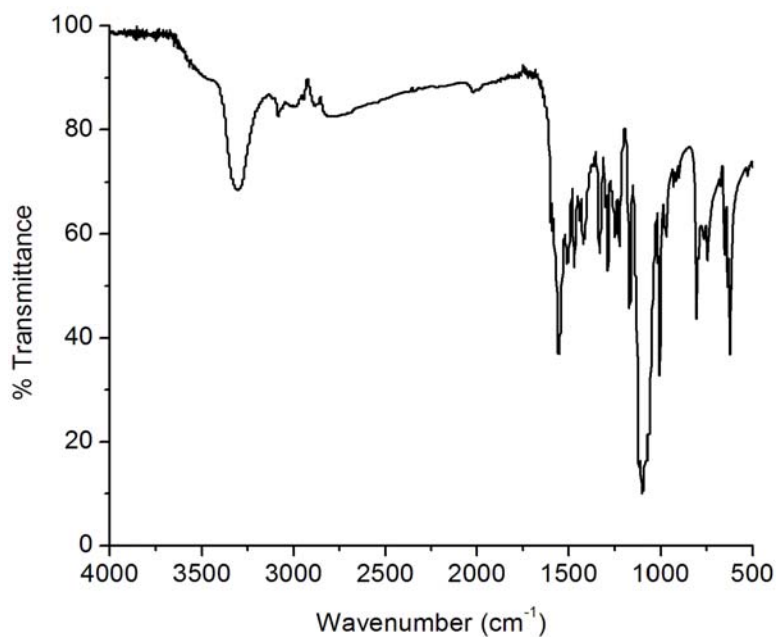
The perchlorate complex shows single broad band at 1098 cm^{-1} and a strong band at 637 cm^{-1}, indicating the presence of ionic perchlorate. The band at 1098 cm^{-1} is assignable to ν_3(ClO$_4$) and the unsplit band at 637 cm^{-1} is assignable to ν_4(ClO$_4$) [22].
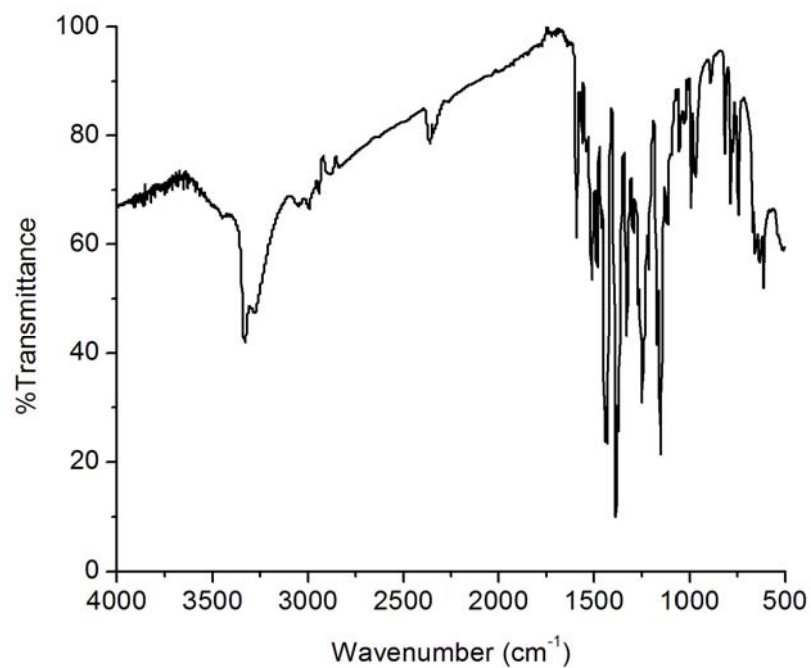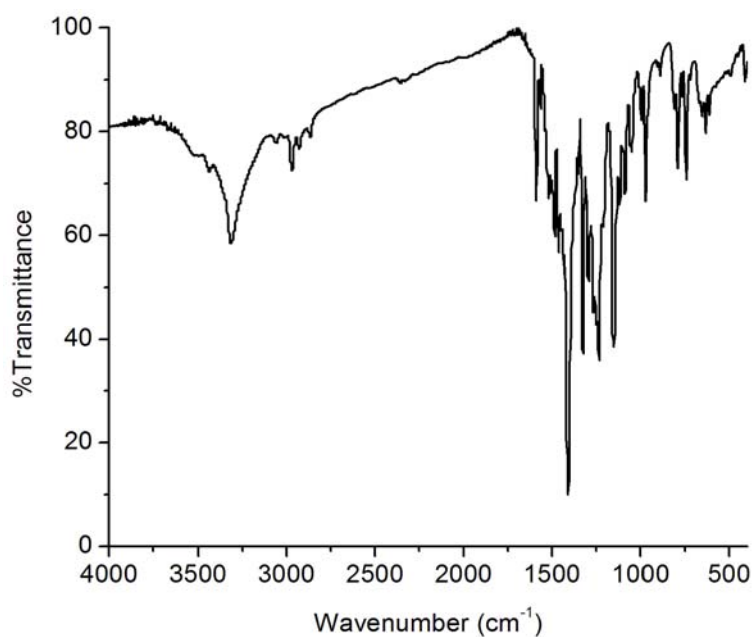
Fig. 4.1. IR spectrum of [Mn(DpyMeTsc)$_2$] (**3**)
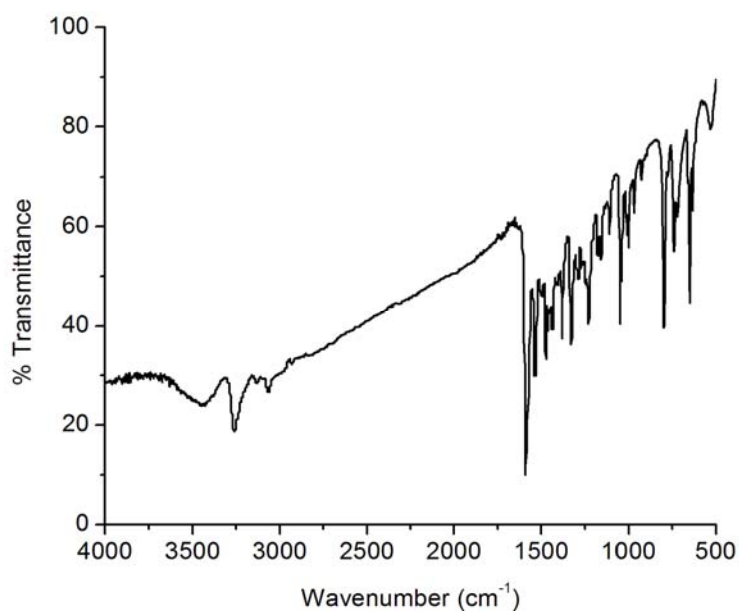
Fig. 4.2. IR spectrum of [Mn(HDpyMeTsc)Cl$_2$] (**4**)

Fig. 4.3. IR spectrum of [Mn(HDpyMeTsc)₂](ClO₄)₂ · H₂O (**5**)

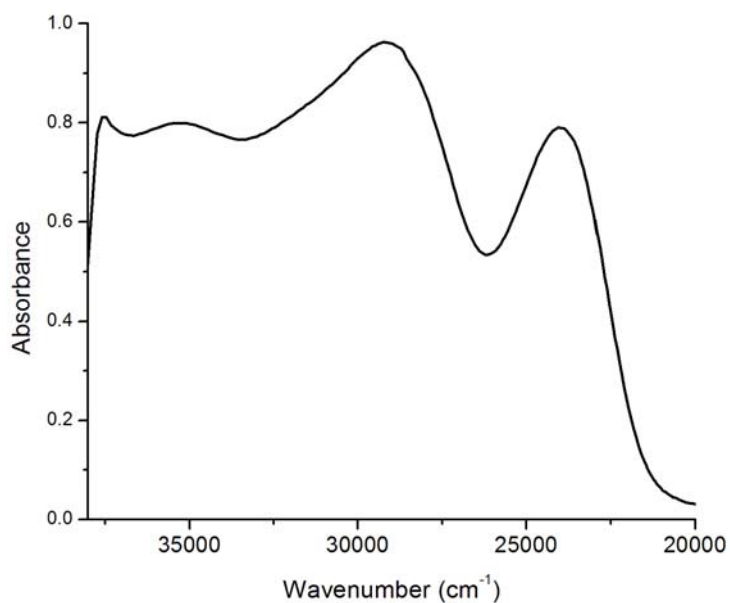**Fig. 4.4**. IR spectrum of [Mn(DpyETsc)₂] · 2H₂O (**6**)

4.3.2. Electronic spectra

The Mn(II) complexes belong to the d^5 system. In the high-spin, octahedrally coordinated Mn(II) complex, the lowest configuration $(t_{2g})^3 (e_g)^2$ gives rise to the ground state $^6A_{1g}$. Since this is the only sextet level present, all the absorption bands must be spin forbidden transitions [23]. Also for octahedral complexes, transitions are Laporte forbidden. Thus these transitions are doubly forbidden, and consequently the transition intensities of octahedral manganese(II) complexes are very low. The electronic spectra of the Mn(II) complexes were recorded both in acetonitrile and in DMF (Figs. 4.5–4.8).

The high intense intraligand transitions and charge transfer transitions, tailing into the visible region, obscure the very weak d–d absorption bands of the manganese(II) complexes. However some forbidden transitions can occur to the quartet excited states and they are $^4A_{1g}(G)$, $^4E_g(G) \leftarrow {}^6A_{1g}$, $^4E_g(D) \leftarrow {}^6A_{1g}$, $^4T_{1g}(G) \leftarrow {}^6A_{1g}$ and $^4T_{2g}(G) \leftarrow {}^6A_{1g}$. The very weak bands $ca.$ 18000 cm^{-1} assigned to $^6A_{1g} \rightarrow {}^4T_{1g} \, (^4G)$ transitions are obtained for all the complexes [24]. The electronic spectral assignments are summarized in Table 4.2.

**Table 4.2.** Electronic spectral data (cm^{-1}) of manganese(II) complexes

| Compound	UV absorption bands (cm^{-1})				
HDpyMeTsc	35890	29280			
[Mn(DpyMeTsc)$_2$](3)	37500	35300	29160	23940	18790
[Mn(HDpyMeTsc)Cl$_2$] (4)	43060	35700	29480	23450	17360
[Mn(HDpyMeTsc)$_2$](ClO$_4$)$_2$ · H$_2$O (5)	42390	35820	29250	24680	18110
HDpyETsc	35860	29360			
[Mn(DpyETsc)$_2$] · 2H$_2$O (6)	29240	23900	18690		

Fig. 4.5. Electronic spectrum of [Mn(DpyMeTsc)$_2$] **(3)**
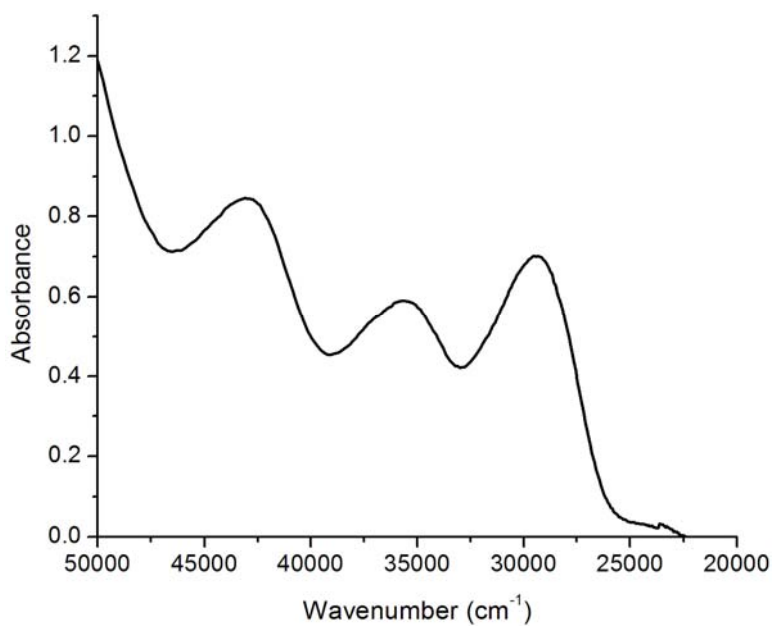
Fig. 4.6. Electronic spectrum of [Mn(HDpyMeTsc)Cl$_2$] **(4)**
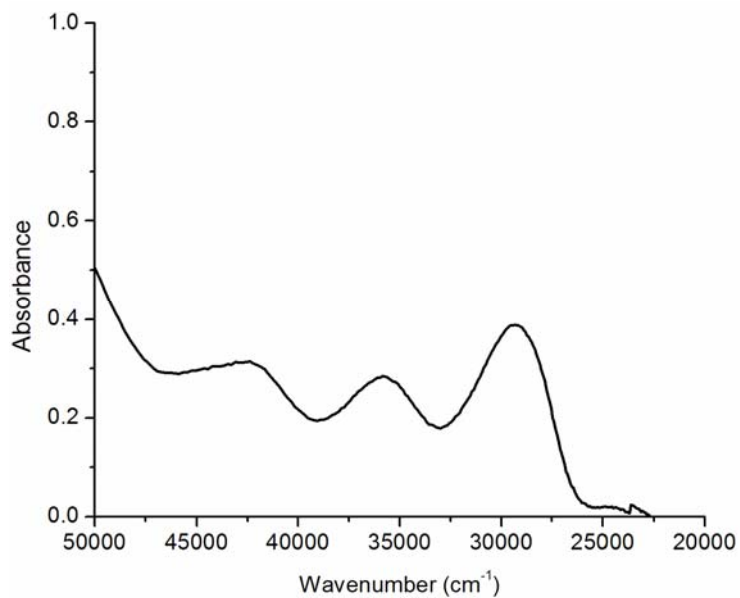
Fig. 4.7. Electronic spectrum of [Mn(HDpyMeTsc)$_2$](ClO$_4$)$_2$ · H$_2$O (**5**)
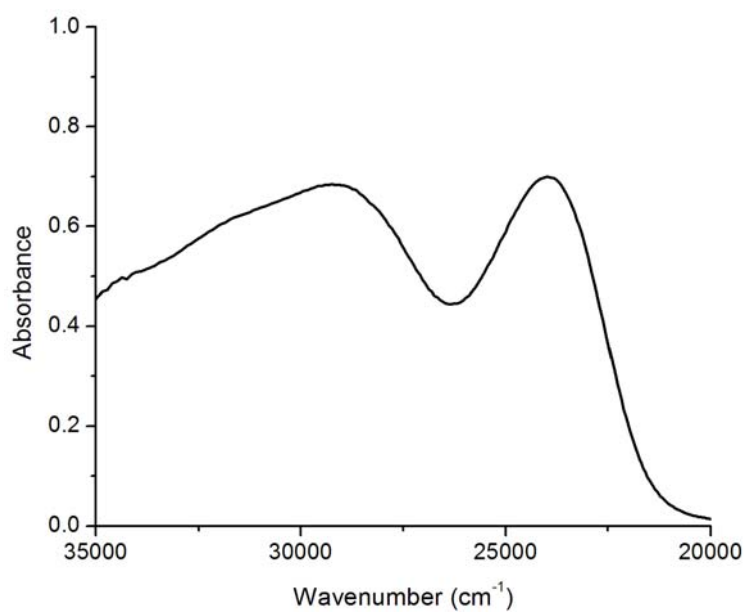
Fig. 4.8. Electronic spectrum of [Mn(DpyETsc)$_2$] · 2H$_2$O (**6**)

4.3.3. Electron paramagnetic resonance spectra

Manganese complexes show a wide variety of bonding geometries and EPR spectroscopy has been used successfully to probe the structures of these compounds [25,26]. The ground state of Mn^{2+} ion, with a d^5 configuration, is unique among d^n configurations in that there is only one state with maximum spin multiplicity ($^6S_{5/2}$). This splits into three Kramers doublets ($\pm 5/2$, $\pm 3/2$ and $\pm 1/2$) in an orthorhombic crystalline field, which are further split in the presence of an applied magnetic field. These six levels give rise to five fine structure transitions. Each fine structure transition will be split into six hyperfine components due to ^{55}Mn hyperfine coupling, giving, in all 30 allowed transitions.

The EPR spectra of Mn(II) may be described by the spin Hamiltonian

$$\hat{H} = g\beta BS + D[S_z^2 - S(S+1)/3] + E(S_x^2 - S_y^2)$$

where B is the magnetic field vector, g is the spectroscopic splitting factor, β is the Bohr magneton, D is the axial zero field splitting parameter, E is rhombic zero field splitting parameter and S is the electron spin vector [27]. If D and E are both zero, then the only contributor to the spectrum is the first-order Zeeman term and the result for Mn^{2+} is an isotropic spectrum, with a single signal with g_{eff} near 2.0. In weak ligand fields, Mn(II) centers give a single transition at $g = 2$, which splits into six hyperfine lines by the ^{55}Mn nucleus ($I = 5/2$). If D and E are very small compared to $g\beta BS$, five EPR transitions corresponding to $\Delta m_s = \pm 1$, viz., $|+5/2>\leftrightarrow|+3/2>$, $|+3/2>\leftrightarrow|+1/2>$, $|+1/2>\leftrightarrow|-1/2>$, $|-1/2>\leftrightarrow|-3/2>$ and $|-3/2>\leftrightarrow|-5/2>$ are expected. However, for the case where D or E is very large, the lowest doublet has effective g values of $g_\parallel = 2$, $g_\perp = 6$ for $D\neq 0$ and $E=0$ but for $D=0$ and $E\neq 0$, the middle Kramers doublet has an isotropic g value of 4.29 [28].

The X-band EPR spectra of the manganese complexes were recorded in polycrystalline state at 298 K and in frozen DMF at 77 K. The EPR spectrum of compound **3** in the polycrystalline state at room temperature shows five *g* values, $g_1 = 2.037$, $g_2 = 2.882$, $g_3 = 4.261$, $g_4 = 5.700$ and $g_5 = 11.605$, due to zero field splitting and Kramers degeneracy. However, the solution spectrum in DMF at 77 K, displayed two *g* values, $g_1 = 2.093$ and $g_2 = 4.133$.
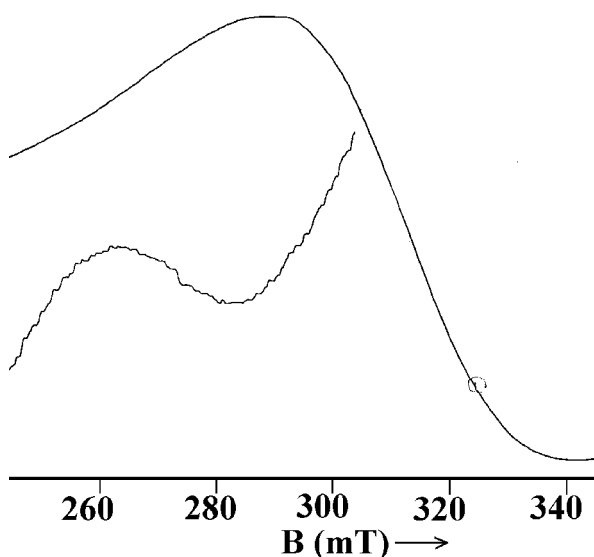
The polycrystalline state EPR spectrum of the compound **4** at 298 K exhibits a broad signal with a *g* value at 2.031 with no hyperfine splitting. The broadness of the signals is a characteristic feature of Mn(II) complex in the polycrystalline state, which arises due to dipolar interactions and enhanced spin lattice relaxation [29]. The spectrum in DMF at 77 K (Fig. 4.9) displayed a hyperfine sextet with *g* value 1.999 and hyperfine coupling constant, A_{iso} 99 x 10^{-4} cm^{-1}. The observance of hyperfine sextet is due to the interaction of the unpaired electron with the Mn(II) nucleus of spin $I = 5/2$, resulting in $2nI+1$ lines. Thus the six lines observed corresponds to $m_s = +5/2, +3/2, +1/2, -1/2, -3/2, -5/2$ with $\Delta m_I = 0$.
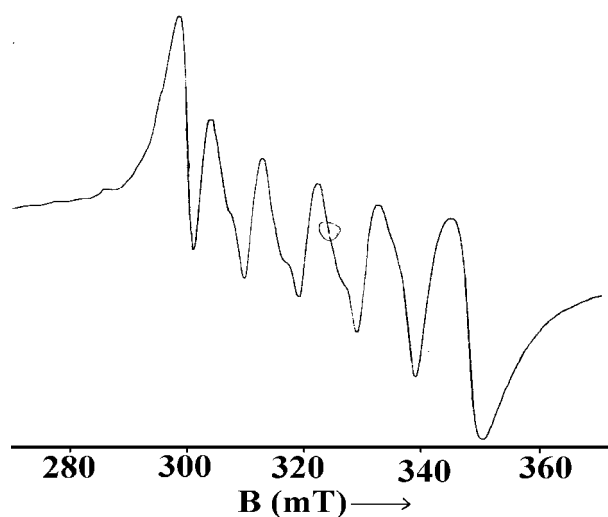
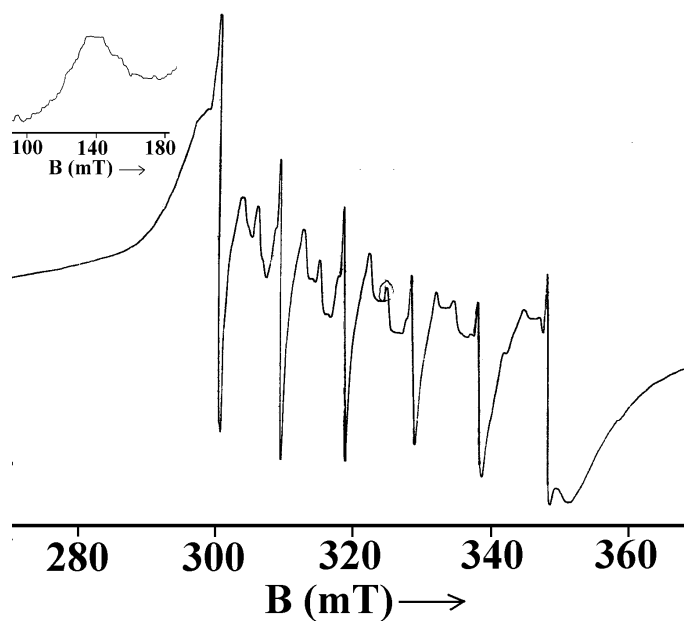**Fig. 4.9.** EPR spectrum of [Mn(HDpyMeTsc)Cl$_2$] **(4)** in DMF at 77 K

The EPR spectrum of compound **5** in the polycrystalline state at 298 K gave two *g* values; $g_1 = 2.073$ and $g_2 = 5.241$ (Fig. 4.10). The spectrum is broad with no hyperfine splitting. However, the solution spectrum in DMF at 77 K, displayed two g values, $g_1 = 1.997$ and $g_2 = 4.642$ (Fig. 4.11). Only the high field signal exhibited hyperfine splitting and a sextet pattern was observed.

A broad isotropic signal with $g_{iso} = 2.097$ was found for the compound **6** in polycrystalline state at 298 K (Fig. 4.12). In DMF at 77 K, the EPR spectrum displays two g values at $g_1 = 2.054$ and $g_2 = 4.763$.


Fig. 4.10. EPR spectrum of [Mn(HDpyMeTsc)$_2$](ClO$_4$)$_2$ · H$_2$O **(5)** in polycrystalline state at 298 K

The observed *g* values are very close to the free electron spin value, suggestive of the absence of spin orbit coupling in the ground state. The A_{iso} values are somewhat lower than pure ionic compounds, which reflects the covalent nature of the metal-ligand bond in the complexes. The mixing of the nuclear hyperfine levels with the zero field splitting factor produces low intensity forbidden lines lying between each of the two main hyperfine lines in the frozen solution spectra of the complexes [30].

Fig. 4.11. EPR spectrum of [Mn(HDpyMeTsc)$_2$](ClO$_4$)$_2$ · H$_2$O **(5)** in DMF at 77 K
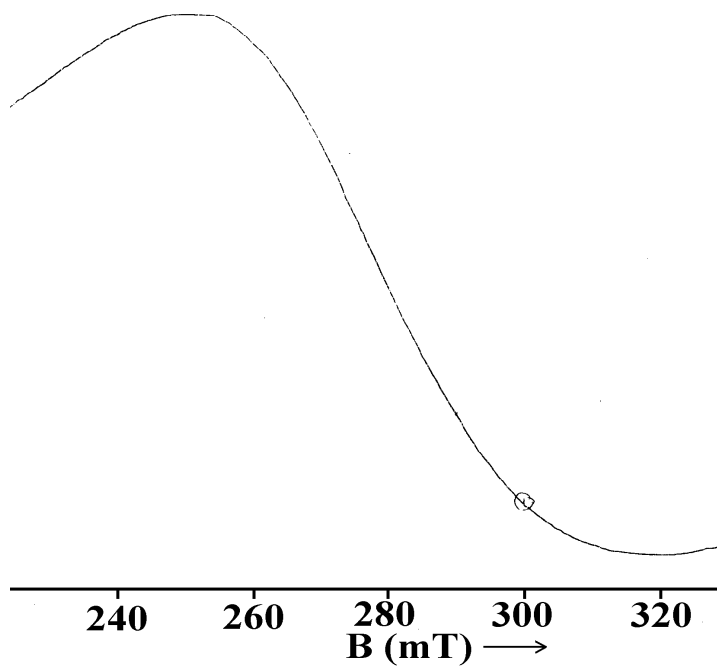
Fig. 4.12. EPR spectrum of [Mn(DpyETsc)$_2$] · 2H$_2$O **(6)** in polycrystallinestate at 298 K

4.3.4. Thermal analyses

Thermogravimetric anlyses are based on the change in weight of the substance with respect to temperature or time. Thermogravimetric analyses are used to get (i) informations regarding thermal stability of these new complexes (ii) decide whether the water molecules (if present) are inside or outside of the inner coordination sphere of the central metal ion and (iii) suggest a general scheme for thermal decomposition of the ligands [31]. Thermogram of complex **6** shows weight loss in the range 50-90 °C, indicating the presence of water molecules outside the coordination sphere. Complex is thermally stable and decomposition of ligand starts after 200 °C. TG-DTG curve of complex **6** is shown in Fig. 4.13.
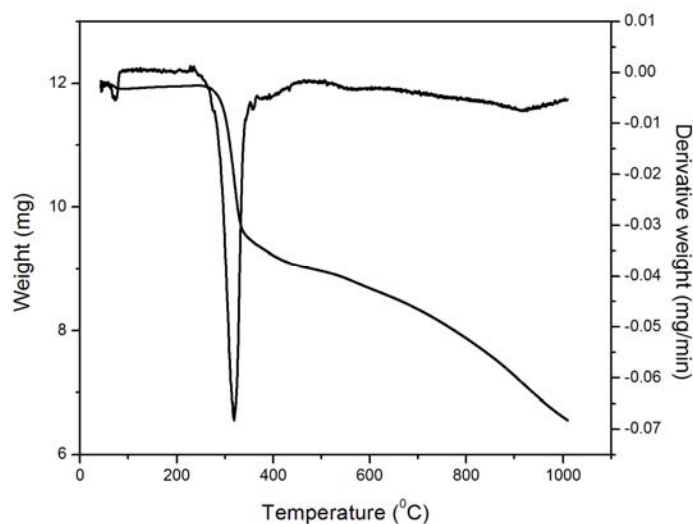

Fig. 4.13. TG-DTG curve of complex **6**

4.3.5. Crystal structure of [Mn(DpyMeTsc)₂] (3)

Reddish brown crystals for the single crystal X-ray diffraction were grown by slow evaporation of the complex in ethanol/methanol (1:1) mixture. The crystallographic data and structure refinement parameters are given in

Table 4.3. The data reduction and cell refinement were carried out using a CrysAlis RED, Oxford Diffraction Ltd. at the National Single Crystal X-ray Diffraction facility, IIT, Bombay, India. The trial structure was solved using SHELXS-97 and refinement was carried out by full-matrix least squares on F^2 (SHELXL-97) [32]. The molecular graphics employed were PLATON [33] and DIAMOND [34].

The molecular structure of the complex along with the atom-numbering scheme is given in Fig. 4.14. The compound crystallizes into a monoclinic space group $P2_1/n$. The two molecules of monodeprotonated ligand, coordinate to manganese *via* pyridyl nitrogen, azomethine nitrogen and thiolato sulfur atoms to form four five membered chelate rings. The coordination of sulfur occurs through deprotonation after enolization, and was confirmed by the lengthening of the bond C1–S1 [1.728(5) Å] and shortening of the bond N1–C1 [1.323(6) Å].
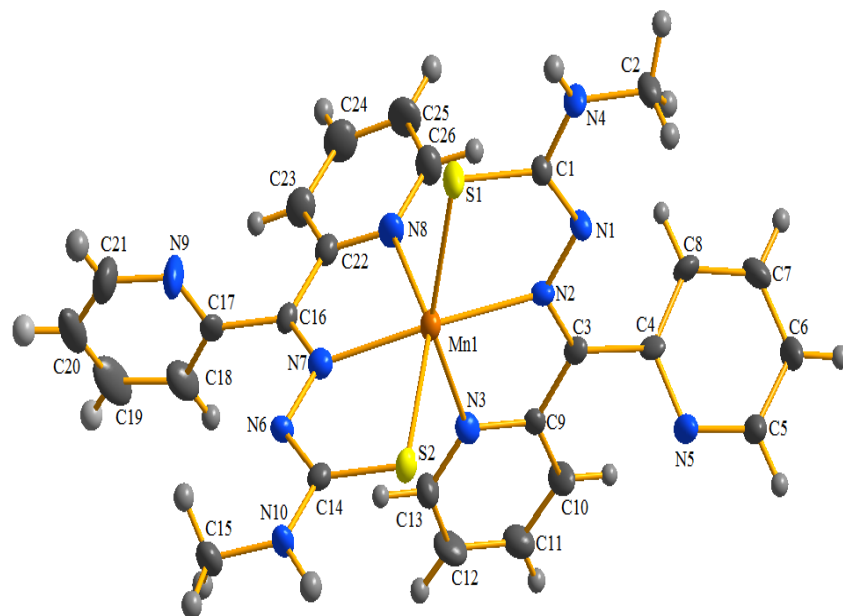
Fig. 4.14. The molecular structure of [Mn(DpyMeTsc)₂] **(3)**.

Table 4.3. Crystal refinement parameters of [Mn(DpyMeTsc)$_2$]

| Empirical formula	C$_{26}$ H$_{24}$Mn$_1$N$_{10}$ S$_2$
Formula weight (M)	595.63
Temperature (T) K	120(2)
Wavelength (Mo Kα) (Å)	0.71073
Crystal system	Monoclinic
Space group	$P2_1$/n
Lattice constants	
a(Å)	10.6433(7)
b(Å)	15.1466(9)
c(Å)	17.2816(10)
α (°)	90.00
β (°)	92.179(6)
γ(°)	90.00
Volume V (Å^3)	2784.0(3)
Z	4
D$_{calc}$(ρ) (Mg m^{-3})	1.421
Absorption coefficient, μ (mm^{-1})	0.660
F(000)	1228
Crystal size (mm^3)	0.19x 0.15x 0.13
θ range for data collection	2.94 -25
Limiting Indices	-12 $\leq$ h $\leq$ 12, -18 $\leq$ k $\leq$ 18, -20 $\leq$ l $\leq$ 20
Reflections collected	21200
Unique reflections	4883 [R(int) $=$ 0.1276]
Refinement method	Full-matrix least-squares on F^2
Data / restraints / parameters	4883/0/362
Goodness-of-fit on F^2	1.026
Final R indices [I $>$ 2σ (I)]	R$_1$ $=$ 0.0636, wR$_2$ $=$0.0869
R indices (all data)	R$_1$ $=$ 0.1463, wR$_2$$=$0.1142
Largest difference peak and hole (e Å^{-3})	0.43 and -0.427

$R_1 = \Sigma||F_o| - |F_c|| / \Sigma|F_o$
$wR_2 = [\Sigma w(F_o^2-F_c^2)^2 / \Sigma w(F_o^2)^2]^{1/2}$

There is a slight shortening of Mn–N$_{azomethine}$ bond distance compared to Mn–N$_{py}$ distances; this may be attributed to the fact that the azomethine nitrogen is a stronger base compared with the pyridyl nitrogen. The ligands with their donor atoms are arranged around the manganese ion in a meridional fashion. In this compound, while S1, S2, N3 and N8 lie in the equatorial plane, N2 and N7 occupy the axial positions of the distorted octahedron. The MnN$_2$S$_2$ fragment is distorted from the mean plane by 0.013 Å. Each thiosemicarbazone fragment is subtending an angle of 147.38 and 148.41° at the Mn center, which is smaller than 180° that is expected for an ideal octahedron. The planes containing Mn, S1, N2, N3, N7 and Mn, S2, N2, N8, N7 are deviated from the mean plane by 0.179 and 0.166 Å (Mn), respectively. These factors suggest considerable distortion from an octahedral geometry around the Mn(II) center. The significant deviation from regular octahedron coordination geometry around the central metal is evident from the observed values of bond distances and angles as summarized in Table 4.4.

The molecules are connected in the crystal lattice through weak intermolecular hydrogen bonds; N4(H) of one molecule with S1 of another molecule [symmetry code: 2 - x, -y, 1- z; with a H⋯S distance of 2.60(6) Å and angle 166(5)°] and vice-versa and N10(H) of same molecule with N(9) of another [symmetry code: 5/2-x, 1/2+y, 1/2-z; with a H⋯N distance of 2.28(6) Å and angle 169(5)°] leading to a three dimentional network (Fig. 4.15). The network of electron delocalization brought about by the aromatic and metallo-aromatic [35] rings gives rise to diverse π-π and C–H⋯π interactions, invoking stable molecular arrangement in the unit cell. The interaction parameters are listed in Table 4.5.

Table 4.4. Selected bond lengths (Å) and bond angles (°) of [Mn(DpyMeTsc)₂]

Bond lengths (Å)		Bond angles (°)	
Mn(1)—N(2)	2.231(4)	N(2)—Mn(1)—N(7)	160.60(14)
Mn(1)—N(7)	2.249(4)	N(7)—Mn(1)—N(3)	94.95(14)
Mn(1)—N(3)	2.269(4)	N(2)—Mn(1)—N(3)	72.07(15)
Mn(1)—N(8)	2.254(4)	N(7)—Mn(1)—N(8)	72.23(14)
Mn(1)—S(1)	2.558(14)	N(2)—Mn(1)—N(8)	92.20(14)
Mn(1)—S(2)	2.495(15)	N(8)—Mn(1)—N(3)	86.55(14)
S(1)—C(1)	1.728(5)	N(7)—Mn(1)—S(1)	115.52(10)
N(2)—C(3)	1.298(5)	N(2)—Mn(1)—S(1)	75.45(11)
N(1)—N(2)	1.375(5)	N(3)—Mn(1)—S(1)	147.38(11)
N(1)—C(1)	1.323(6)	N(8)—Mn(1)—S(1)	91.73(10)
C(1)—N(4)	1.356(6)	N(7)—Mn(1)—S(2)	76.57(10)
N(6)—N(7)	1.375(5)	N(2)—Mn(1)—S(2)	117.10(10)
N(7)—C(16)	1.292(5)	N(3)—Mn(1)—S(2)	91.35(11)
C(14)—S(2)	1.738(5)	N(8)—Mn(1)—S(2)	148.41(11)
N(6)—C(14)	1.342(5)	S(2)—Mn(1)—S(1)	106.23(5)
N(10)—C(14)	1.335(6)		
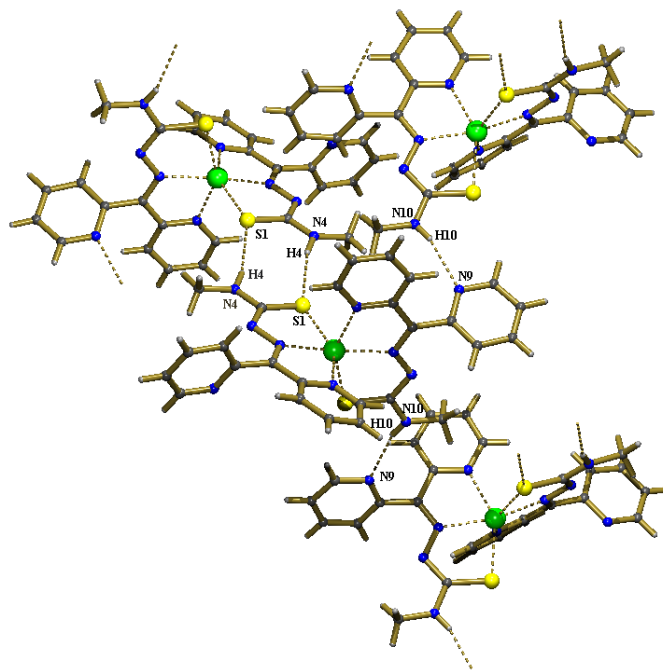
Fig. 4.15. Packing diagram of compound **3** showing H-bonding

Table 4.5. Interaction parameters of [Mn(DpyMeTsc)$_2$]

Hydrogen bonding

D—H···A	D—H (Å)	H···A (Å)	D···A (Å)	D—H···A (°)
N4(H)···S(1)	0.97	2.60	3.550	166
N10(H)···N(9)	0.83	2.28	3.100	169

(D=Donor, A=acceptor)

π-π interactions

Cg(I)···Cg(J)	Cg—Cg (Å)	α (°)	β (°)
Cg(2)···Cg(6)^a	4.023	20.76	23.74
Cg(6)···Cg(2)^b	4.023	20.76	43.30

Equivalent position codes: a = 1 + x, y, z; b = -1 + x, y, z

Cg(2) = Mn(1), S(2),C(14), N(6), N(7);

Cg(6) = N(5), C(4), C(5), C(6), C(7), C(8)

α (°) = Dihedral angle between planes I and J;

β (°) = Angle between Cg(I)-Cg(J) vector and normal to plane I.

C–H···π interaction

X—H(I)···Cg(J)	H···Cg (Å)	XH···Cg (°)	X···Cg (°)
C(19)—H(19)···Cg(1)^a	2.57	160	3.476

Equivalent position code: a = ½ + x, ½ - y, −½ + z

Cg(1) = Mn(1), S(1), C(1), N(1), N(2)

References

[1]   S. Chandra, L.K. Gupta, Spectrochim. Acta Part A 61 (2005) 2549.

[2]   K. Weighardt, Angew. Chem. Int. Ed. 28 (1989) 1153.

[3]   J.M. McCord, I. Fridovich, J. Biol. Chem. 244 (1969) 6049.

[4]   T.A. Stich, S. Lahiri, G. Yeagle, M. Dicus, M. Brynda, A. Gunn, C. Aznar, V.J. DeRose, R.D. Britt, Appl. Magn. Reson. 31 (2007) 321.

[5]   M. Bakir, O. Green, C. Gyles, Inorg. Chim. Acta 358 (2005) 1835.

[6]   M. Devereux, M. McCann, V. Leon, V. McKee, R.J. Ball, Polyhedron 21 (2002) 1063.

[7]   D. Kovala-Demertzi, U. Gangadharmath, M.A. Demertzis, Y. Sanakis, Inorg. Chem. Commun. 8 (2005) 619.

[8]   T.D. Tzima, G. Sioros, C. Duboc, D. Kovala-Demertzi, V.S. Melissas, Y. Sanakis, Polyhedron 28 (2009) 3257.

[9]   V. Philip, V. Suni, M.R.P. Kurup, M. Nethaji, Spectrochim. Acta Part A 64 (2006) 171.

[10]   V.K. Yachandra, Chem. Rev. 96 (1996) 2927.

[11]   M. Yagi, M. Kaneko, Chem. Rev. 101 (2001) 21.

[12]   G.C. Dismukes, Chem. Rev. 96 (1996) 2909.

[13]   N. Tamura, M. Ikeuchi, Y. Inoue, Biochim. Biophys. Acta 973 (1989) 281.

[14]   O. Kahn, Molecular Magnetism, VCH, New York (1993).

[15]   J.S. Miller, M. Drillon (Eds.), Magnetism: Molecules to Materials, Wiley-VCH, Weinheim (2002).

[16] Y. Kono, I. Fridovrich, J. Biol. Chem. 258 (1983) 6015.

[17] R.C. Valeutine, B.M. Shapire, E.R. Stadtman, Biochem. 7 (1968) 2143.

[18] W.J. Geary, Coord. Chem. Rev. 7 (1971) 81.

[19] F.A. Cotton, G. Wilkinson, C.A. Murillo, M. Bochmann, Advanced Inorganic Chemistry, 6th ed., Wiley, New York, 1999, pp.839.

[20] S. Renjusha, M.R.P. Kurup, Polyhedron 27 (2008) 3294.

[21] A. Sreekanth, M. Joseph, H.-K. Fun, M.R.P. Kurup, Polyhedron 25 (2006) 1408.

[22] K. Nakamoto, Infrared and Raman Spectra of Inorganic and Coordination Compounds, Part B, 5th edition, Wiley, New York, 1997.

[23] S. Chandra, L.K. Gupta, Spectrochim. Acta Part A 61 (2005) 2549.

[24] S. Chandra, G. Singh, V.P. Tyagi, S. Raizada, Synth. React. Inorg. Met. –Org. Chem. 31(10) (2001) 1759.

[25] R. Luck, R. Stosser, O.P. Poluektov, O. Ya. Grinberg, S. Ya. Lebedev, G.M. Woltermann, J.R. Wasson, Inorg. Chem. 12 (1973) 2366.

[26] E. Meirovitch, R. Poupko, J. Phys. Chem. 82 (1978) 1920.

[27] D.J.E. Ingram, Spectroscopy at Radio and Microwave Frequencies, 2nd Ed., Butterworth, London (1967).

[28] K.B. Pandeya, R. Singh, P.K. Mathur, R.P. Singh, Trans. Met. Chem. 11 (1986) 347.

[29] B.S. Garg, M.R.P. Kurup, S.K. Jain, Y.K. Bhoon, Trans. Met. Chem. 13 (1988) 92.

[30] P.F. Rapheal, E. Manoj, M.R.P. Kurup, Polyhedron 26 (2007) 5088.

[31] H. Cesur, T.K. Yazicilar, B. Bati, V.T. Yilmaz, Syntth. React. Inorg. Met. –Org. Chem. 31 (2001) 1271.

[32] G.M. Sheldrick SHELXL-97 and SHELXS-97, Program for the Solution of Crystal Structures, University of Gottingen, Germany,1997.

[33] A.L. Spek, J. Appl. Cryst. 36 (2003) 7.

[34] K. Brandenburg, Diamond Version 3.1f, Crystal Impact GbR, Bonn,Germany, 2008.

[35] H. Masui, Coord. Chem. Rev. 219 (2001) 957.

........................ॐॐॐ........................

SYNTHESES AND SPECTRAL CHARACTERIZATION OF NICKEL(II) COMPLEXES OF KETONE BASED N(4)-SUBSTITUTED THIOSEMICARBAZONES

5.1. Introduction

The redox chemistry of nickel has received considerable attention in the last few years due to its essential role in bioinorganic chemistry and the presence of nickel in several enzymes [1,2]. Nickel species in various coordination environments are of interest to inorganic biochemists, for instance, some nickel complexes of thiosemicarbazone derivatives are observed to exhibit antitumour activity [3]. The chemistry of divalent and trivalent nickel complexes with nitrogen-sulfur donor ligands has received much attention particularly since the discovery that a number of dehydrogenases contain nickel at their active sites, surrounded by more than one thiolate ligand, as well as one or two nitrogen donors [4]. Nickel(II) is also used as a spectroscopic probe in metal replacement studies of other metalloenzyme systems [5-9]. Some mono- and bis-chelated nickel complexes of di-2-pyridyl ketone derivatives of *S*-methyldithiocarbazate are observed to have antifungal and antibacterial properties [10]. Ni(II) complexes of substituted thiosemicarbazones and their di-2-pyridyl ketone derivatives have been previously reported [11].

The most common oxidation state of nickel is +2, though 0, +1, +3 and +4 Ni complexes are observed. In the divalent state, nickel exhibits wide and interesting variety of coordination numbers and stereochemistries. The most frequently encountered coordination numbers of Ni(II) are four, five and six. Four coordinate complexes may be tetrahedral or square planar. The five coordinate complexes may exhibit square pyramidal or trigonal bipyramidal geometry. Six coordinate complexes are usually octahedral. The d^8 configuration is especially prone to form four coordinate diamagnetic square planar derivatives, particularly with strong field ligands or where steric hindrance impedes higher coordination numbers. The square planar complexes are diamagnetic, while all others are paramagnetic.

This chapter focuses on the syntheses and spectral characterization of nickel(II) complexes of the two thiosemicarbazone ligands, viz., di-2-pyridyl ketone-*N*(4)-methylthiosemicarbazone (HDpyMeTsc) and di-2-pyridyl ketone-*N*(4)-ethylthiosemicarbazone (HDpyETsc).

5.2. Experimental

5.2.1. Materials

All the chemicals and solvents used for the syntheses were of analytical grade. Di-2-pyridyl ketone (Aldrich), *N*(4)-methyl thiosemicarbazide (Aldrich), *N*(4)-ethyl thiosemicarbazide (Aldrich), nickel(II) acetate tetrahydrate (C.D.H. Chemicals), nickel(II) perchlorate hexahydrate (Fluka), sodium azide (Reidel-De Haen), potassium thiocyanate (E-Merck), ethanol and methanol were used as supplied.

5.2.2. Syntheses of ligands

The ligands HDpyMeTsc and HDpyETsc were prepared as described previously in Chapter 2.

5.2.3. Syntheses of nickel(II) complexes

5.2.3a. Synthesis of [Ni(DpyMeTsc)$_2$] (7)

To a solution of HDpyMeTsc (0.542 g, 2 mmol) in hot ethanol was added a methanolic solution of nickel(II) acetate tetrahydrate (0.248 g, 1 mmol) and refluxed for 4 hours. The brown solution obtained was kept for slow evaporation. The dark brown precipitate separated out was filtered, washed with ether and dried over P$_4$O$_{10}$ *in vacuo*.

λ_m (DMF): 2 ohm^{-1} cm^2 mol^{-1}, μ_{eff} *(B.M.)*: 3.03, Elemental Anal. Found (Calcd.) (%): C: 51.61 (52.10); H: 3.73 (4.04); N: 23.34 (23.37).

5.2.3b. Synthesis of [Ni(DpyMeTsc)N$_3$] (8)

HDpyMeTsc (0.271 g, 1 mmol) was dissolved in ethanol by heating. To this solution, NaN$_3$ (0.065 g, 1 mmol) in water and nickek(II) acetate tetrahydrate (0.248 g, 1 mmol) in methanol were added and stirred the mixture for 3 hours. Brown precipitate obtained was filtered, washed with ethanol followed by ether and dried over P$_4$O$_{10}$ *in vacuo*.

λ_m (DMF): 4 ohm^{-1} cm^2 mol^{-1}, μ_{eff} *(B.M.)*: 0.42, Elemental Anal. Found (Calcd.) (%): C: 42.68 (42.08); H: 3.25 (3.26); N: 30.04 (30.20).

5.2.3c. Synthesis of [Ni(HDpyMeTsc)$_2$](ClO$_4$)$_2$ · H$_2$O (9)

HDpyMeTsc (0.271 g, 1 mmol) in hot ethanol and nickel(II) perchlorate hexahydrate (0.365 g, 1 mmol) in methanol were mixed and refluxed for 4 hours. The reaction mixture was cooled and filtered. The brown precipitate

obtained was washed with ethanol followed by ether and then dried over P_4O_{10} *in vacuo*.

λ_m (DMF): 135 ohm^{-1} cm^2 mol^{-1}, μ_{eff} *(B.M.)*: 3.07, Elemental Anal. Found (Calcd.) (%): C: 38.06 (38.16); H: 3.03 (3.45); N: 17.26 (17.12).

5.2.3d. Synthesis of [Ni(HDpyETsc)₂](ClO₄)₂ · 2H₂O (10)

HDpyETsc (0.285 g, 1 mmol) in hot ethanol and nickel(II) perchlorate hexahydrate (0.365 g, 1 mmol) in methanol were mixed and refluxed for 4 hours. The reaction mixture was cooled and filtered. The brown precipitate obtained was washed with ethanol followed by ether and then dried over P_4O_{10} *in vacuo*.

λ_m (DMF): 149 ohm^{-1} cm^2 mol^{-1}, μ_{eff} *(B.M.)*: 2.97, Elemental Anal. Found (Calcd.) (%): C: 38.91 (39.20); H: 3.96 (3.55); N: 16.20 (15.98).

5.2.3e. Synthesis of [Ni(DpyETsc)NCS] · H₂O (11)

HDpyETsc (0.285 g, 1 mmol) was dissolved in ethanol by heating. To this, an aqueous solution of KSCN (0.097 g, 1 mmol) was added dropwise and refluxed for half an hour. This was followed by the addition of methanolic solution of nickel(II) acetate tetrahydrate (0.248 g, 1 mmol) and again refluxed for 4 hours. The dark brown precipitate separated out was filtered, washed with ethanol followed by ether and dried over P_4O_{10} *in vacuo*.

λ_m (DMF): 10 ohm^{-1} cm^2 mol^{-1}, μ_{eff} (B.M.): 0, Elemental Anal. Found (Calcd.) (%): C: 38.47 (38.00); H: 3.77 (3.19); N: 16.09 (15.83).

Caution: Azide and perchlorate complexes of metals with organic ligands are potentially explosive and should be handled with care.

5.3. Results and discussion

Based on spectral and magnetic susceptibility studies, compounds **7, 9** and **10** are found to be six coordinate around the Ni(II) centers, while other compounds are four coordinate. The stoichiometries of the compounds are in agreement with the partial elemental analyses and spectral studies. In complexes **9** and **10**, the thiosemicarbazone moiety is in the thioamido form, while in all other complexes, the thiosemicarbazone deprotonate and chelate in thiolate form as evidenced by the IR spectral data. The molar conductivities of the complexes in DMF (10^{-3} M) solution were measured at 298 K with a Systronic model 303 direct-reading conductivity bridge, which suggest that complexes **9** and **10** are probably 2:1 electrolytes, while all other complexes are non-electrolytic in nature [12].

All the Ni(II) complexes are paramagnetic and the effective magnetic moments are found to be in the range 2.62 – 3.07 *B.M.* consistent with two unpaired electrons, except complexes **8** and **11**. Complex **11** is diamagnetic with $\mu_{eff} = 0$ indicating probable square planar geometry. Though square planar Ni(II) complexes are diamagnetic, weakly paramagnetic systems with low spin also have been reported [13]. The anomalous magnetic moment of 0.42 *B.M.* shown by complex **8** may be due to deviation from a perfect square planar geometry or the presence of impurity [14].

5.3.1. Infrared spectra

IR spectroscopy is a useful tool to confirm the coordination of various atoms and groups to the metal atom from the positions and natures of the bands associated with them. The characteristic IR bands of the complexes differ from their free ligands HDpyMeTsc and HDpyETsc, and provide significant

indications regarding the coordination and bonding sites of the ligands. Relevant characteristic bands of ligands and complexes are listed in Table 5.1.

A broad band around 3400 cm^{-1} in the IR spectra of complexes **9**, **10** and **11** is assigned to the –OH stretching vibrations of lattice water. The azomethine stretching vibrations are observed at 1588 and 1585 cm^{-1} in the ligands. However, in complexes these bands are shifted to lower wavenumbers as the azomethine nitrogen is coordinated to the Ni(II) centre. The shifts in the v(N–N) bands to higher frequencies also support coordination through azomethine nitrogen in all the complexes. Coordination *via* thiolate sulfur is indicated by the negative shift of the two bands assigned to v(C=S) and δ(C=S) vibrations. The new bands seen at frequencies 1589, 1572 and 1582 cm^{-1} for complexes **7**, **8** and **11** are assigned to the newly formed –C=N– moiety and this band is absent in the spectra of **9** and **10**, support the above observation. The in-plane bending vibrations of the pyridine ring in uncomplexed ligands shift to higher frequencies on complexation, confirming the coordination of ligands to the metal *via* the pyridine nitrogen [15] (Fig. 5.1).

The azido complex **8** exhibited the asymmetric v(NNN) vibration as a sharp band observed at 2052 cm^{-1}. Another band at 1350 cm^{-1} is assigned to symmetric v(NNN) of the coordinated azido group [16]. The band observed at 683 cm^{-1} in the spectrum of the complex is assigned to δ(NNN) band. The Ni–N$_{azido}$ band is observed at 421 cm^{-1} (Fig. 5.2).

The perchlorate complexes **9** and **10** show broad band around 1100 cm^{-1} and strong band at 624 cm^{-1}, indicating the presence of ionic perchlorate [17]. The band around 1100 cm^{-1} are assignable to v_3(ClO$_4$) and the unsplit band at 624 cm^{-1} is assignable to v_4(ClO$_4$) [18]. The other bands around 975 and 430

cm^{-1}, assignable to ν_1 and ν_2 vibrations of perchlorate, are very weak (Figs. 5.3 & 5.4).

Thiocyanato complex **11** has a very strong and sharp bands at 2116 and 785 cm^{-1} and several bands of low intensity near 420 cm^{-1} corresponding to ν(CN), ν(CS) and δ(NCS) modes of the thiocyanate group [19]. The intensities and positions of these bands indicate the unidentate coordination of the thiocyanate group through the sulfur atom (Fig. 5.5).

Table 5.1. IR spectral data (cm^{-1}) of thiosemicarbazones and their nickel(II) complexes

Compound	ν(C=N)	ν(C=N)^a	ν/δ(C–S)	ν(N–N)	py(ip)
HDpyMeTsc	1588	...	1431, 800	1110	618
[Ni(DpyMeTsc)₂] **(7)**	1560	1589	1384, 781	1153	640
[Ni(DpyMeTsc)N₃] **(8)**	1515	1572	1404, 784	1170	647
[Ni(HDpyMeTsc)₂](ClO₄)₂ · H₂O **(9)**	1566	...	1333, 797	1168	649
HDpyETsc	1585	...	1431, 799	1109	615
[Ni(HDpyETsc)₂](ClO₄)₂ · 2H₂O **(10)**	1560	...	1333, 772	1171	642
[Ni(DpyETsc)NCS] · H₂O **(11)**	1552	1582	1339, 741	1145	637

^{a} Newly formed C=N
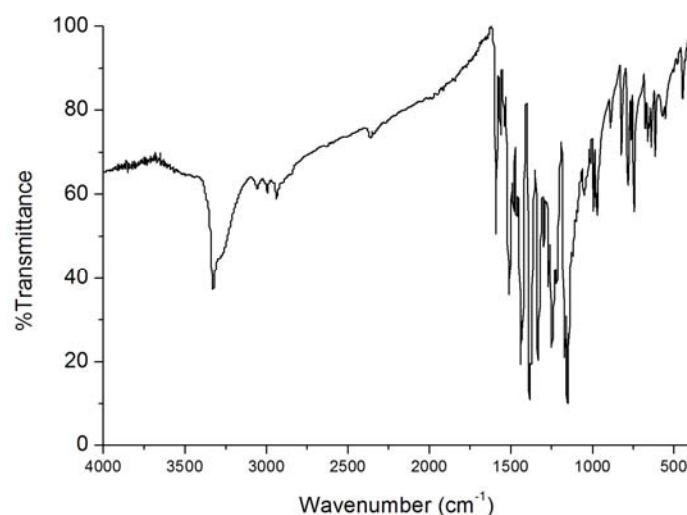
Fig. 5.1. IR spectrum of [Ni(DpyMeTsc)₂] **(7)**
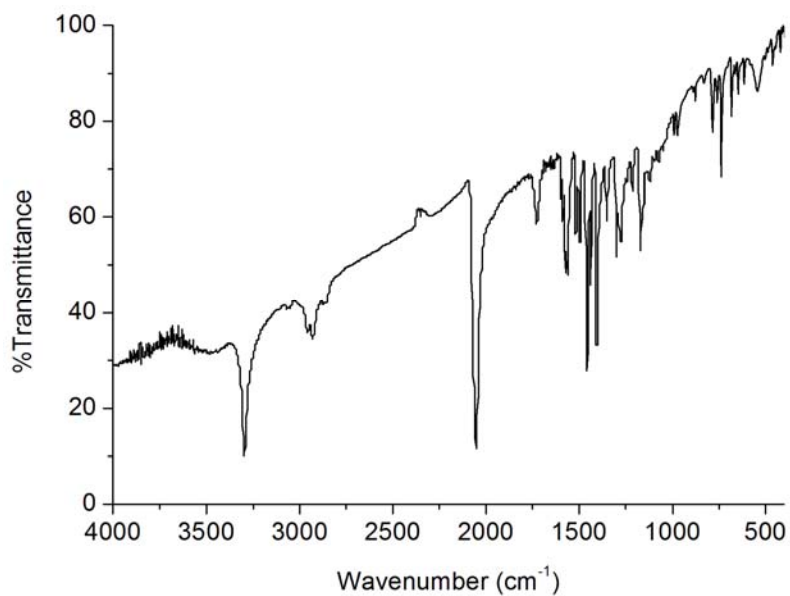
Fig. 5.2. IR spectrum of [Ni(DpyMeTsc)N$_3$] (**8**)
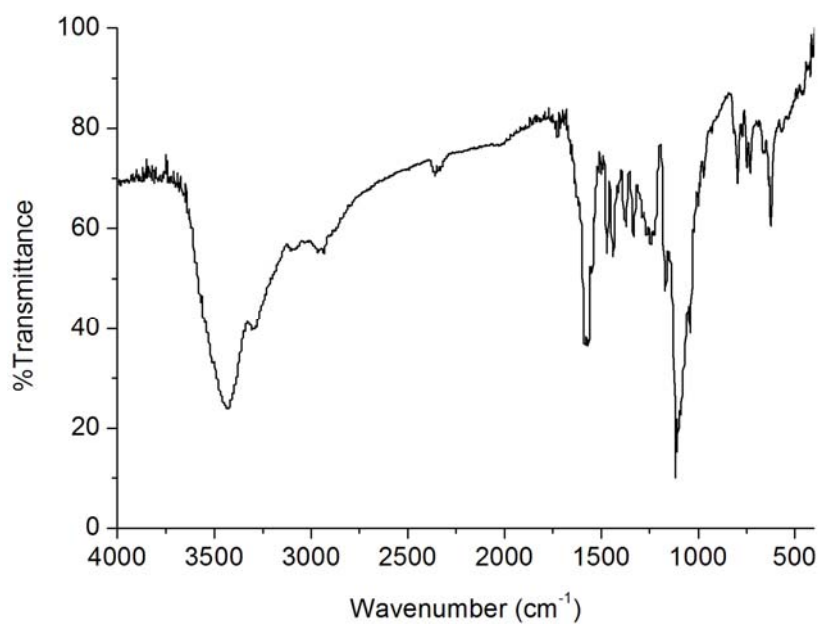
Fig. 5.3. IR spectrum of [Ni(HDpyMeTsc)$_2$](ClO$_4$)$_2$ · H$_2$O (**9**)
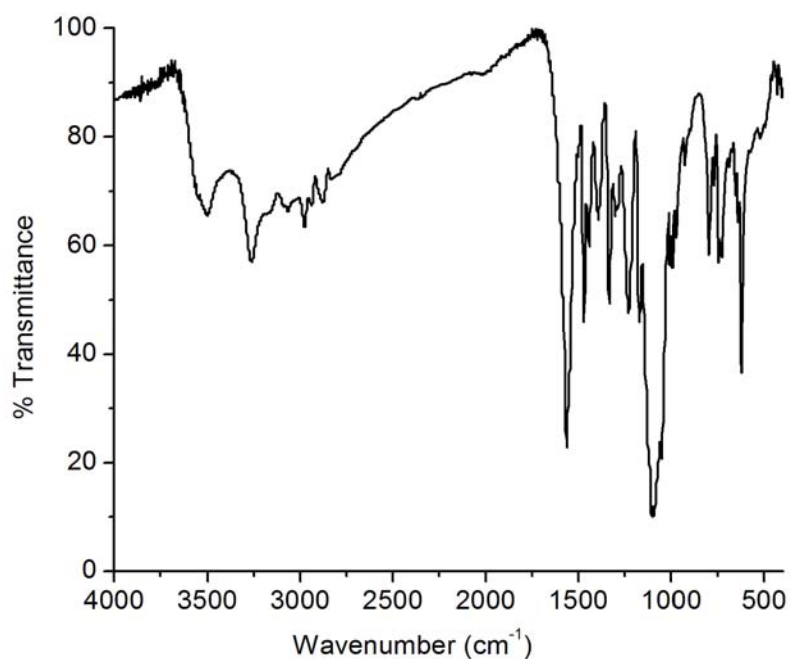
Fig. 5.4. IR spectrum of [Ni(HDpyETsc)₂](ClO₄)₂ · 2H₂O (**10**)
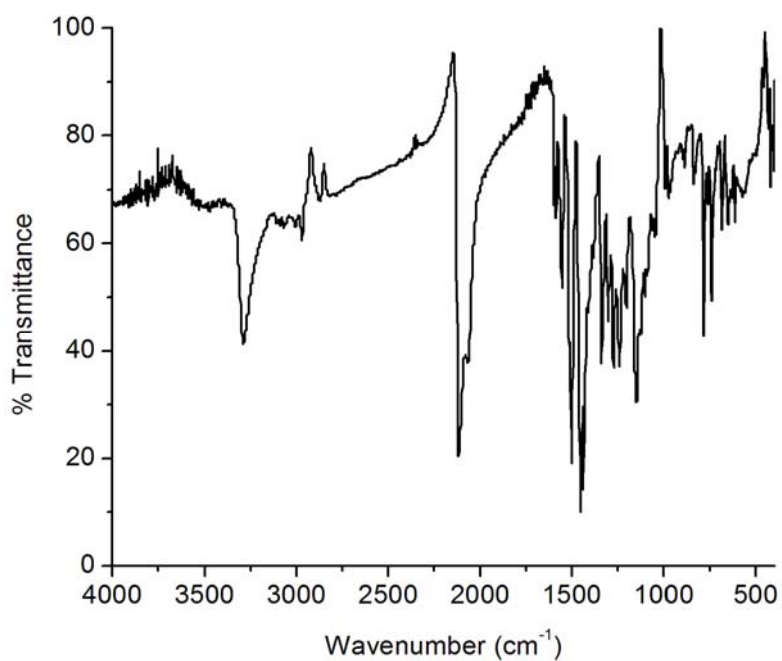
**Fig. 5.5.** IR spectrum of [Ni(DpyETsc)NCS] · H₂O (**11**)

5.3.2. Electronic spectra

The intraligand electronic transitions of HDpyMeTsc and HDpyETsc suffered considerable shift on coordination, as evidenced by the absorptions obtained for complexes. The ground state of Ni(II) in an octahedral coordination is $^3A_{2g}$ and expects three spin allowed transitions $^3T_{2g}(F) \leftarrow {}^3A_{2g}(F)(\nu_1)$, $^3T_{1g}(F) \leftarrow {}^3A_{2g}(F)(\nu_2)$ and $^3T_{1g}(P) \leftarrow {}^3A_{2g}(F)(\nu_3)$ in an increasing order of energy. However we could not locate any of these bands, probably due to masking by the high-intensity charge transfer bands [13]. For a diamagnetic Ni(II) complex, as a consequence of eight electrons being paired in the four low-lying d orbitals with the upper orbital being $d_{x^2-y^2}$, the four lower orbitals are often so close in energy that individual transitions from them to upper d level cannot be distinguished, resulting in a single absorption band. The shoulder band obtained at 17070 cm^{-1} for complex **8** may be attributed to a *d-d* band of this type. The *d-d* bands appearing as weak shoulders centered around the 20000 cm^{-1} region are typical of square-planar monoligated nickel(II) complexes [20].

The significant electronic absorption bands in the spectra of ligands and their nickel (II) complexes (Figs. 5.6–5.11) are summarized in Table 5.2. The spectra of all the compounds were recorded in acetonitrile solutions in the range 50000-20000 cm^{-1} and in DMF in the range 20000-10000 cm^{-1}.

**Table 5.2.** Electronic spectral data of thiosemicarbazones and their nickel(II) complexes

| Compound	UV-vis absorption bands (cm^{-1})			
HDpyMeTsc	35890,	29280		
[Ni(DpyMeTsc)$_2$] (**7**)	31410,	27520,	22680	
[Ni(DpyMeTsc)N$_3$] (**8**)	35740,	30770,	25350,	17070
[Ni(HDpyMeTsc)$_2$](ClO$_4$)$_2$ · H$_2$O (**9**)	35130,	30120		
HDpyETsc	35860,	29360		
[Ni(HDpyETsc)$_2$](ClO$_4$)$_2$ · 2H$_2$O (**10**)	34790,	30340,	23390	
[Ni(DpyETsc)NCS] · H$_2$O (**11**)	32250	25280		
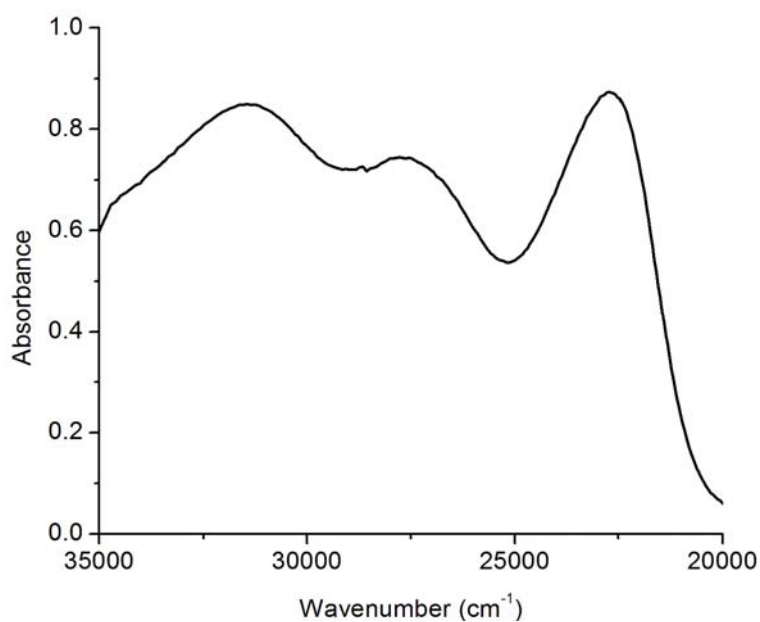
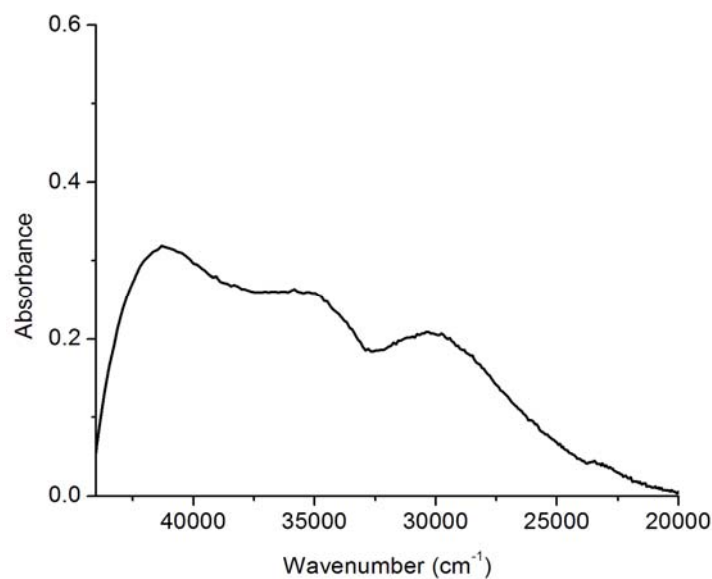**Fig. 5.6.** Electronic spectrum of [Ni(DpyMeTsc)₂] (**7**)
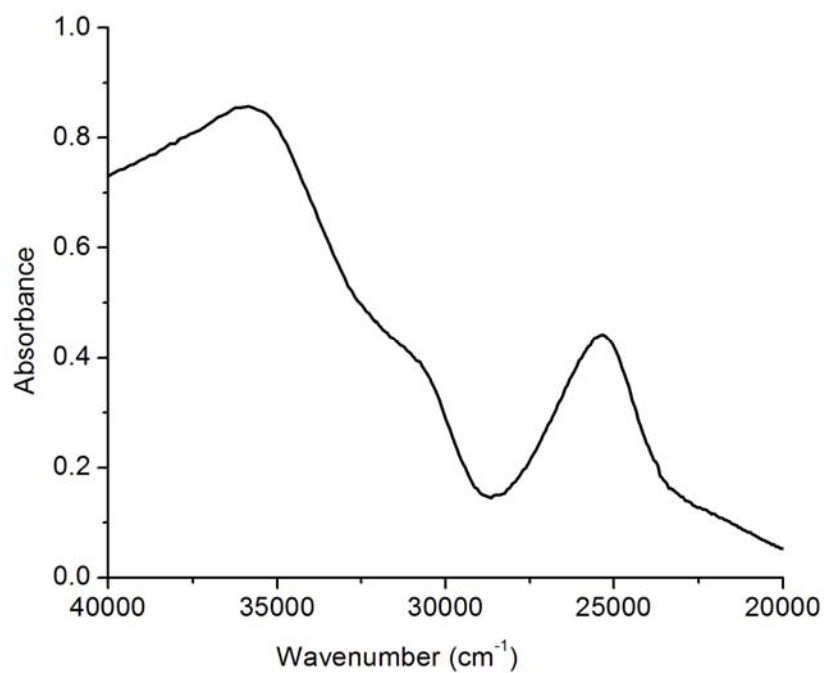
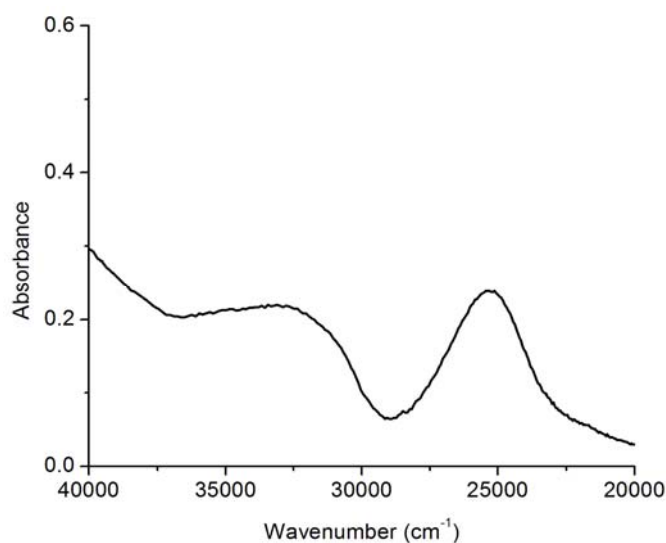**Fig. 5.7.** Electronic spectrum of [Ni(DpyMeTsc)N₃] (**8**)
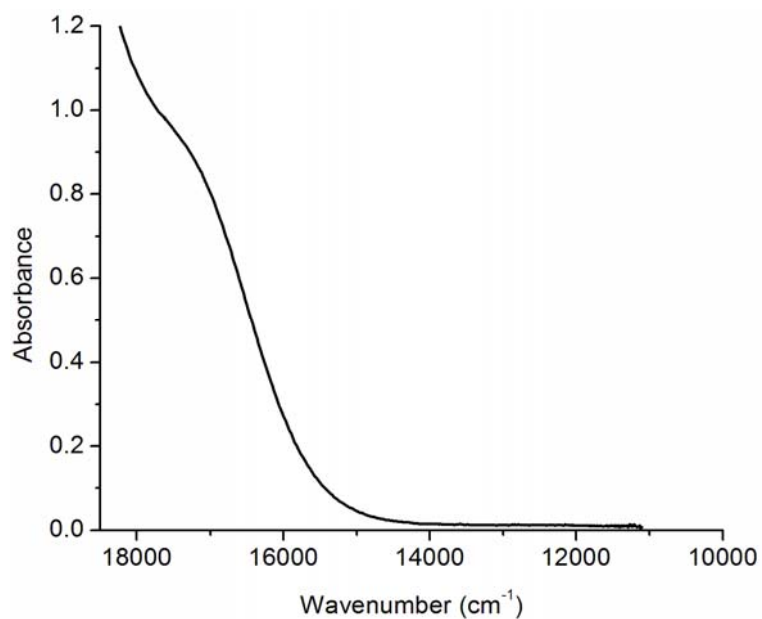
Fig. 5.8. Electronic spectrum of [Ni(DpyMeTsc)N₃] (**8**) in the visible region
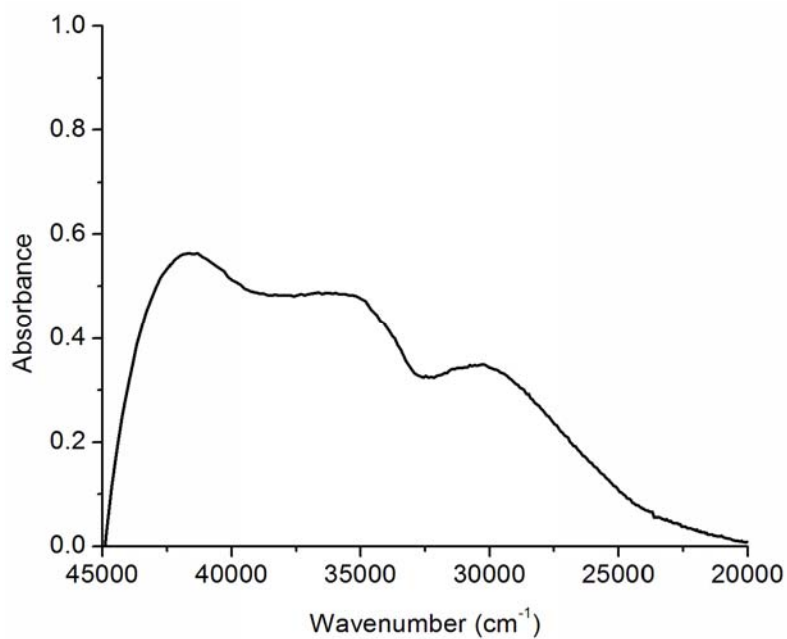
Fig. 5.9. Electronic spectrum of [Ni(HDpyMeTsc)₂](ClO₄)₂ · H₂O (**9**)

**Fig. 5.10.** Electronic spectrum of [Ni(HDpyETsc)$_2$](ClO$_4$)$_2$ · 2H$_2$O (**10**)



Fig. 5.11. Electronic spectrum of [Ni(DpyETsc)NCS] · H$_2$O (**11**)

5.3.3. Thermal analyses

TG curves are drawn as weight (mg) versus temperature (°C). For complex **7**, no weight loss upto 250 °C, suggest that there is no water molecules

inside or outside the coordination sphere. Complex **11** showed weight loss in the range 50-130 °C, suggest that water molecule is outside the coordination sphere [21,22]. Both complexes are thermally stable and decomposition of ligand starts around 300 °C. TG-DTG curves of complexes **7** and **11** are shown in Figs 5.12 and 5.13 respectively.
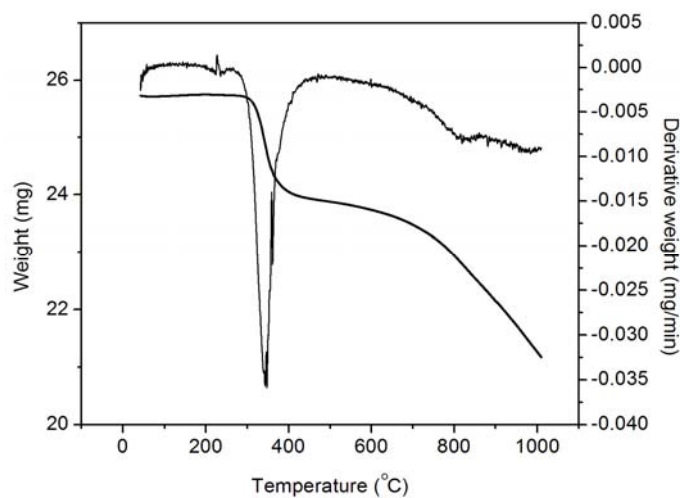
Fig. 5.12. TG-DTG curve of complex **7**
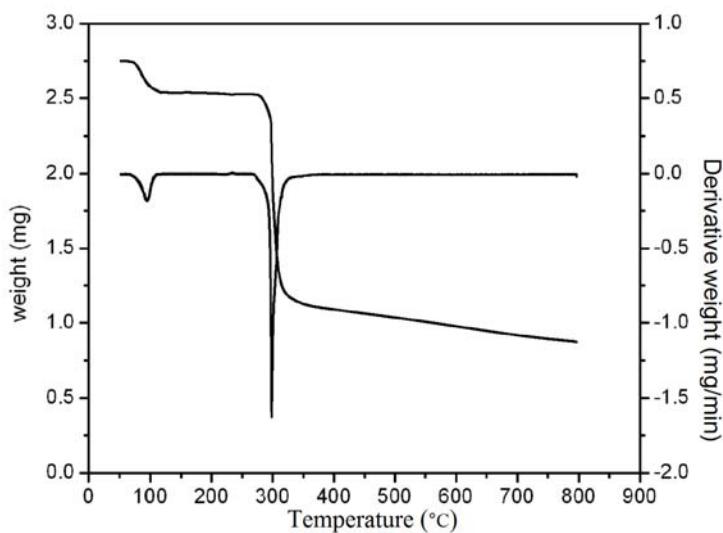
Fig. 5.13. TG-DTG curve of complex **11**

References

[1]   A.F. Kolodziej, Prog. Inorg. Chem. 41 (1994) 493.

[2]   D.X. West, H. Gebremedhin, R.J. Butcher, J.P. Jasinski, A.E. Liberta, Polyhedron 12 (1993) 2489.

[3]   M. Wang, L.-F. Wang, Y.-Z. Li, Q.-X. Li, Z.-D. Xu, D.-M. Qu, Transit. Met. Chem. 26 (2001) 307.

[4]   S.K. Chattopadhyay, D. Chattopadhyay, T. Banerjee, R. Kuroda, S. Gosh, Polyhedron 16 (1997) 1925.

[5]   R. Cammack, D.S. Patil, E.C. Hatchikian, V.M. Fernande, Biochem. Biophys. Acta 98 (1987) 912.

[6]   D.L. Tennent, R.D. McMillin, J. Am. Chem. Soc. 101 (1979) 2307.

[7]   V. Lum, H.B. Gray, Isr. J. Chem. 21 (1981) 23.

[8]   H.R. Engeseth, D.R. McMillin, E.L. Ulrich, Inorg. Chim. Acta 67 (1982) 145.

[9]   J.A. Blaszak, E.L. Ulrich, J.L. Markley, D.R. McMillin, Biochemistry 21 (1981) 6253.

[10]   M.A. Ali, A.H. Mirza, M. Nazimuddin, H. Rahman, R.J. Butcher, Transit. Met. Chem. 27 (2002) 268.

[11]   V. Suni, M.R.P. Kurup, M. Nethaji, Polyhedron 26 (2007) 3097.

[12]   W.J. Geary, Coord. Chem. Rev. 81 (1971).

[13]   M. Mathew, G.J. Palenik, G.R. Clark, J. Inorg. Chem. 12 (1973) 446.

[14]   E. Manoj, M.R.P. Kurup, Polyhedron 27 (2008) 275.

[15]   K. Nakamoto, Infrared and Raman Spectra of Inorganic and Coordination Compounds, Part B, 5th edition, Wiley, New York, 1997.

[16]   M. Joseph, V. Suni, M.R.P. Kurup, M. Nethaji, A. Kishore, S.G. Bhat, Polyhedron 23 (2004) 3069**.**

[17]   B.S. Garg, M.R.P. Kurup, S.K. Jain, Y.K. Bhoon, Transit. Met. Chem. 13 (1988) 92.

[18]   F. Hueso-Urena, A.L. Penas-Chamorro, M.N. Moreno-Carretero, J.M. Amigo, V. Esteve, T. Debaerdemaekar, Polyhedron 18 (1999) 2205.

[19]   K.B. Yatsimirskii, Pure and Appl. Chem. 49 (1977) 115.

[20]   M. Akbar Ali, G. Hossain, S.M.M.H. Majumder, M. Nazimuddin, M.T.H. Tarafder, Polyhedron 6 (1987) 1653**.**

[21]   M.R. Maurya, N. Bharti, Transit. Met. Chem. 24 (1999) 389.

[22]   S.M. Abdallah, G.G. Mohamed, M.A. Zayed, M.S. Abou El-Ela, Spectrochim. Acta Part A 73 (2009) 833.

........................≪≪≪........................

SYNTHESES, SPECTRAL AND STRUCTURAL CHARACTERIZATION OF COPPER(II) COMPLEXES OF KETONE BASED N(4)-SUBSTITUTED THIOSEMICARBAZONES

6.1. Introduction

Copper has continued to be one of man's most important metal. Copper is an essential trace element for life processes, and several copper-containing proteins have been identified [1]. It is widely distributed in the plant and animal worlds, and its redox chemistry is involved in a variety of oxidation processes.

Since the late 1980s, the study of mono- and dinuclear copper(II) complexes has attracted considerable attention, due to the relevance of Cu(II) in biological systems. There have been several attempts to model the active centre of biological molecules that include two metal copper atoms on their structure, such as haemocyanin or other biological proteins [2]. Copper (II) complexes have been found to be possible medical uses in the treatment of many diseases including cancer [3].

The coordination chemistry of copper (II) has developed very rapidly over the last four decades due to a number of reasons. From the standpoint of bioinorganic chemistry, copper(II) coordination complexes have been used for the modelling of active sites in copper(II) biomolecules [4], while from the

perspective of magneto-chemistry dinuclear complexes of this ion have been synthesized to establish magneto-structural correlations [5-10], and trinuclear complexes have got attention in order to study spin frustration and antisymmetric exchange phenomena, as well as for the rational synthesis of ferromagnetic entities [11-13]. Copper(II) polynuclear complexes with aesthetically pleasing structures and interesting magnetic properties are a hot topic in current research.

Common oxidation states of copper include the less stable copper(I) state (d^{10}) and the more stable copper(II) state (d^9). The most common oxidation state of copper is +2 and Cu (II) complexes have been extensively studied. Cu(II) ions readily form coordination complexes involving coordination numbers 4, 5 and 6 with tetrahedral, square planar, trigonal bipyramidal, square pyramidal, octahedral and distorted octahedral geometries [14]. Regular geometries are rare and the distinction between square planar and tetragonally distorted octahedral coordination is generally not easily made. The reason for this is ascribed to the Jahn-Teller effect arising from the unequal occupation of the e_g pair of orbitals ($d_z{}^2$ and $d_x{}^2{}_{-y}{}^2$) when a d^9 ion is subjected to an octahedral crystal field.

It has been reported that copper(II) complexes of heterocyclic N(4)-substituted thiosemicarbazones exercise bio-activity through a mechanism involving either inhibition of the enzyme ribonucleotide reductase, or creation of lesions in DNA strands. Studies have also shown that, for these ligands, nature of substitution on the terminal N(4) atom is crucial for the antifungal activity [15]. This chapter presents the optimal conditions for the syntheses of eleven copper(II) complexes with the two ligands, di-2-pyridyl ketone-*N*(4)-methylthiosemicarbazone (HDpyMeTsc) and di-2-pyridyl ketone-*N*(4)-ethylthiosemicarbazone (HDpyETsc) and their characterization by

physicochemical methods, together with X-ray crystal structure of one of the copper complexes, viz. $[Cu_3(DpyETsc)_2(NO_3)_4(H_2O)_2] \cdot H_2O$.

6.2. Experimental

6.2.1. Materials

All the chemicals and solvents used for the syntheses were of analytical grade. Di-2-pyridyl ketone (Aldrich), *N*(4)-methylthiosemicarbazide (Aldrich), *N*(4)-ethylthiosemicarbazide (Aldrich), copper(II) nitrate trihydrate (S.D.Fine-chemicals Ltd), copper(II) acetate monohydrate (E-Merk), copper(II) chloride dihydrate (E-Merck), copper(II) sulphate pentahydrate (E-Merk), copper(II) perchlorate hexahydrate (Aldrich), sodium azide (Reidel-De Haen), potassium thiocyanate (E-Merck), ethanol and methanol were used as supplied.

6.2.2. Syntheses of ligands

The syntheses of thiosemicarbazone ligands, HDpyMeTsc and HDpyETsc are described already in Chapter 2.

6.2.3. Syntheses of copper(II) complexes of di-2-pyridyl ketone-*N*(4)-methyl thiosemicarbazone

6.2.3a. Synthesis of [Cu(HDpyMeTsc)(NO₃)₂] · 4H₂O (12)

To a solution of the ligand, HDpyMeTsc (0.271 g, 1 mmol) in hot ethanol, was added a solution of $Cu(NO_3)_2 \cdot 3H_2O$ (0.241 g, 1 mmol) in methanol. The mixture was refluxed for 4 hours and allowed to stand at room temperature. Dark green precipitate obtained was washed with ethanol followed by ether and dried over P_4O_{10} *in vacuo*.

λ_m (DMF): 10 ohm⁻¹ cm² mol⁻¹, μ_{eff} (B.M.): 1.98, Elemental Anal. Found (Calcd.) (%): C: 29.57 (29.41); H: 3.51 (3.99); N: 18.20 (18.47).

6.2.3b. Synthesis of [Cu₂(DpyMeTsc)₂SO₄] · 3H₂O (13)

HDpyMeTsc (0.271 g, 1 mmol) was dissolved in ethanol by heating. To this solution, $CuSO_4 \cdot 5H_2O$ (0.249 g, 1 mmol) in methanol was added and refluxed for 4 hours. Green precipitate obtained was filtered, washed with ethanol followed by ether and dried over P_4O_{10} *in vacuo*.

λ_m (DMF): 2 ohm^{-1} cm^2 mol^{-1}, μ_{eff} (B.M.): 1.37, Elemental Anal. Found (Calcd.) (%): C: 38.10 (38.18); H: 3.63 (3.70); N: 17.54 (17.13).

6.2.3c. Synthesis of [Cu(DpyMeTsc)N₃] · H₂O (14)

HDpyMeTsc (0.271 g, 1 mmol) was dissolved in ethanol by heating. To this solution, NaN_3 (0.065 g, 1 mmol) in water and $Cu(OAc)_2 \cdot H_2O$ (0.199 g, 1 mmol) in hot methanol were added and stirred the mixture for 3 hours. Green precipitate obtained was filtered, washed with ethanol followed by ether and dried over P_4O_{10} *in vacuo*.

λ_m (DMF): 5 ohm^{-1} cm^2 mol^{-1}, μ_{eff} (B.M.): 1.80, Elemental Anal. Found (Calcd.) (%): C: 40.30 (39.64); H: 3.30 (3.58); N: 28.76 (28.45).

6.2.3d. Synthesis of [Cu₂(DpyMeTsc)₂](ClO₄)₂ · 2H₂O (15)

A methanolic solution of $Cu(ClO_4)_2 \cdot 6H_2O$ (0.370 g, 1 mmol) was added to a solution of ligand, HDpyMeTsc (0.271 g, 1 mmol) in hot ethanol. The mixture was refluxed for 4 hours and the dark green precipitate obtained was filtered, washed with ethanol followed by ether and dried over P_4O_{10} *in vacuo*.

λ_m (DMF): 166 ohm^{-1} cm^2 mol^{-1}, μ_{eff} (B.M.): 1.45, Elemental Anal. Found (Calcd.) (%): C: 34.45 (34.59); H: 2.65 (3.13); N: 15.83 (15.52).

6.2.3e. Synthesis of [Cu(DpyMeTsc)(CH₃COO)] · 2H₂O (16)

HDpyMeTsc (0.271 g, 1 mmol) was dissolved in ethanol by heating. To this solution, $Cu(OAc)_2 \cdot H_2O$ (0.199 g, 1 mmol) in hot methanol was added and refluxed the solution for 4 hours. Dark green precipitate obtained was cooled and filtered. It is then washed with ethanol followed by ether and dried over P_4O_{10} *in vacuo*.

λ_m (DMF): 6 ohm^{-1} cm^2 mol^{-1}, μ_{eff} (B.M.): 1.75, Elemental Anal. Found (Calcd.) (%): C: 42.40 (42.00); H: 4.14 (4.46); N: 16.63 (16.33).

6.2.4. Syntheses of copper(II) complexes of di-2-pyridyl ketone-*N*(4)-ethyl thiosemicarbazone

6.2.4a. Synthesis of [Cu₃(DpyETsc)₂(NO₃)₄(H₂O)₂] · H₂O (17)

To a solution of the ligand, HDpyETsc (0.285 g, 1 mmol) in hot ethanol, was added a solution of $CuNO_3 \cdot 3H_2O$ (0.241 g, 1 mmol) in methanol. The mixture was refluxed for 4 hours and allowed to stand at room temperature. The green crystalline precipitate formed was filtered, washed with ethanol followed by ether and dried over P_4O_{10} *in vacuo*.

λ_m (DMF): 11 ohm^{-1} cm^2 mol^{-1}, μ_{eff} (B.M.): 0.85, Elemental Anal. Found (Calcd.) (%): C: 31.68 (31.09); H: 3.23 (3.11); N: 18.47 (18.38).

6.2.4b. Synthesis of [Cu₂(DpyETsc)₂SO₄]₂ · 4H₂O (18)

HDpyETsc (0.285 g, 1 mmol) was dissolved in ethanol by heating. To this solution, $CuSO_4 \cdot 5H_2O$ (0.249 g, 1 mmol) in methanol was added and refluxed the solution for 4 hours. Dark green precipitate obtained was cooled and filtered. It is then washed with ethanol followed by ether and dried over P_4O_{10} *in vacuo*.

λ_m (DMF): 9 ohm^{-1} cm^2 mol^{-1}, μ_{eff} (B.M.): 1.35, Elemental Anal. Found (Calcd.) (%): C: 40.00 (40.62); H: 3.25 (3.90); N: 16.83 (16.92).

6.2.4c. Synthesis of [Cu(DpyETsc)N₃]₂ · 2 H₂O (19)

HDpyETsc (0.285 g, 1 mmol) was dissolved in ethanol by heating. To this solution, NaN$_3$ (0.065 g, 1 mmol) in water and Cu(OAc)$_2$ · H$_2$O (0.199 g, 1 mmol) in hot methanol were added and stirred the mixture for 3 hours. Dark green precipitate obtained was filtered, washed with ethanol followed by ether and dried over P$_4$O$_{10}$ *in vacuo*.

λ_m (DMF): 6 ohm^{-1} cm^2 mol^{-1}, μ_{eff} (B.M.): 1.64, Elemental Anal. Found (Calcd.) (%): C: 41.03 (41.22); H: 3.70 (3.95); N: 27.41 (27.47).

6.2.4d. Synthesis of [Cu₂(DpyETsc)₂](ClO₄)₂ · H₂O (20)

A methanolic solution of Cu(ClO$_4$)$_2$ · 6H$_2$O (0.370 g, 1 mmol) was added to a solution of ligand, HDpyETsc (0.285 g, 1 mmol) in hot ethanol. The mixture was refluxed for 4 hours and the green precipitate obtained was filtered, washed with ethanol followed by ether and dried over P$_4$O$_{10}$ *in vacuo*.

λ_m (DMF): 155 ohm^{-1} cm^2 mol^{-1}, μ_{eff} (B.M.): 1.25, Elemental Anal. Found (Calcd.) (%): C: 36.56 (36.85); H: 2.93 (3.31); N: 15.44 (15.35).

6.2.4e. Synthesis of [Cu(DpyETsc)Cl]₂ · H₂O (21)

HDpyETsc (0.285 g, 1 mmol) was dissolved in ethanol by heating. To this solution, CuCl$_2$ · 2H$_2$O (0.170 g, 1 mmol) in hot methanol was added and refluxed the solution for 4 hours. Then it is cooled and filtered. The dark brown precipitate of **21** was washed with ethanol followed by ether and then dried over P$_4$O$_{10}$ *in vacuo*.

λ_m (DMF): 10 ohm^{-1} cm^2 mol^{-1}, μ_{eff} (B.M.): 1.29, Elemental Anal. Found (Calcd.) (%): C: 42.38 (42.86); H: 3.27 (3.85); N: 17.88 (17.85).

6.2.4f. Synthesis of [Cu(DpyETsc)(NCS)]$_2$ (22)

HDpyETsc (0.570 g, 2 mmol) was dissolved in ethanol by heating. To this, an aqueous solution of KSCN (0.097 g, 1 mmol) was added dropwise and stirred for half an hour. This was followed by the addition of methanolic solution of Cu(CH$_3$COO)$_2$ · H$_2$O (0.199 g, 1 mmol) and again stirred for 2 hours. The dark green precipitate separated out was filtered, washed with ethanol followed by ether and dried over P$_4$O$_{10}$ *in vacuo*.

λ_m (DMF): 18 ohm^{-1} cm^2 mol^{-1}, μ_{eff} (B.M.): 1.21, Elemental Anal. Found (Calcd.) (%): C: 44.00 (44.38); H: 3.11 (3.48); N: 20.63 (20.70).

Caution: Although no problems were encountered during this research, azide and perchlorate salts of metal complexes with organic ligands are potentially explosive. So they should be prepared in small quantities and handled with care.

6.3. Results and discussion

Eleven copper(II) complexes of thiosemicarbazones were prepared. The green and brown colors are common to complexes involving thiosemicarbazone coordination due to the sulfur-to-metal charge-transfer bands, which dominate their visible spectra [16]. In all complexes, except complex **12,** thiosemicarbazone deprotonates and chelates in thiolate form as evidenced by the IR spectra. In complex **12,** the thiosemicarbazone is in the thioamido form.

The molar conductance of the complexes in DMF (10^{-3} M) solution were measured at 298 K with a Systronic model 303 direct-reading conductivity bridge, which showed that compounds **15** and **20** are 2:1 electrolytes while all other complexes are non-electrolytic in nature. The magnetic moments of the

complexes were calculated from the magnetic susceptibility measurements at room temperature. The effective magnetic moment (μ_{eff}) values for the mononuclear copper(II) complexes (d^9 system) were found to be close to the spin only value, which corresponds to a single unpaired electron. The low magnetic moment values for some complexes may be due to some interaction between metal centers.

6.3.1. Infrared spectra

The characteristic IR bands of the complexes differ from their free ligands, and provide significant indications regarding the coordination and bonding sites of the ligands. The selected IR bands of ligands and complexes along with their tentative assignments are listed in Table 6.1. The strong bands at 3263 and 3199 cm^{-1} in the spectra of ligands have been assigned to $\nu(^4\text{N–H})$ vibrations. In the spectra of complexes, these bands shift to both higher and lower energies, suggesting differences in hydrogen bonding of N(4)H between the uncomplexed and complexed thiosemicarbazones [17, 18].

On coordination of the azomethine nitrogen, $\nu(\text{C=N})$ bands around 1590 cm^{-1} in uncomplexed thiosemicarbazones shift to lower wavenumbers in the spectra of all complexes. The bonding of the imine nitrogen as one of the coordinating sites is further confirmed by the presence of bands around 400 cm^{-1} assigned to a $\nu(\text{Cu–N})$ vibrations for these complexes [19]. The increase for the $\nu(\text{N–N})$ frequency in the spectra of the complexes is probably due to enhanced double bond character through chelation, thus offsetting the loss of electron density *via* donation to the metal atom, and is supportive of azomethine nitrogen coordination [18]. For complexes containing the anionic ligands, a

second band due to newly formed –C=N– moiety is often found. This indicates that the ligand enolizes and coordinates in the thiolate form. Coordination *via* thiolate sulfur is also indicated by the downward shift of frequencies of *v/δ*(CS) bands. The in-plane bending vibrations of the pyridine ring in uncomplexed ligands shift to higher frequencies on complexation, confirming the coordination of ligands to the metal *via* the pyridine nitrogen (Figs. 6.1–6.11).

It is rather very difficult to differentiate the coordination modes of nitrato anion by IR spectroscopy. According to Gatehouse *et al*., for nitrato complexes, the unidentate and bidentate NO_3 groups exhibit three NO stretching bands. The separation of the two highest-frequency bands is greater for the bidentate than for the monodentate nitrate group. We found that the compound **12** exhibits three strong bands at 1384, 1277 and 1036 cm^{-1} corresponding to stretching bands of the nitrato group indicating the presence of a terminal monodentate coordination of the nitrato group [20]. The fact that the nitrato group is terminally bonded is understood from the separation of 107 cm^{-1} between two highest-frequency bands just mentioned above. The spectrum of **17** exhibits bands at 1384, 1275 and 1036 cm^{-1} with a separation of 109 cm^{-1} between two highest-frequency bands, indicating the presence of monodentate nitrato ion. Also, in the spectrum we can find stretching bands of the nitrato group with a separation of 251 cm^{-1} between two highest-frequency bands. It shows that bidentate nitrato group is also present in this complex.

Table 6.1. IR spectral data (cm^{-1}) of thiosemicarbazones and their copper(II) complexes

Compound	v(C=N)	v(C=N)^a	v/δ(C–S)	v(N–N)	py(ip)
HDpyMeTsc	1588	...	1431, 800	1110	618
[Cu(HDpyMeTsc)(NO$_3$)$_2$] · 4H$_2$O (**12**)	1523	...	1328, 792	1161	629
[Cu$_2$(DpyMeTsc)$_2$SO$_4$] · 3H$_2$O (**13**)	1537	1595	1388, 791	1146	652
[Cu(DpyMeTsc)N$_3$] · H$_2$O (**14**)	1524	1586	1340, 790	1163	648
[Cu$_2$(DpyMeTsc)$_2$](ClO$_4$)$_2$ · 2H$_2$O (**15**)	1534	1602	1388, 790	1160	655
[Cu(DpyMeTsc)(CH$_3$COO)] · 2H$_2$O (**16**)	1537	1594	1383, 787	1164	669
HDpyETsc	1585	...	1431, 799	1109	615
[Cu$_3$(DpyETsc)$_2$(NO$_3$)$_4$(H$_2$O)$_2$] · H$_2$O (**17**)	1524	1570	1416, 796	1157	635
[Cu$_2$(DpyETsc)$_2$SO$_4$]$_2$ · 4H$_2$O (**18**)	1525	1592	1337, 785	1157	686
[Cu(DpyETsc)N$_3$]$_2$ · 2H$_2$O (**19**)	1517	1590	1401, 788	1118	652
[Cu$_2$(DpyETsc)$_2$](ClO$_4$)$_2$ · H$_2$O (**20**)	1518	1599	1307, 788	1168	623
[Cu(DpyETsc)Cl]$_2$ · H$_2$O (**21**)	1518	1593	1333, 783	1152	644
[Cu(DpyETsc)(NCS)]$_2$ (**22**)	1512	1593	1338, 781	1130	666

^{a} Newly formed C=N
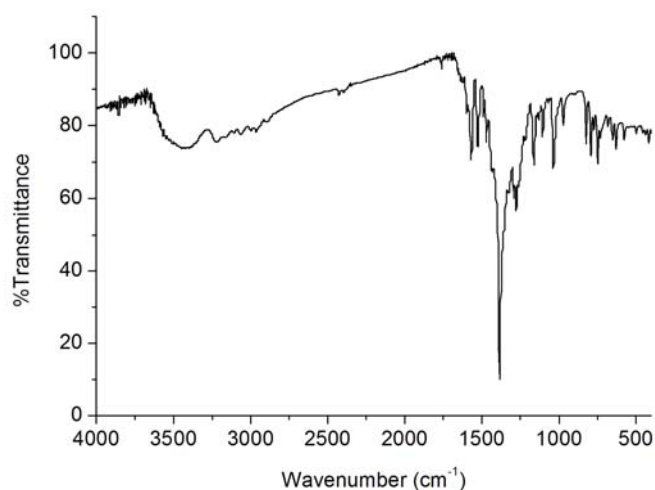
Fig. 6.1. IR spectrum of [Cu(HDpyMeTsc)(NO$_3$)$_2$] · 4H$_2$O (**12**)
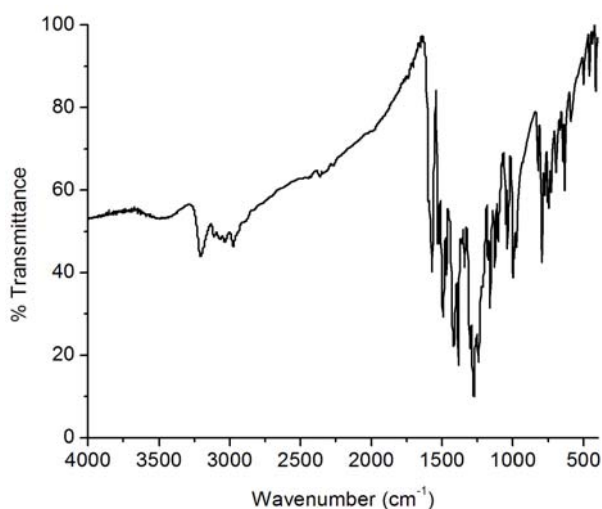
Fig. 6.2. IR spectrum of $[Cu_3(DpyETsc)_2(NO_3)_4(H_2O)_2] \cdot H_2O$ **(17)**

The free sulfate ion belongs to the high-symmetry point group T_d. It shows four fundamental vibrations, of these only v_3 and v_4 are infrared-active. If the symmetry of the ion is lowered by complex formation, the degenerate vibrations split and Raman-active modes appear in the infrared spectrum. On complexation the symmetry is lowered to C_{2v} for bidentate complexes. In bidentate complexes v_1 and v_2 appear with medium intensity, and v_3 and v_4, each split into three bands. It was found that both sulfato complexes **13** and **18** exhibit four fundamental vibrations. Bands at ~975 cm^{-1} due to v_1 and medium bands around 450 cm^{-1} due to v_2. Strong bands at 1164, 1106 and 1032 cm^{-1} corresponding to v_3 for complex **13** and at 1181, 1120 and 1035 cm^{-1} for complex **18**. The v_4 bands are found in the region 580-610 cm^{-1} for the two complexes. Thus sulfato groups in the complexes are concluded to be bridging bidentate in nature [21].
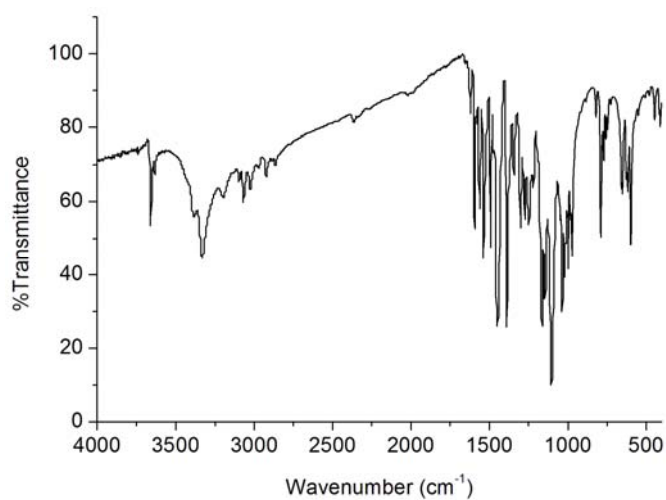
**Fig. 6.3.** IR spectrum of [Cu$_2$(DpyMeTsc)$_2$SO$_4$] · 3H$_2$O (**13**)
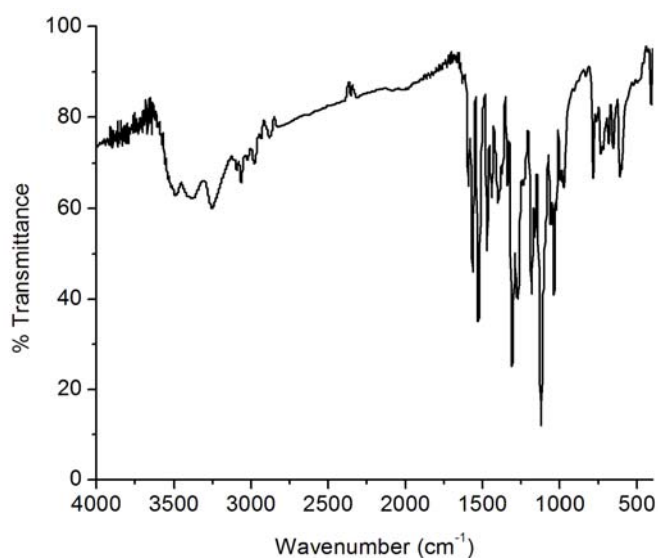
Fig. 6.4. IR spectrum of [Cu$_2$(DpyETsc)$_2$SO$_4$]$_2$ · 4H$_2$O (**18**)

The azido complexes **14** and **19** showed sharp bands at 2060 and 2051 cm^{-1} respectively due to asymmetric ν(N$_3$) mode of the coordinated azido group. The bands associated with the symmetric ν(N$_3$) modes are located at 1396 and 1378 cm^{-1} respectively. The broad band observed at 680 cm^{-1} for **14** and 687 cm^{-1} for **19** are assigned to δ(N–N–N) vibrations.
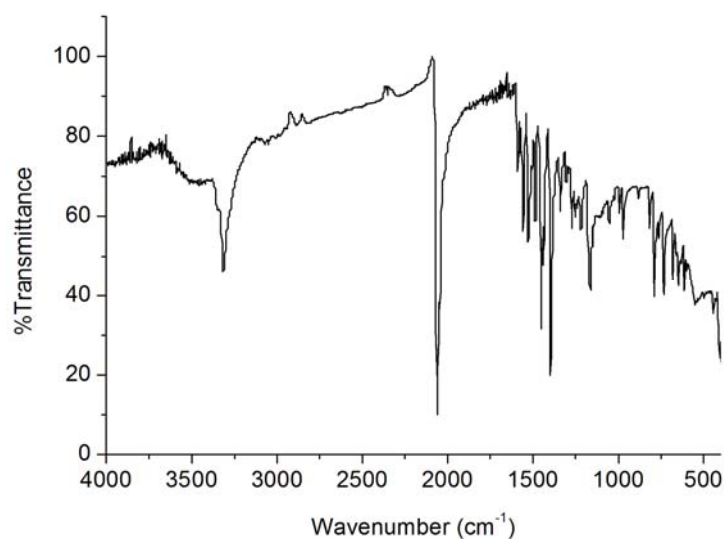
Fig. 6.5. IR spectrum of [Cu(DpyMeTsc)N$_3$] · H$_2$O (**14**)
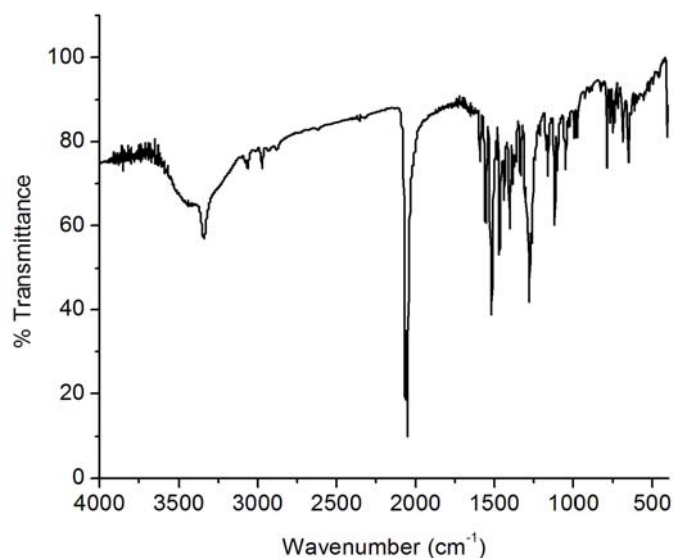
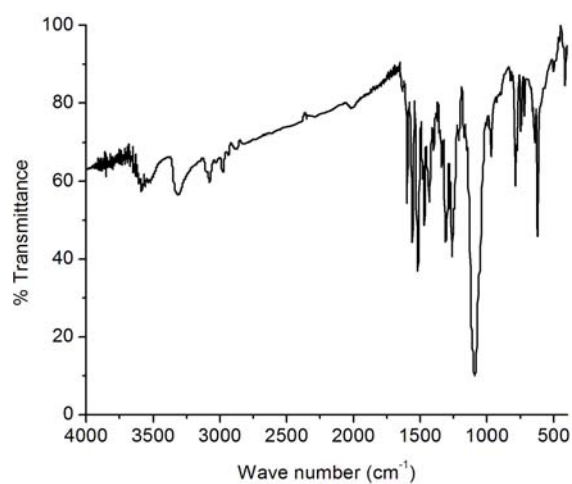**Fig. 6.6.** IR spectrum of [Cu(DpyETsc)N$_3$]$_2$ · 2H$_2$O (**19**)

The perchlorate complexes **15** and **20** showed single broad band around 1090 cm^{-1} and strong band at 623 cm^{-1}, indicating the presence of ionic perchlorate. The band around 1090 cm^{-1} are assignable to ν_3(ClO$_4$) and the unsplit band at 623 cm^{-1} are assignable to ν_4(ClO$_4$). Also in the spectrum of the

compounds, medium band around 965 cm^{-1} may be due to $\nu_1(ClO_4)$ suggesting the presence of ionic perchlorate group [22].

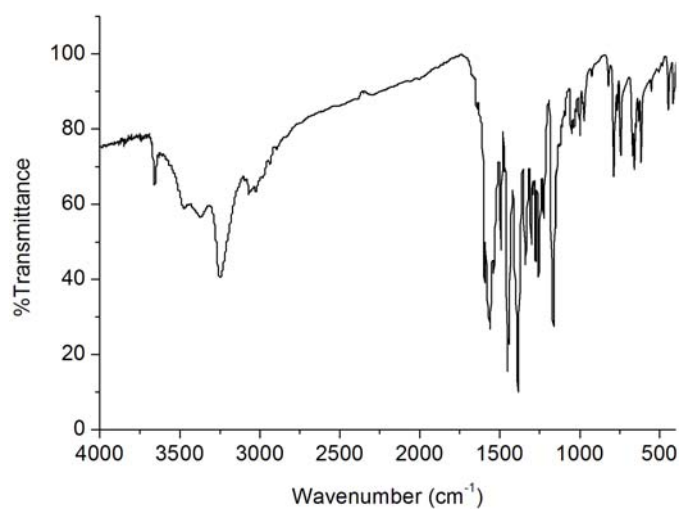The spectrum of the acetate-containing complex **16** displayed relatively strong bands at 1560 [ν_a(COO)] and 1339 cm^{-1} [ν_s(COO)] support the unidentate nature of the acetate group in this compound [23].
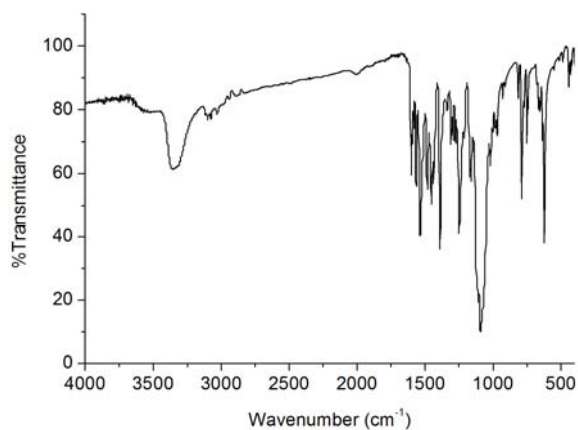
Fig. 6.7. IR spectrum of [Cu$_2$(DpyMeTsc)$_2$](ClO$_4$)$_2$ · 2H$_2$O (**15**)

Fig. 6.8. IR spectrum of [Cu$_2$(DpyETsc)$_2$](ClO$_4$)$_2$ · H$_2$O (**20**)

Fig. 6.9. IR spectrum of [Cu(DpyMeTsc)(CH$_3$COO)] · 2H$_2$O (**16**)

Thiocyanato complex **22** has a very strong and sharp band at 2075 cm^{-1} and a medium band at 781 cm^{-1} corresponding to v(CN) and v(CS) modes of the NCS group. The intensities and positions of these bands indicate the unidentate coordination of the thiocyanate group through the nitrogen atom [24].
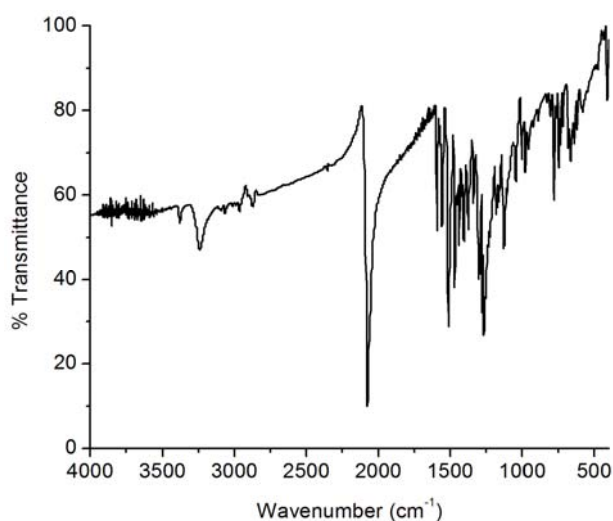
Fig. 6.10. IR spectrum of [Cu(DpyETsc)(NCS)]$_2$ (**22**)
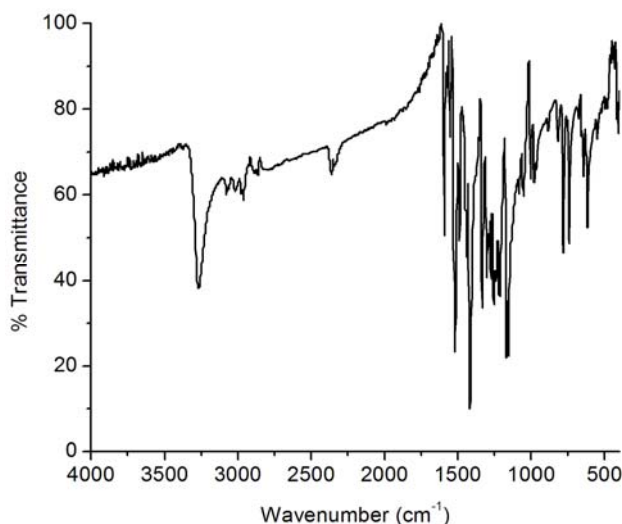
Fig. 6.11. IR spectrum of $[Cu(DpyETsc)Cl]_2 \cdot H_2O$ (**21**)

6.3.2. Electronic spectra

The copper(II) ion is a typical transition metal ion which forms coordination complexes of different stereochemistry, but it is reluctant to take up regular octahedral or tetrahedral stereochemistry. The copper(II) ion form coordination complexes of the type in which coordination numbers four, five or six predominate. Due to large distortion in bond lengths, the splitting of electronic energy levels in copper(II) ions tend to be larger than other first row transition metals. Thus the electronic properties of copper(II) complexes are relatively sensitive to stereochemistry.

The electronic spectra are concerned with energy difference between ground and excited states. A precise knowledge of ground state and excited state is necessary to understand electronic spectra. The variety of colors among transition metal complexes arises from the electronic transition between energy levels whose spacing corresponds to the wavelengths available in visible light. In complexes, these transitions are frequently referred to as *d-d* transitions

because they involve the molecular orbitals that are mainly metal *d* in character [25]. Since this spacing depends on factors such as the geometry of the complex, the nature of the ligands present, and the oxidation state of the central metal atom, the electronic spectra of complexes can provide valuable information relating to bonding and structure [26].

Copper(II) has the spectroscopic ground state term ^2D which will be split by an octahedral field into two levels, $^2T_{2g}$ and ^2E_g. However, if the geometry around copper(II) complex is of lower symmetry, the energy levels again split resulting in more transitions and its electronic spectrum is somewhat more complicated. In a tetragonal field, with $d_{x^2-y^2}$ (B_{1g}) ground state, three spin allowed transitions are possible *viz.* $d_{x^2-y^2} \rightarrow d_{z^2}$, $d_{x^2-y^2} \rightarrow d_{xy}$ and $d_{x^2-y^2} \rightarrow d_{xz}$, d_{yz} ($^2A_{1g} \leftarrow {}^2B_{1g}$, $^2B_{2g} \leftarrow {}^2B_{1g}$ and $^2E_g \leftarrow {}^2B_{1g}$) and they occur in the ranges 12000-17000, 15500-18000 and 17000-20000 cm^{-1} respectively.

In the case of square planar complexes also, three allowed *d-d* transitions are expected in the visible region as in the case of octahedral complexes, but often these theoretical expectations are unseen in practice and these bands usually appear overlapped due to the very small energy difference between the *d* levels. For five coordinated complexes two extreme structures, the square pyramid and trigonal bipyramid are possible, along with many distorted intermediates. Although the electronic spectra of Cu(II) complexes do not in general provide a good indication of geometry, a criterion for distinguishing between square pyramidal and trigonal bipyramidal geometries has been proposed [27-29]. A regular trigonal bipyramidal complex is characterized by peaks extending from 850 – 800 nm, with the greater absorption intensity for the lower energy. The square pyramid has a similar band envelope with peaks extending from 670 – 530 nm, but with greater intensity in the higher energy [30].

The high intense ligand-to-metal charge transfer (LMCT) transitions are observed at the higher energy region. The intensity of these transitions reflects the overlap of the ligand and metal orbitals involved in the charge transfer. Strong bands in the range 23350–23800 cm^{-1} observed in the spectra of all Cu(II) complexes are assigned to S $\rightarrow$ Cu and py $\rightarrow$ Cu charge-transfer bands [31], which are absent in ligands. The remaining bands of the complexes correspond to the intraligand transitions which suffered marginal shifts on complexation.

The significant electronic absorption bands in the spectra of thiosemicarbazones and their copper(II) complexes (Figs. 6.12–6.28) are summarized in Table 6.2. The spectra of all the compounds were recorded in acetonitrile solutions in the range 50000-20000 cm^{-1} and in DMF in the range 20000-10000 cm^{-1}.

Table 6.2. Electronic spectral data (cm^{-1}) of thiosemicarbazones and their copper(II) complexes

| Compound	UV-vis absorption bands (cm^{-1})					
HDpyMeTsc	35890	29280				
[Cu(HDpyMeTsc)(NO$_3$)$_2$] · 4H$_2$O (12)	39040	32700	23570	16440		
[Cu$_2$(DpyMeTsc)$_2$SO$_4$] · 3H$_2$O (13)	39600	34260	31470	23340	18870	
[Cu(DpyMeTsc)N$_3$] · H$_2$O (14)	38600	34490	28920	23570	16980	
[Cu$_2$(DpyMeTsc)$_2$](ClO$_4$)$_2$ · 2H$_2$O (15)	39270	33140	23450	15860		
[Cu(DpyMeTsc)(CH$_3$COO)] · 2H$_2$O (16)	39040	34030	28360	23680	17350	
HDpyETsc	35860	29360				
[Cu$_3$(DpyETsc)$_2$(NO$_3$)$_4$(H$_2$O)$_2$] · H$_2$O (17)	38820	34370	28250	23800	16340	
[Cu$_2$(DpyETsc)$_2$SO$_4$]$_2$ · 4H$_2$O (18)	38600	34700	28020	23340	17570	
[Cu(DpyETsc)N$_3$]$_2$ · 2H$_2$O (19)	39380	33810	29250	23570	18500	
[Cu$_2$(DpyETsc)$_2$](ClO$_4$)$_2$ · H$_2$O (20)	32320	23710	16420			
[Cu(DpyETsc)Cl]$_2$ · H$_2$O (21)	38380	34490	28020	23350	16460	
[Cu(DpyETsc)(NCS)]$_2$ (22)	39380	33590	28250	23450	16900	
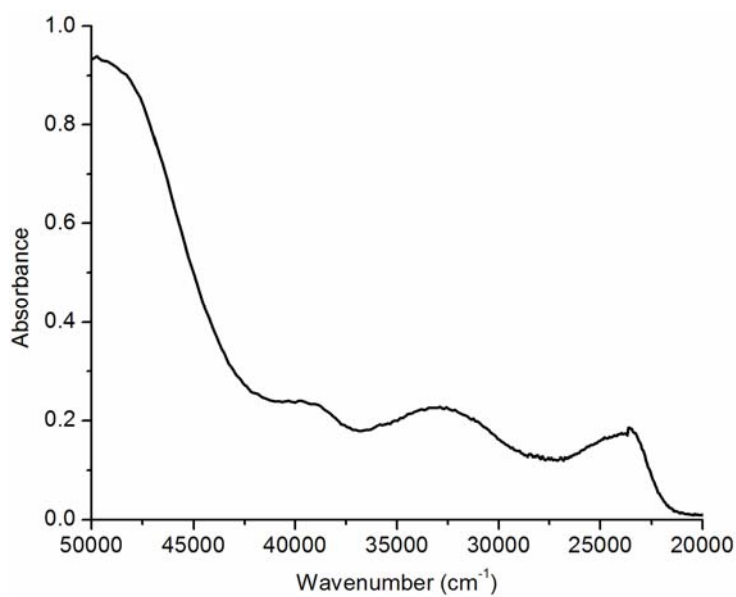
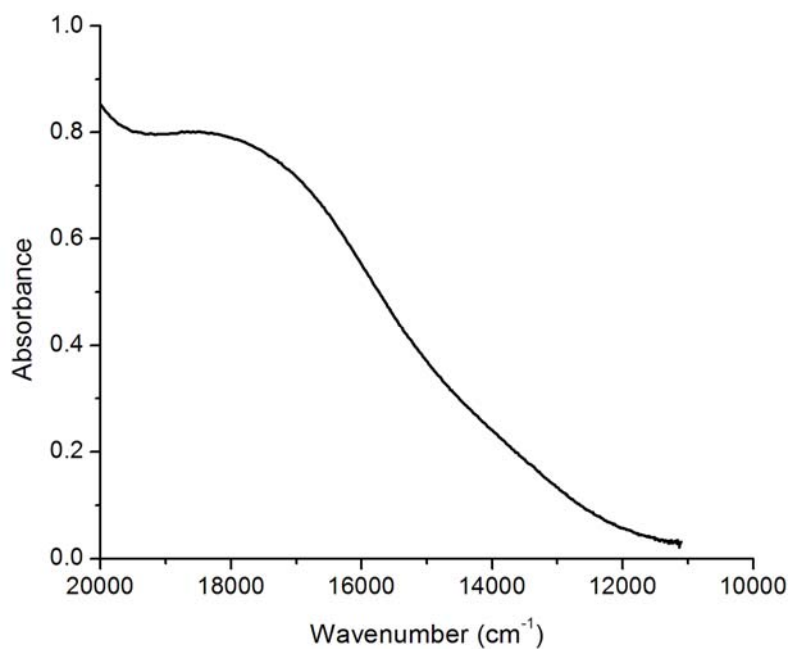**Fig. 6.12.** Electronic spectrum of [Cu(HDpyMeTsc)(NO$_3$)$_2$] · 4H$_2$O (**12**)
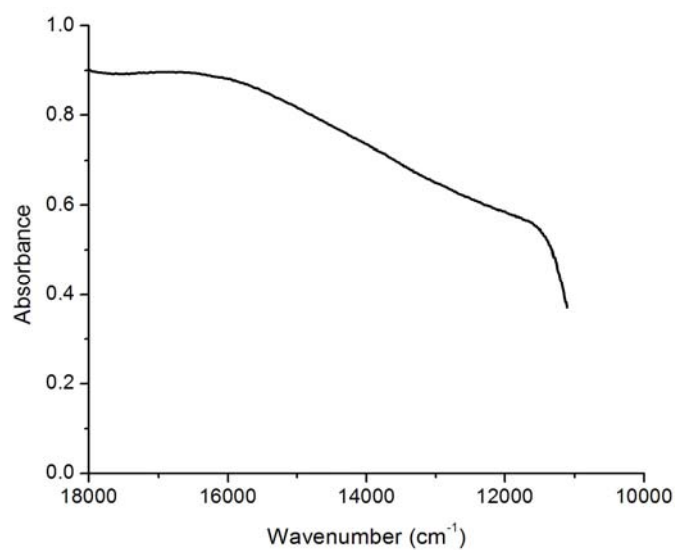
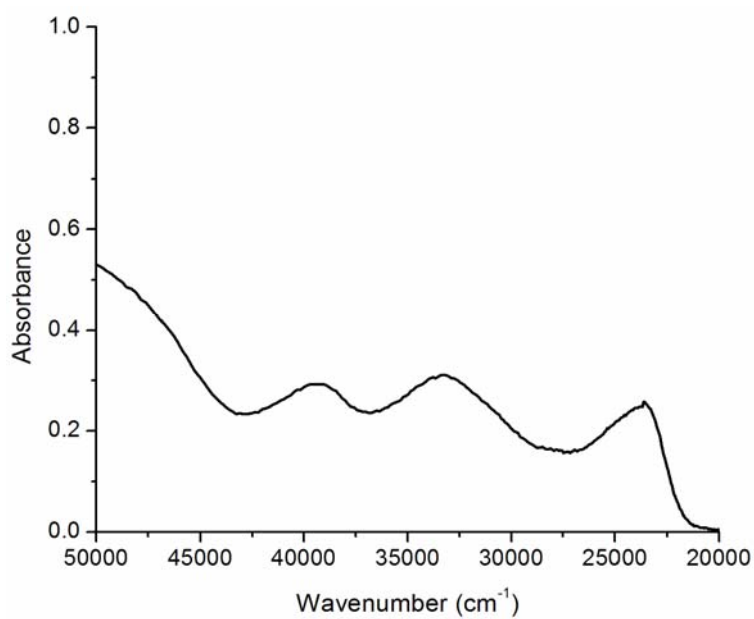**Fig. 6.13.** Electronic spectrum of [Cu(HDpyMeTsc)(NO$_3$)$_2$] · 4H$_2$O (**12**) in the visible region
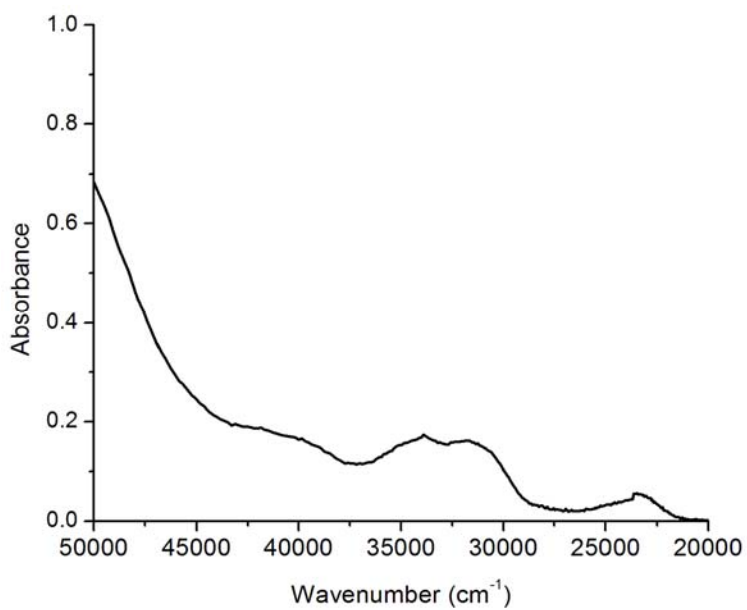
Fig. 6.14. Electronic spectrum of $[Cu_2(DpyMeTsc)_2SO_4] \cdot 3H_2O$ (**13**)
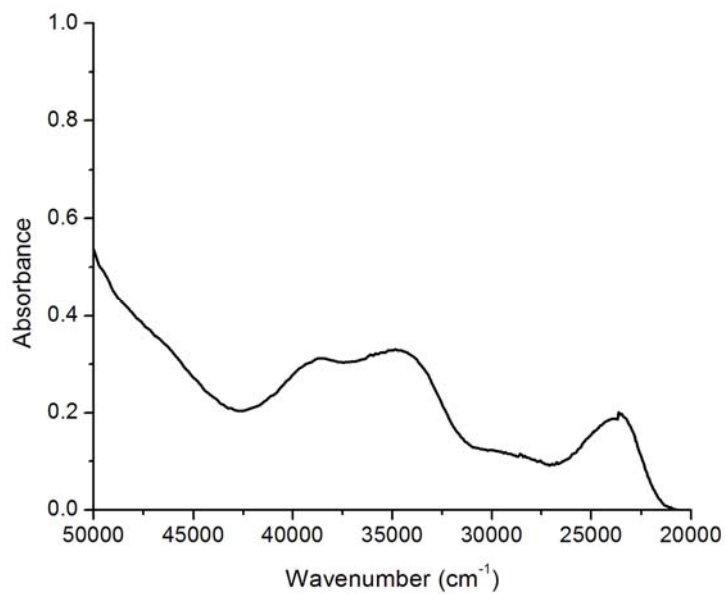
Fig. 6.15. Electronic spectrum of $[Cu(DpyMeTsc)N_3] \cdot H_2O$ (**14**)

Fig. 6.16. Electronic spectrum of [Cu(DpyMeTsc)N$_3$] · H$_2$O (**14**) in the visible region

Fig. 6.17. Electronic spectrum of [Cu$_2$(DpyMeTsc)$_2$](ClO$_4$)$_2$ · 2H$_2$O (**15**)
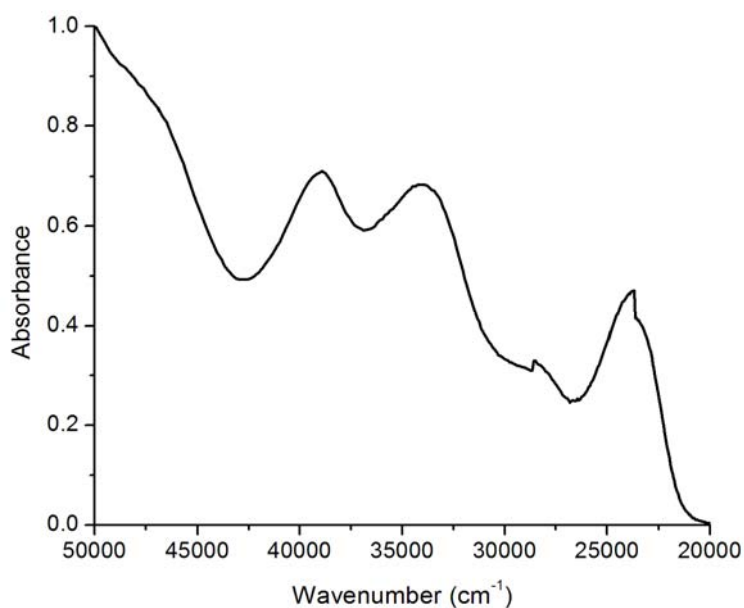
Fig. 6.18. Electronic spectrum of [Cu(DpyMeTsc)(CH$_3$COO)] · 2H$_2$O (**16**)
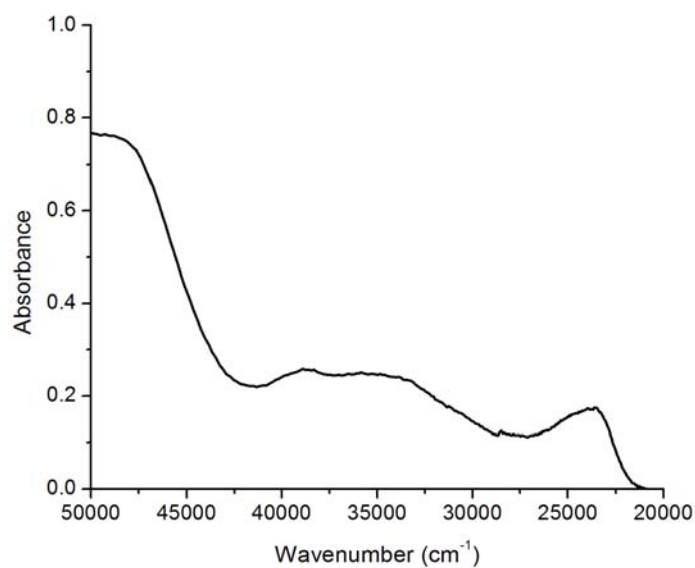
Fig. 6.19. Electronic spectrum of [Cu$_3$(DpyETsc)$_2$(NO$_3$)$_4$(H$_2$O)$_2$] · H$_2$O (**17**)
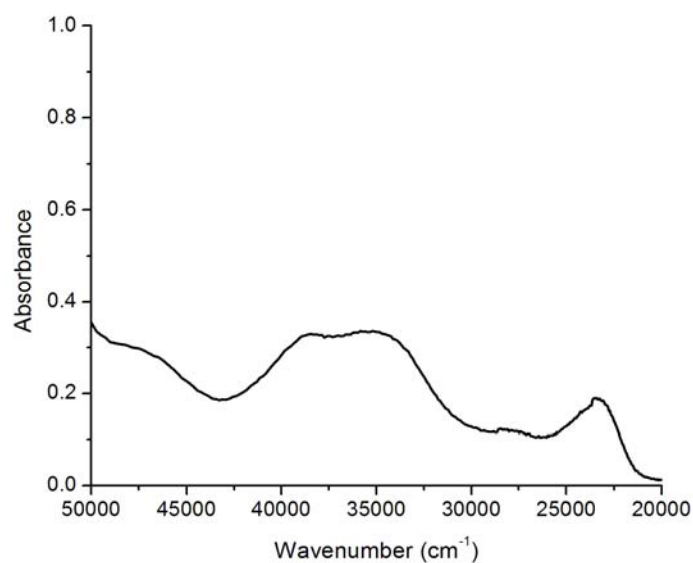
Fig. 6.20. Electronic spectrum of $[Cu_2(DpyETsc)_2SO_4]_2 \cdot 4H_2O$ (**18**)
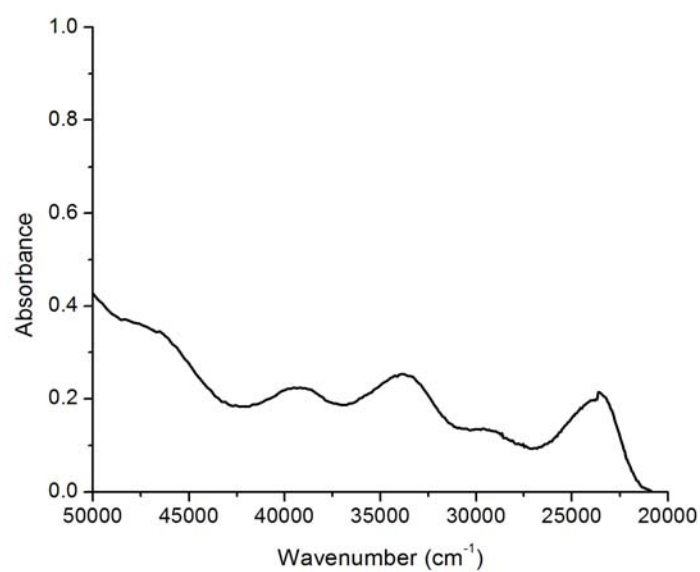
Fig. 6.21. Electronic spectrum of $[Cu(DpyETsc)N_3]_2 \cdot 2H_2O$ (**19**)
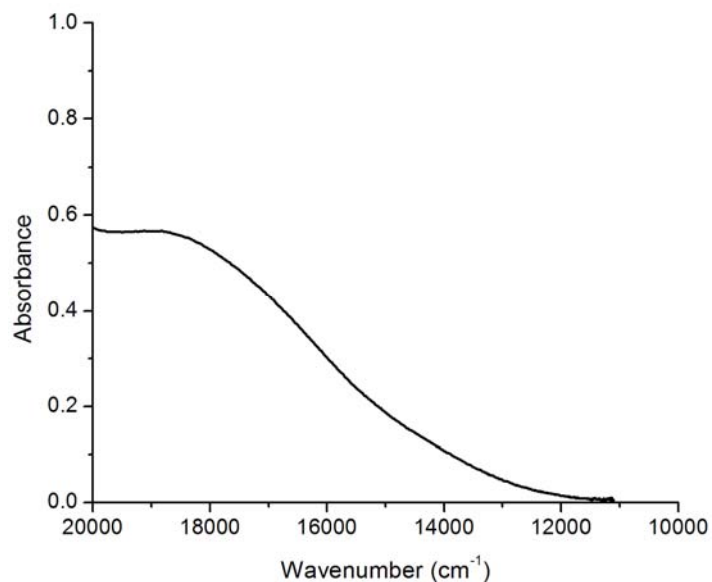
Fig. 6.22. Electronic spectrum of [Cu(DpyETsc)N$_3$]$_2$ · 2H$_2$O (**19**) in the visible region
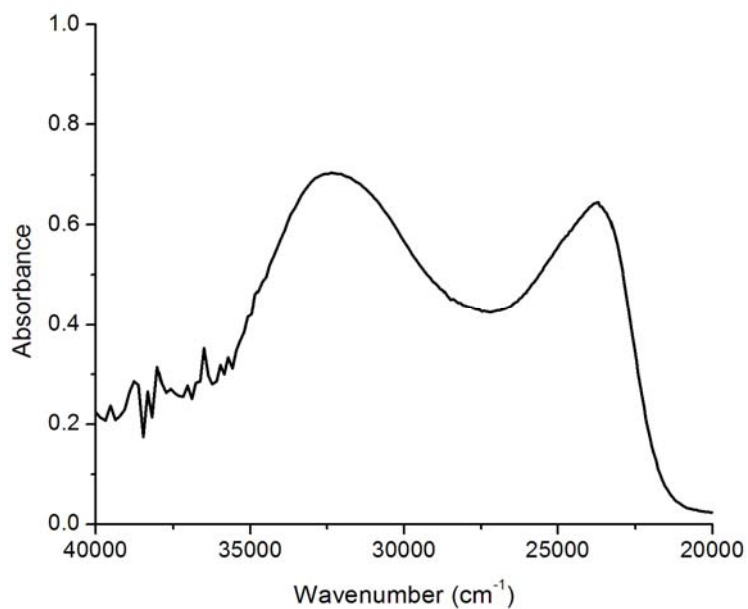
Fig. 6.23. Electronic spectrum of [Cu$_2$(DpyETsc)$_2$](ClO$_4$)$_2$ · H$_2$O (**20**)
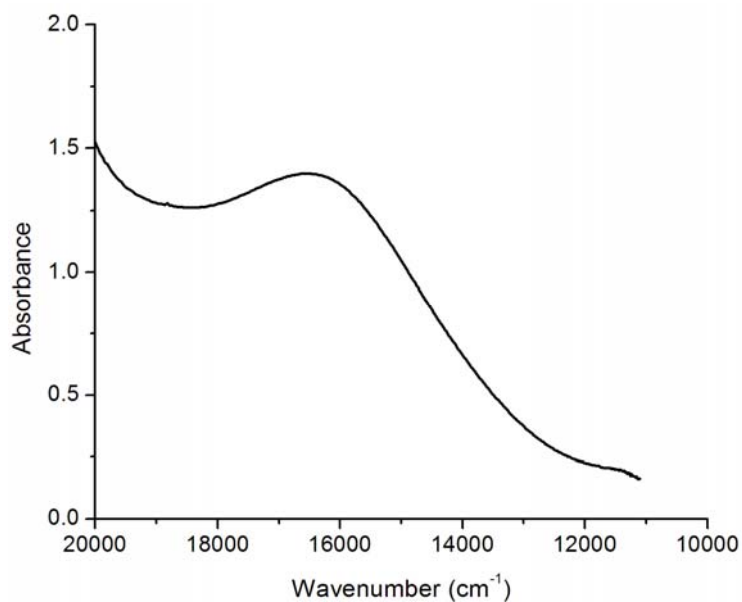
Fig. 6.24. Electronic spectrum of $[Cu_2(DpyETsc)_2](ClO_4)_2 \cdot H_2O$ (**20**) in the visible region
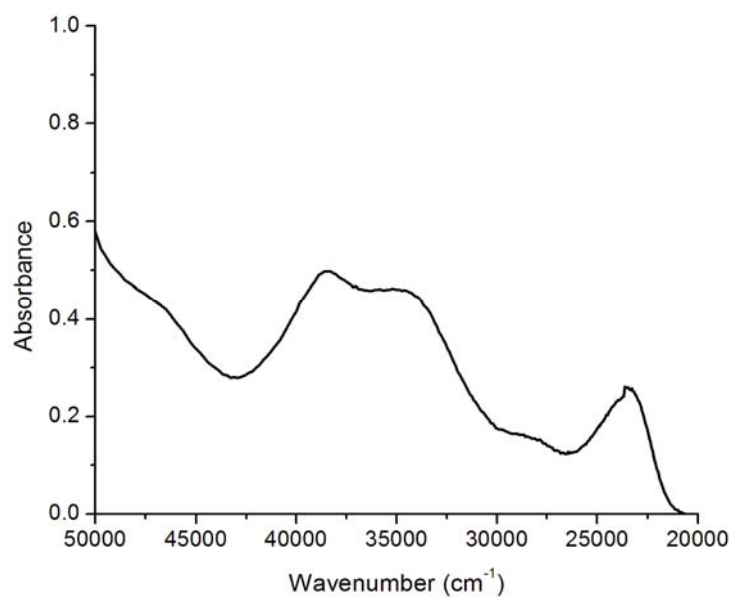
Fig. 6.25. Electronic spectrum of $[Cu(DpyETsc)Cl]_2 \cdot H_2O$ (**21**)
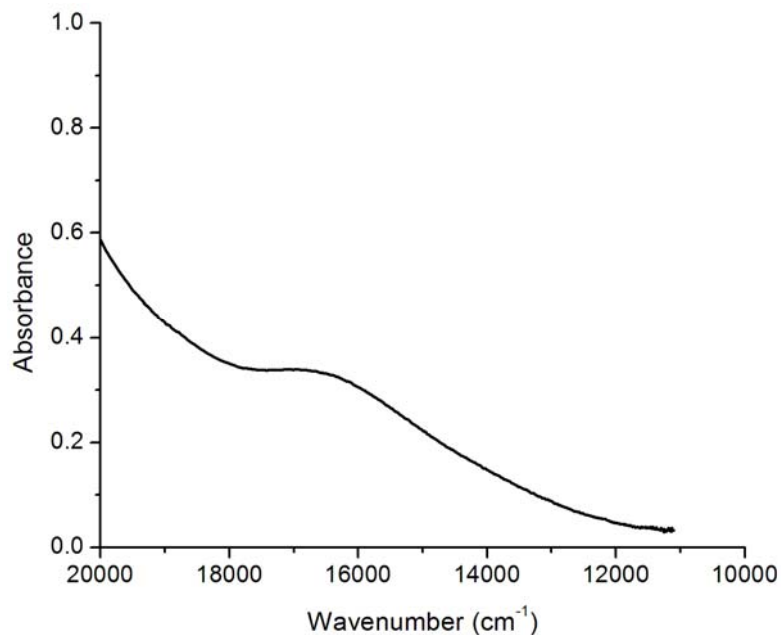
Fig. 6.26. Electronic spectrum of [Cu(DpyETsc)Cl]$_2$ · H$_2$O (**21**) in the visible region
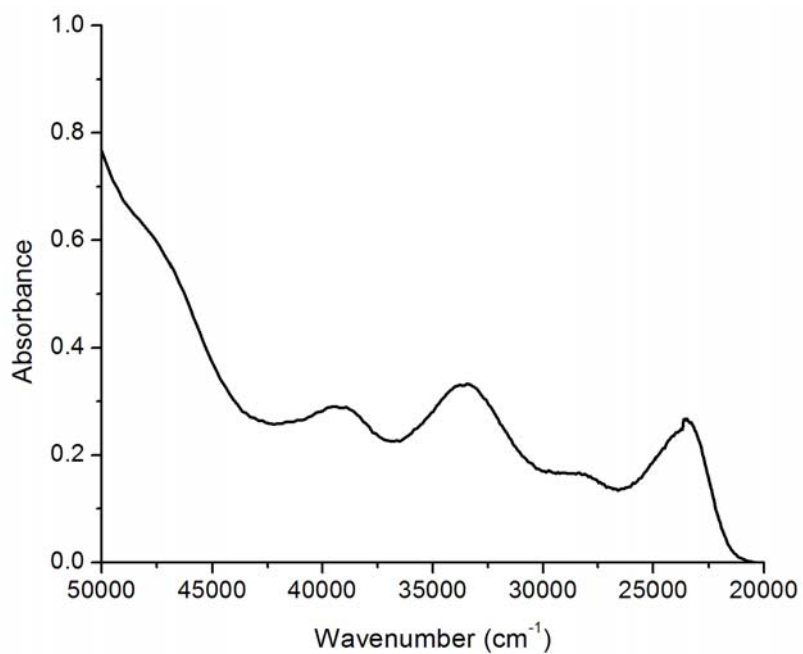
Fig. 6.27. Electronic spectrum of [Cu(DpyETsc)(NCS)]$_2$ (**22**)
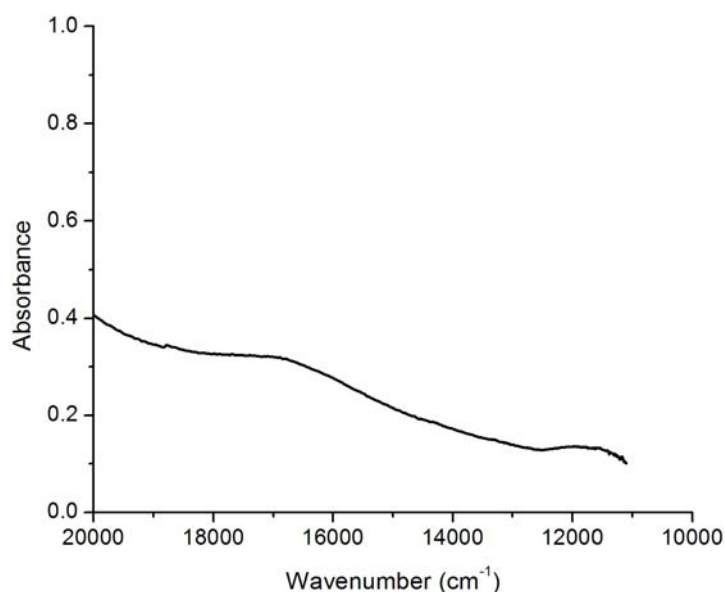
Fig. 6.28. Electronic spectrum of [Cu(DpyETsc)(NCS)]₂ (**22**) in the visible region

6.3.3. Thermal analyses

TGA was performed for all complexes except azido and perchlorate complexes and selected TG-DTG curves are presented in Fig. 6.29. TG curves are drawn as weight (mg) versus temperature (°C). Thermogram of complex **17** showed weight loss above 130 °C, indicate the presence of water molecules inside the coordination sphere. All other complexes show weight loss in the range 50-130 °C, suggest that water molecules are outside the coordination sphere. Complexes are thermally stable and decomposition of ligands starts after 200 °C.
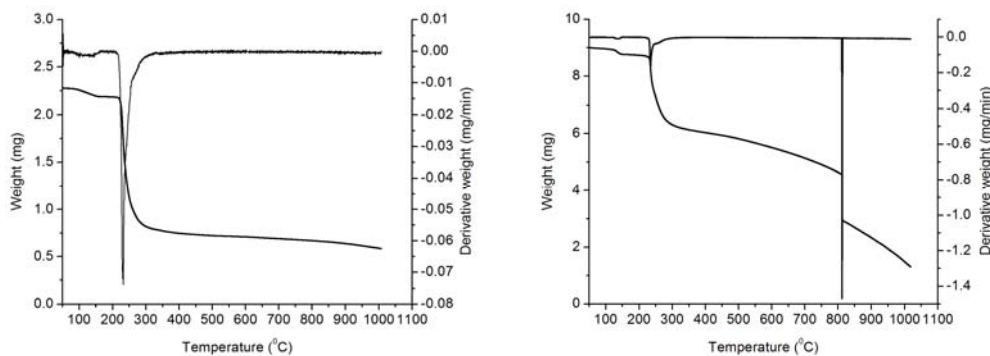
Fig. 6.29. TG-DTG curves of the copper complexes **13** (left) and **17** (right)

6.3.4. Electron paramagnetic resonance spectra

EPR spectral studies on paramagnetic complexes are effective tool for determining the stereochemistry of the ligand around the metal ion. Copper(II) complexes are extensively studied using EPR spectroscopy. EPR is the most powerful spectroscopic method to discriminate between monomeric and dimeric Cu(II) complexes in solution.

The copper(II) ion, with a d^9 configuration, has an effective spin of $S = ½$ and associated spin angular momentum $m_s = ± ½$, leading to a doubly degenerate spin state in the absence of a magnetic field. In a magnetic field this degeneracy is removed and the energy difference between these two states is given by $E = hv = g\beta B$, where h is Planck's constant, v is the frequency, g is the Lande splitting factor (equal to 2.0023 for a free electron), β is the electronic Bohr magneton and B is the magnetic field strength. For the free copper(II) ion there is also an interaction with the magnetic field due to the orbital angular momentum L of the electron, and the total interaction becomes $E = (2.0023S + L)B$. The orbital degeneracy is removed by the crystal field and the orbital angular momentum is said to be quenched for the ground states of copper(II) complexes. Spin-orbit coupling mixes into the ground state some orbital angular momentum from certain excited states, the extent of which is reflected in the modification to the Lande splitting factor g. For the case of a $3d^9$ copper(II) ion, the appropriate spin Hamiltonian assuming a B_{1g} ground state is given by [32]:

$$\hat{H} = \beta[g_{\parallel} B_z S_z + g_{\perp} (B_x S_x + B_y S_y)] + A_{\parallel} I_z S_z + A_{\perp} (I_x S_x + I_y S_y)$$

The copper(II) ion having a d^9 configuration with an effective spin $S = ½$ couples with nuclear spin of ^{63}Cu ($I = {^3}/_2$) and give rise to four ($2nI + 1 = 4$) hyperfine lines. The EPR spectra of the complexes in the polycrystalline state

at 298 K and in solution at 77 K were recorded in the X-band, using 100-kHz field modulation and the g factors were quoted relative to the standard marker TCNE (g = 2.00277). EPR spectral assignments of the copper(II) complexes along with the spin Hamiltonian and orbital reduction parameters are given in Tables 6.3 and 6.4.

The EPR spectra for complexes **12, 14, 15, 17, 18, 19** and **20** in polycrystalline state at 298 K showed only one broad signal with g_{iso} 2.096, 2.086, 2.106, 2.095, 2.083, 2.134 and 2.073 respectively (Figs. 6.30-6.33). Such isotropic spectra, consisting of a broad signal and hence only one g value (g_{iso}), arise from extensive exchange coupling through misalignment of the local molecular axes between the different molecules in the unit cell (dipolar broadening) and enhanced spin lattice relaxation. This type of spectra unfortunately give no information on the electronic ground state of the Cu(II) ions present in complexes.
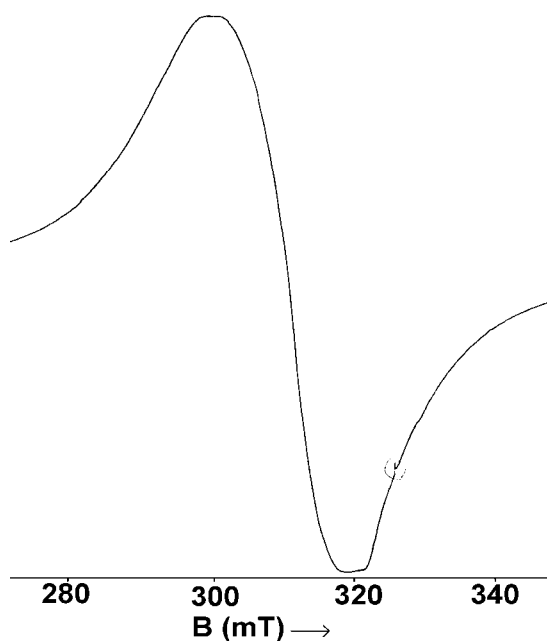
Fig. 6.30. EPR spectrum of [Cu(HDpyMeTsc)(NO$_3$)$_2$] · 4H$_2$O (**12**) in polycrystalline state at 298 K
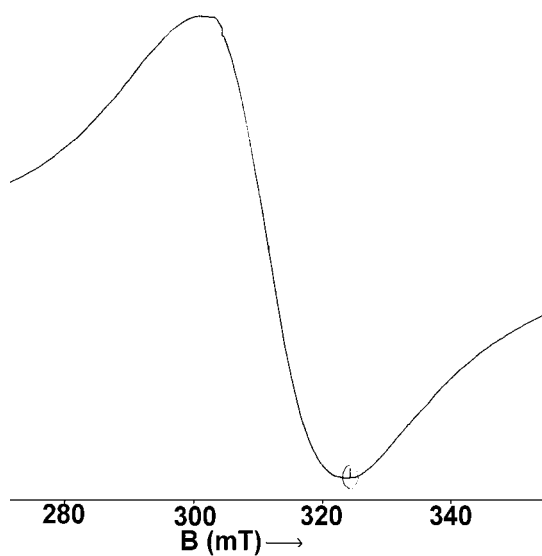
Fig. 6.31. EPR spectrum of $[Cu(DpyMeTsc)N_3] \cdot H_2O$ **(14)** in polycrystalline state at 298 K
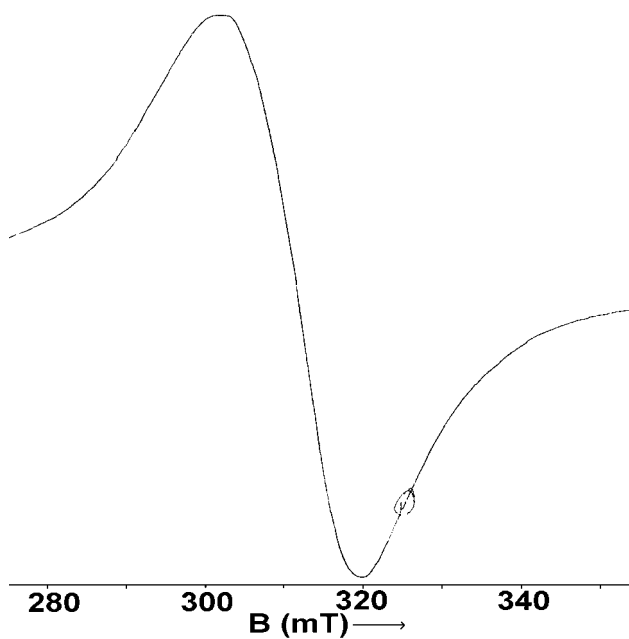
Fig. 6.32. EPR spectrum of $[Cu_3(DpyETsc)_2(NO_3)_4(H_2O)_2] \cdot H_2O$ **(17)** in polycrystalline state at 298 K
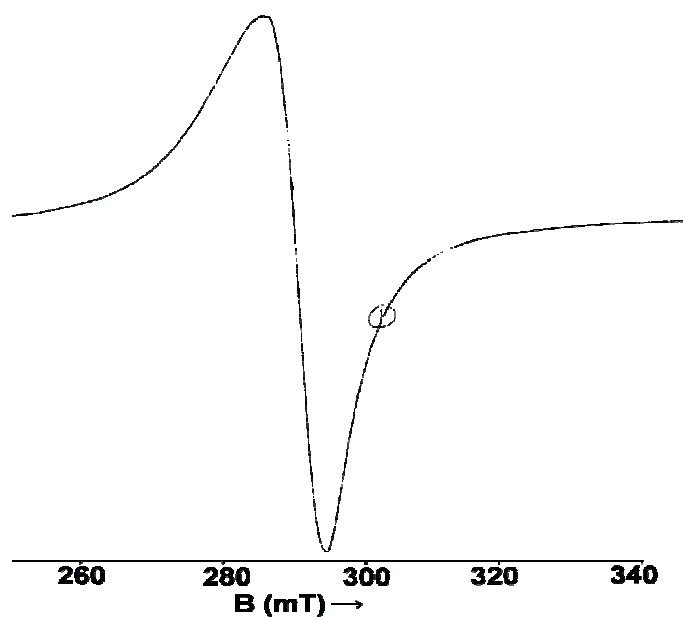
Fig. 6.33. EPR spectrum of $[Cu_2(DpyETsc)_2SO_4]_2 \cdot 4H_2O$ **(18)** in polycrystalline state at 298 K

However the spectra of compounds **13, 16, 21** and **22** showed typical axial behavior with a well defined $g_\parallel$ and $g_\perp$ values (Figs. 6.34-6.37). The variations in the g values indicate that the geometry of the compound is affected by the nature of the coordinating anions [33]. The geometric parameter G, which is a measure of the exchange interaction between copper centers in the polycrystalline compound, is calculated using the equation: $G = (g_\parallel-2.0023)/g_\perp-2.0023)$. If $G > 4$, exchange interaction is negligible and if it is less than 4, considerable exchange interaction is indicated in the solid complex [34,35]. The G values being less than 4 indicate that exchange interactions are strong in all these complexes. In all the copper(II) complexes $g_\parallel > g_\perp > 2.0023$ indicate $d_{x^2-y^2}$ ground state [36].

B (mT) ⟶
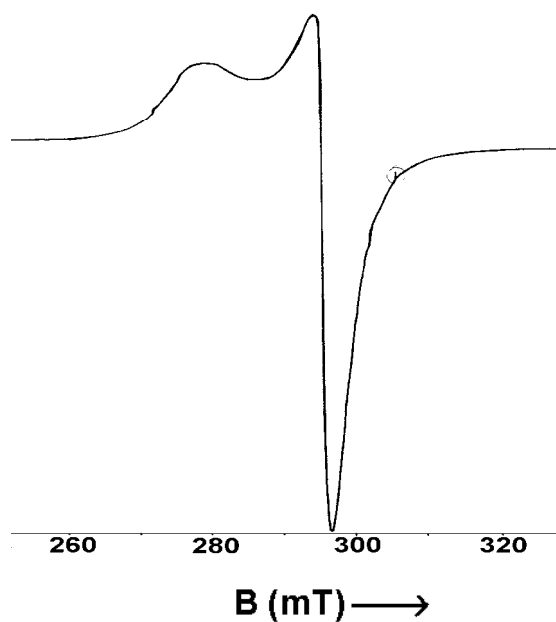
Fig. 6.34. EPR spectrum of [Cu$_2$(DpyMeTsc)$_2$SO$_4$] · 3H$_2$O (**13**) in polycrystalline state at 298 K

B (mT) →
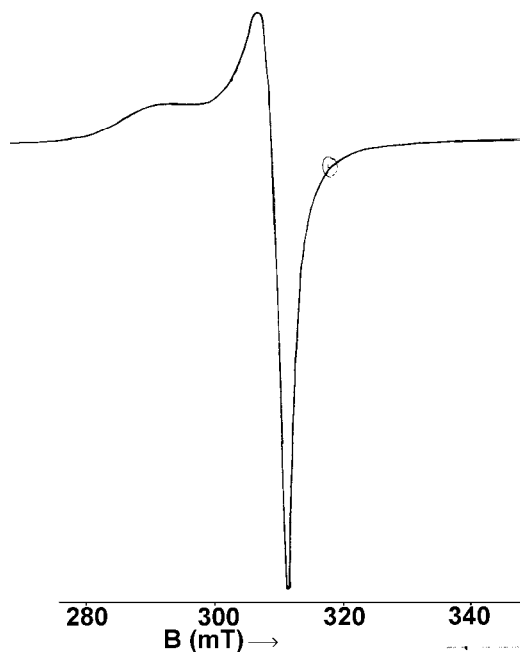
Fig. 6.35. EPR spectrum of [Cu(DpyMeTsc)(CH$_3$COO)] · 2H$_2$O (**16**) in polycrystalline state at 298 K
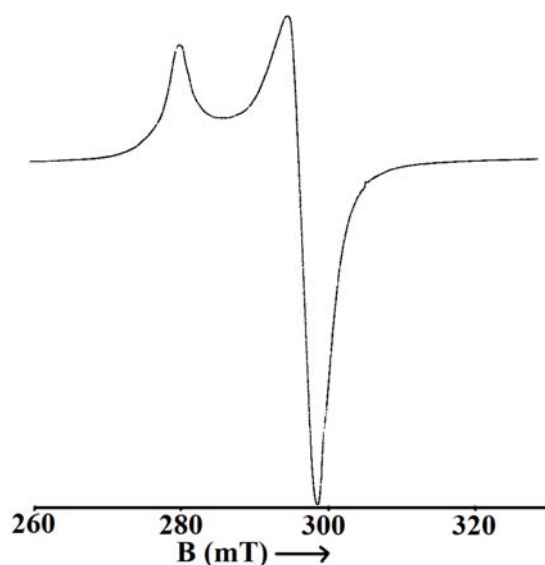
Fig. 6.36. EPR spectrum of [Cu(DpyETsc)Cl]$_2$ · H$_2$O (**21**) in polycrystalline state at 298 K
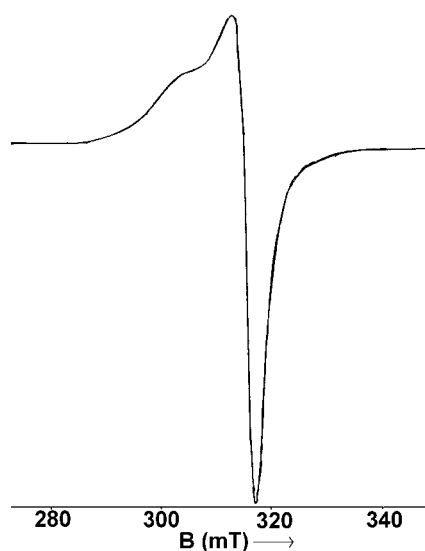
Fig. 6.37. EPR spectrum of [Cu(DpyETsc)(NCS)]$_2$ (**22**) in polycrystalline state at 298 K

In DMF at 77 K, the five coordinated complex [Cu(HDpyMeTsc)(NO$_3$)$_2$] · 4H$_2$O (**12**) displays well-resolved axial spectrum with four hyperfine splittings in the parallel region (Fig. 6.38) resulting from coupling of the electron spin with the spin of the ^{63}Cu nucleus (I = 3/2). The $g_\parallel > g_\perp$ values accounts to the

distorted square based pyramid structure in five coordinated complex and rules out the possibility of a trigonal bipyramidal structure, which would be expected to have $g_{\parallel} < g_{\perp}$ [37,38].
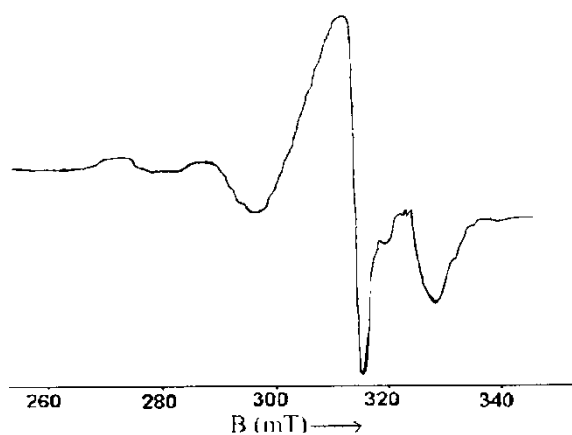
Fig. 6.38. EPR spectrum of $[Cu(HDpyMeTsc)(NO_3)_2] \cdot 4H_2O$ (**12**) in DMF at 77 K

For complexes $[Cu_2(DpyMeTsc)_2SO_4] \cdot 3H_2O$ (**13**) and $[Cu_2(DpyMeTsc)_2](ClO_4)_2 \cdot 2H_2O$ (**15**), axial spectra with seven (not well resolved) hyperfine lines (Figs. 6.39 & 6.40) in the parallel region were obtained, suggesting a dimeric state with two copper centers. This seven line hyperfine splittings are due to the interaction of electrons with two copper nuclei (^{63}Cu, $I = 3/2$). The most important aspect found in the spectrum of complex **15** is the presence of a half field signal with seven hyperfine splittings ($g_{\parallel} = 4.178$ and $g_{\perp} = 4.148$) due to the coupling of the electron spin with the nuclear spin of the two copper centers ($2nI + 1 = 2 \times 2 \times {}^3/_2 + 1$). This aspect is rarely found and is a good evidence for the dinuclear species. Apart from this, a weak signal is observed at half field for complex **13.**
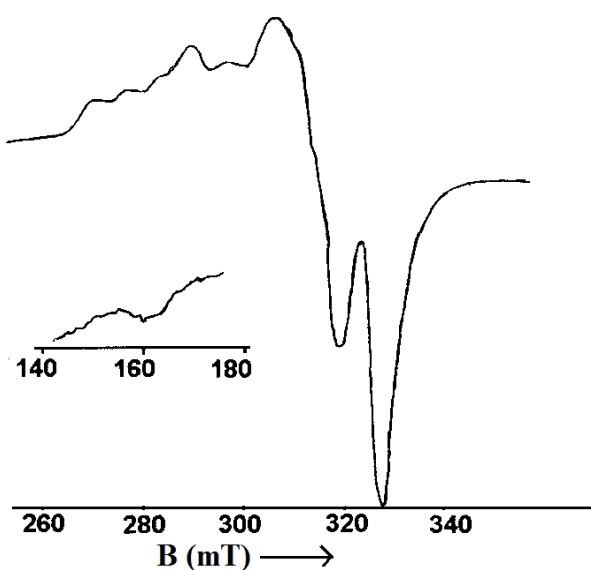
Fig. 6.39. EPR spectrum of [Cu$_2$(DpyMeTsc)$_2$SO$_4$] · 3H$_2$O (**13**) in DMF at 77 K
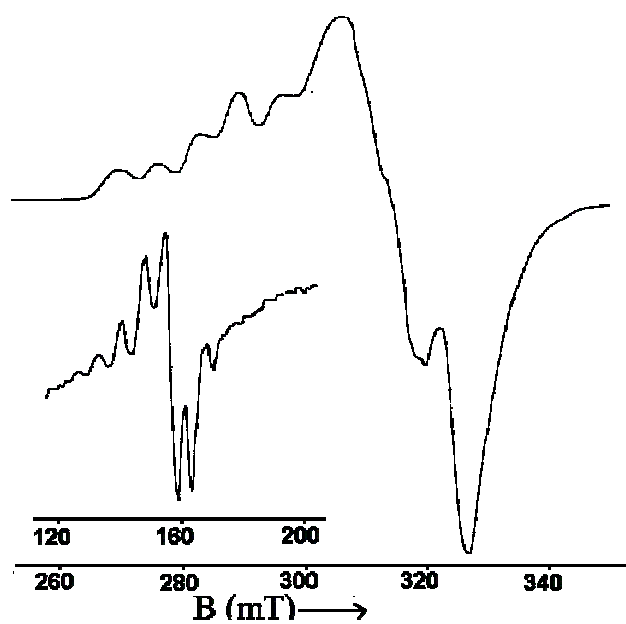
Fig. 6.40. EPR spectrum of [Cu$_2$(DpyMeTsc)$_2$](ClO$_4$)$_2$ · 2H$_2$O (**15**) in DMF at 77 K

For complexes **14** and **16**, well-resolved axial spectra with four hyperfine lines in the parallel region (Figs. 6.41 & 6.42) were obtained in DMF solution at 77 K.
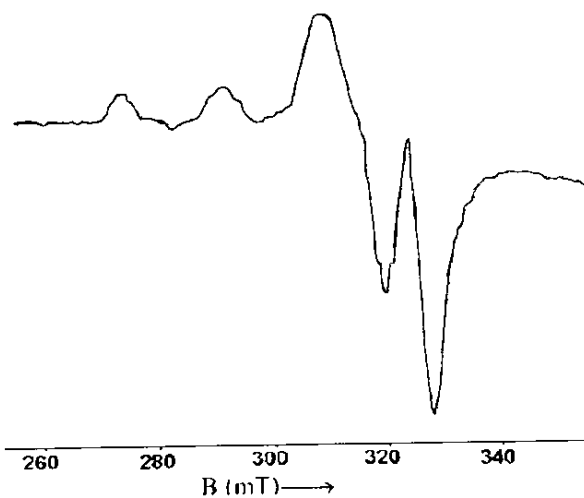
Fig. 6.41. EPR spectrum of [Cu(DpyMeTsc)N$_3$] · H$_2$O **(14)** in DMF at 77 K
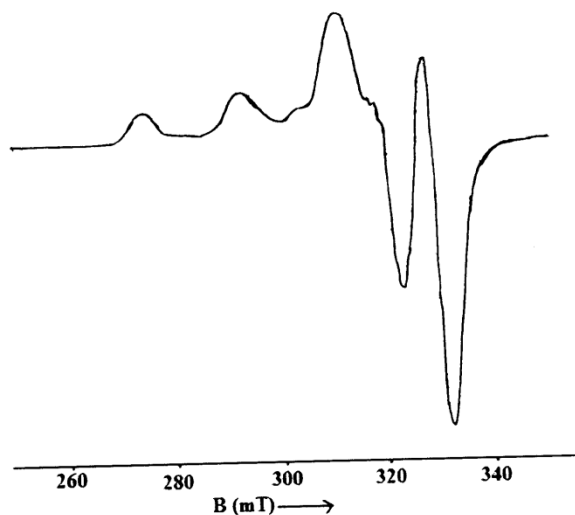
Fig. 6.42. EPR spectrum of [Cu(DpyMeTsc)(CH$_3$COO)] · 2H$_2$O **(16)** in DMF at 77 K

For the trinuclear complex [Cu$_3$(DpyETsc)$_2$(NO$_3$)$_4$(H$_2$O)$_2$] · H$_2$O **(17),** the spectrum shows an axial type with four main hyperfine peaks in the $g_{\parallel}$ region due to the central Cu(II) ion and a signal at $g = 4.147$ that is attributed to a $\Delta M_s = \pm 2$ transition from the two triplet states formed from the interactions of the central Cu(II) ion with each one of the two terminal copper ions.

In DMF solution at 77 K, complexes **18**, **19** and **21** gave axial spectra with four hyperfine splittings in the parallel region (Figs. 6.43 & 6.44). But the hyperfine structure is not well-resolved for complex **18** and this may be due to the poor glass formation. Moreover, splitting seen in the perpendicular region of the spectra for complexes **19** and **21** corresponds to the interaction of electrons with nuclear spin of nitrogens, which gives an evidence for the coordination of pyridyl and azomethine nitrogens. The binuclear nature of complexes **19** and **21** were confirmed by the presence of half-field signals ($\Delta M_s = \pm 2$) *ca.* 160 mT.
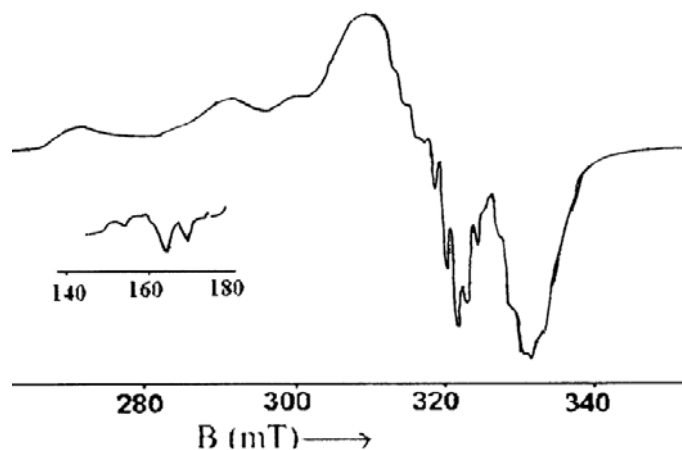
Fig. 6.43. EPR spectrum of [Cu(DpyETsc)N$_3$]$_2$ · 2H$_2$O (**19**) in DMF at 77 K
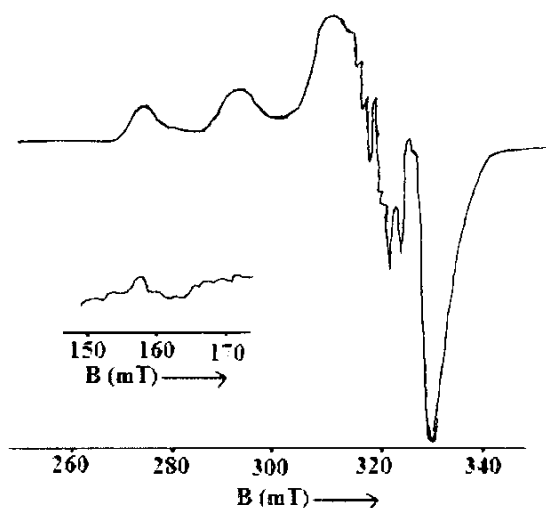
Fig. 6.44. EPR spectrum of [Cu(DpyETsc)Cl]$_2$ · H$_2$O (**21**) in DMF at 77 K

The spectra of complexes **20** and **22** clearly indicates dimeric copper(II) species as evidenced by seven hyperfine lines in the parallel region of the spectra. Half field signals with seven hyperfine splittings with $g = 4.152$ for complex **20** and $g = 4.019$ for complex **22**, indicate the presence of dimeric species, which arises due to the $\Delta M_s = \pm 2$ transitions (Figs. 6.45 & 6.46).
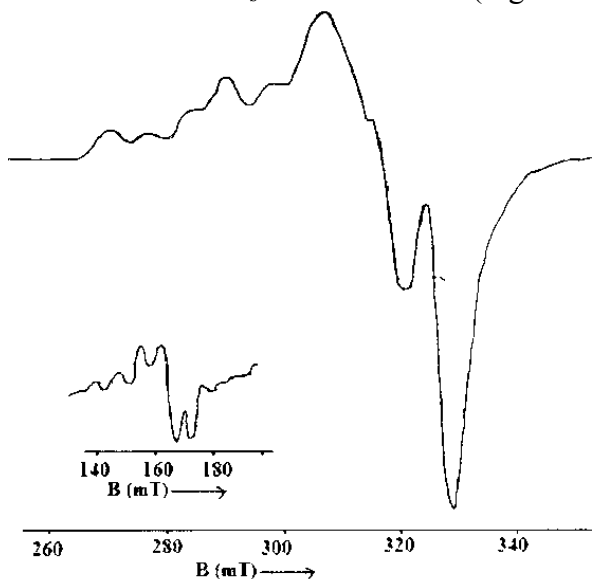
Fig. 6.45. EPR spectrum of $[Cu_2(DpyETsc)_2](ClO_4)_2 \cdot H_2O$ **(20)** in DMF at 77 K
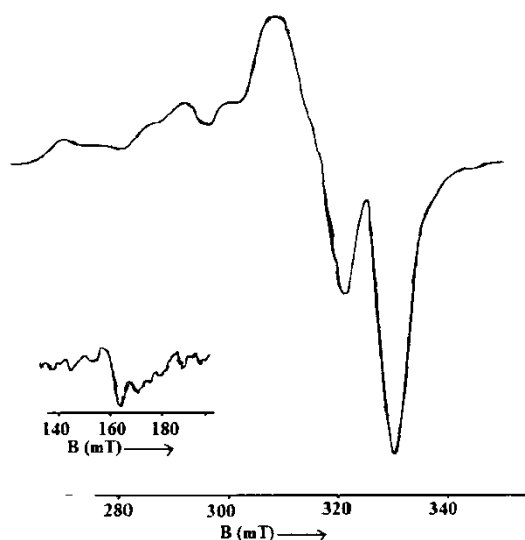
Fig. 6.46. EPR spectrum of $[Cu(DpyETsc)(NCS)]_2$ **(22)** in DMF at 77 K

The EPR parameters $g_\parallel$, $g_\perp$, g_{av}, $A_\parallel$ (Cu) and the energies of *d–d* transitions were used to evaluate the bonding parameters α^2, β^2 and γ^2, which may be regarded as measures of covalency of the in-plane σ-bonds, in-plane π-bonds, and out-of-plane π bonds respectively. The value of in-plane sigma bonding parameter α^2 was estimated from the following expression:

$$\alpha^2 = -A_\parallel /0.036 + (g_\parallel - 2.0023) + {}^3/_7 (g_\perp -2.0023) + 0.04 \text{ [39]}$$

The orbital reduction factors, $K_\parallel = \alpha^2 \beta^2$ and $K_\perp = \alpha^2 \gamma^2$ were calculated using the following expressions [40].

$$K^2_\parallel = (g_\parallel - 2.0023) \, E_{d\text{-}d}/8\lambda_0$$

$$K^2_\perp = (g_\perp - 2.0023) \, E_{d\text{-}d}/2\lambda_0$$

where λ_0 is the spin-orbit coupling constant with a value of -828 cm^{-1} for copper(II) d^9 system. According to Hathaway, $K_\parallel \approx K_\perp \approx 0.77$ for pure σ-bonding and $K_\parallel < K_\perp$ for in-plane π-bonding, while for out-of-plane π- bonding, $K_\parallel > K_\perp$.

In all the copper(II) complexes, it is observed that $K_\parallel < K_\perp$ which indicates the presence of significant in-plane π-bonding. Furthermore α^2, β^2 and γ^2 have values much less than 1.0, which is expected for 100% ionic character of the bonds, and become smaller with increasing covalent nature of the bonding. The evaluated values of α^2, β^2 and γ^2 of the complexes are consistent with both strong in plane σ and in plane π bonding [41]. The $g_\parallel$ values are nearly the same for all the complexes indicating that the bonding is dominated by the thiosemicarbazone moiety but are different from that in the solid state. The fact that $g_\parallel$ values are less than 2.3, is an indication of significant covalent bonding [42]. The empirical factor, $f = g_\parallel/A_\parallel$, is an index of tetragonal distortion and the value depends on the nature of the coordinated atom. The distortion from the plane increases with increasing $g_\parallel$ values and

decreasing $A_{\parallel}$ values. In all the compounds f falls in the range 108 - 118 cm which shows small to medium distortion [43].

Table 6.3. EPR spectral parameters of copper(II) complexes in polycrystalline state at 298 K and in frozen DMF at 77 K

Compound	Polycrystalline (298 K)				DMF Solution (77 K)			
	$g_{\parallel}$	$g_{\perp}$	g_{iso} or g_{av}	G	$g_{\parallel}$	$g_{\perp}$	g_{av}	$A_{\parallel}{}^a$
12	-	-	2.096	-	2.165	2.066	2.099	191.00
13	2.186	2.067	2.106	2.839	2.177	2.065	2.102	195.00
14	-	-	2.086	-	2.160	2.049	2.086	184.66
15	-	-	2.106	-	2.177	2.066	2.103	193.33
16	2.191	2.060	2.104	3.270	2.165	2.046	2.085	196.66
17	-	-	2.095	-	2.174	2.059	2.097	196.66
18	-	-	2.083	-	2.174	2.053	2.093	195.00
19	-	-	2.134	-	2.158	2.044	2.082	186.67
20	-	-	2.073	-	2.176	2.057	2.096	196.66
21	2.151	2.071	2.097	2.180	2.169	2.050	2.089	196.60
22	2.184	2.063	2.103	2.993	2.159	2.051	2.087	182.66

$^a A_{\parallel}$ values in 10^{-4} cm^{-1}

Table 6.4. EPR bonding parameters of copper(II) complexes

Compound	α^2	β^2	γ^2	$K_{\parallel}$	$K_{\perp}$	f
12	0.790	0.831	0.993	0.657	0.785	109.94
13	0.765	0.888	1.108	0.679	0.848	112.17
14	0.694	0.916	0.996	0.636	0.692	116.12
15	0.786	0.822	0.993	0.646	0.781	111.07
16	0.773	0.843	0.877	0.651	0.678	116.42
17	0.748	0.868	0.998	0.650	0.747	109.24
18	0.783	0.861	0.933	0.674	0.730	110.35
19	0.734	0.896	0.924	0.659	0.679	114.85
20	0.792	0.828	0.931	0.656	0.738	108.90
21	0.779	0.836	0.890	0.651	0.694	109.01
22	0.728	0.855	0.958	0.623	0.698	117.40

6.3.5. Crystal structure of $[Cu_3(DpyETsc)_2(NO_3)_4(H_2O)_2] \cdot H_2O$ (17)

The crystal structure of the trinuclear complex $[Cu_3(DpyETsc)_2(NO_3)_4(H_2O)_2] \cdot H_2O$ (**17**) was determined by single-crystal X-ray diffraction. X-ray quality dark green single crystals of compound **17** were grown from its ethanol solution by slow evaporation at room temperature in air. The crystallographic data and structure refinement parameters for the compound **17** are given in Table 6.5. Diffraction data for **17** were collected at 150(2) K using a CrysAlis CCD, Oxford Diffraction Ltd. at the National Single Crystal X-ray Diffraction facility, IIT, Bombay, India. The trial structure was solved using SHELXS-97 [44] and refinement was carried out by full-matrix least square method based on F^2 (SHELXL-97) [44]. Molecular graphics employed were DIAMOND [45] and MERCURY [46].

The molecular structure along with atom labeling scheme of the complex is shown in Fig. 6.47 and selected geometrical parameters are given in Table 6.6. The structure consists of a symmetrical Cu_3L_2 core with the centrally interlocked copper ion as the inversion center. The three copper centers are arranged in a linear fashion with a Cu1⋯Cu2 distance of 4.7079 Å. There is no direct covalent linkage between Cu2 and Cu2a and the trans arrangement of the chelating donors at the central copper ion leads these metals to be separated by a distance of 9.4158 Å. In the trinuclear unit Cu1 is found to have a six coordinated distorted octahedral geometry with two unidentate nitrate groups and each Cu2 has a distorted octahedral geometry with a chelating bidentate nitrate group.

Table 6.5. Crystal refinement parameters of $[Cu_3(DpyETsc)_2(NO_3)_4(H_2O)_2] \cdot H_2O$ **(17)**

Formula	$C_{28} H_{34} Cu_3 N_7 O_{15} S_2$
Formula weight (M)	1079.44
Temperature (T) K	150(2)
Wavelength (Mo Kα) (Å)	0.71073
Crystal system	Triclinic
Space group	P-1
Lattice constants	
a(Å)	8.072(4)
b(Å)	9.661(11)
c(Å)	14.290(8)
α (°)	70.459(17)
β (°)	79.148(3)
γ(°)	74.522(3)
Volume V (Å^3)	1006.1(8)
Z	1
Calculated density (ρ) (Mg m^{-3})	1.782
Absorption coefficient, μ (mm^{-1})	1.763
F(000)	549
Crystal size (mm^3)	0.33 x 0.23x 0.19
θ Range for data collection	2.98-24.99
Limiting Indices	$-9 \leq h \leq 9$, $-11 \leq k \leq 11$, $-16 \leq l \leq 16$
Reflections collected	8952
Independent Reflections	3525 [R(int) = 0.0691]
Refinement method	Full-matrix least-squares on F^2
Data / restraints / parameters	3525 / 0 / 304
Goodness-of-fit on F^2	1.047
Final R indices [I > 2σ (I)]	$R_1 = 0.0750$, wR$_2$ = 0.2001
R indices (all data)	$R_1 = 0.1097$, wR$_2$ =0.2196
Largest difference peak and hole (e Å $^{-3}$)	1.083 and -2.445

$R_1 \quad = \quad \Sigma||F_o| - |F_c|| / \Sigma|F_o|$

$wR_2 \quad = \quad [\Sigma w(F_o^2 - F_c^2)^2 / \Sigma w(F_o^2)^2]^{1/2}$
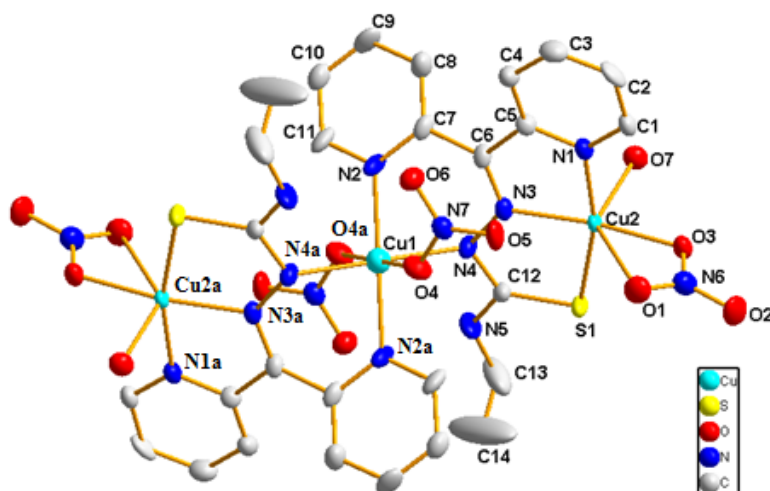
Fig. 6.47. The molecular structure of $[Cu_3(DpyETsc)_2(NO_3)_4(H_2O)_2] \cdot H_2O$ (**17**) along with atom numbering scheme. The hydrogen atoms and water molecule are omitted for clarity

Table 6.6. Selected bond lengths (Å) and bond angles (°) for $[Cu_3(DpyETsc)_2(NO_3)_4(H_2O)_2] \cdot H_2O$ (**17**)

Bond lengths (Å)		Bond angles (°)	
Cu(1)—N(4)	2.058(7)	N(4)—Cu(1)—N(2)	81.8(3)
Cu(1)—N(2)	2.073(7)	N(4a)—Cu(1)—N(4)	180.00(1)
Cu(1)—O(4)	2.398(6)	N(4)—Cu(1)—N(2a)	98.20(3)
Cu(2)—N(3)	1.977(6)	N(2a)—Cu(1)—N(2)	180.00(4)
Cu(2)—N(1)	1.983(7)	N(4a)—Cu(1)—O(4)	89.50(2)
Cu(2)—O(1)	2.760(7)	N(4)—Cu(1)—O(4)	90.50(2)
Cu(2)—O(3)	2.002(6)	N(2a)—Cu(1)—O(4)	79.80(2)
Cu(2)—S(1)	2.250(3)	N(2)—Cu(1)—O(4)	100.20(2)
Cu(2)—O(7)	2.255(8)	N(4)—Cu(1)—O(4a)	89.50(2)
S(1)—C(12)	1.718(8)	N(2)—Cu(1)—O(4a)	79.80(2)
N(3)—C(6)	1.308(11)	O(4)—Cu(1)—O(4a)	180.00(1)
N(4)—C(12)	1.368(10)	N(3)—Cu(2)—N(1)	80.00(3)
N(5)—C(12)	1.312(11)	N(3)—Cu(2)—O(3)	170.10(2)
		N(1)—Cu(2)—O(3)	100.80(3)
		N(3)—Cu(2)—S(1)	85.20(2)
		O(3)—Cu(2)—S(1)	93.34(19)
		N(3)—Cu(2)—O(7)	102.50(3)
		N(1)—Cu(2)—O(7)	86.90(3)
		O(3)—Cu(2)—O(7)	87.40(3)
		S(1)—Cu(2)—O(7)	98.80(3)

The metal ion Cu(2) [and symmetry related Cu(2')] is coordinated by the pyridine N [Cu(2)–N(1) = 1.983(7) Å], azomethine N [Cu(2)–N(3) = 1.977(6) Å] and the thiolato sulfur [Cu(2)–S(1) = 2.250(3) Å] from the ligand. The remaining positions are occupied by oxygens of the chelating bidentate nitrate group [Cu(2)–O(3) = 2.002(6) Å and Cu(2)–O(1) = 2.760(7) Å]. The sixth coordination position is occupied by oxygen of the water molecule at a distance of 2.255(8) Å. The C(12)–S(1) bond length of 1.718(8) Å indicates that the sulfur to be in the deprotonated thiolate form.

The central Cu(1) located at the inversion center of the molecule attains an axially elongated octahedral geometry being surrounded in the equatorial plane by two pyridine nitrogens [Cu(1)–N(2)= 2.073(7) Å] and two nitrogens adjacent to the azomethine nitrogens [Cu(1)–N(4) = 2.058(7) Å] and at the axial positions by oxygens of two monodentate nitrate groups [Cu(1)–O(4) = 2.398(6) Å]. The variations in the N(2)–Cu(1)–N(4) (81.8(3)) and N(2)–Cu(1)–O(4) (100.2(2)) bond angles from 90.0 cause distortion to the octahedral geometry. However this leads to a stable six membered Cu(1)–N(2)–C(7)–C(6)–N(3)–N(4) metallocycle. The centrosymmetric metallocycle with respect to Cu(1) atom is depicted in Fig. 6.48.
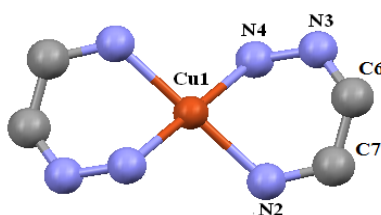
Fig. 6.48. The centrosymmetric six membered metallocycle formed along Cu(1) centre

In the solid state the complex shows a variety of H–bonding interactions involving amino nitrogen and the nitrato oxygen (Table 6.7). Two different hydrogen-bonding motifs are present in the molecule. Intramolecular hydrogen

bonding interactions are observed between the N(5)–H(5) of one ligand with the nitrato oxygen O6 at a distance of 2.895(10) Å. The O(7)–H of Cu(2) bound water molecule is hydrogen bonded to nitrato oxygen O(6) and O(111) of the water molecule [2.813(12) Å and 2.779(14) Å] by intermolecular interaction. H(111) and H(222) of the same water molecule is hydrogen bonded to adjacent nitrato oxygen O(2) coordinated to Cu(2) at a distance of 2.847(13) and 2.813(12) Å. These type of hydrogen bonding interactions are found to be very important in active species of several multinuclear metalloenzymes [47]. The lattice water held among the units is shown in Fig. 6.49.
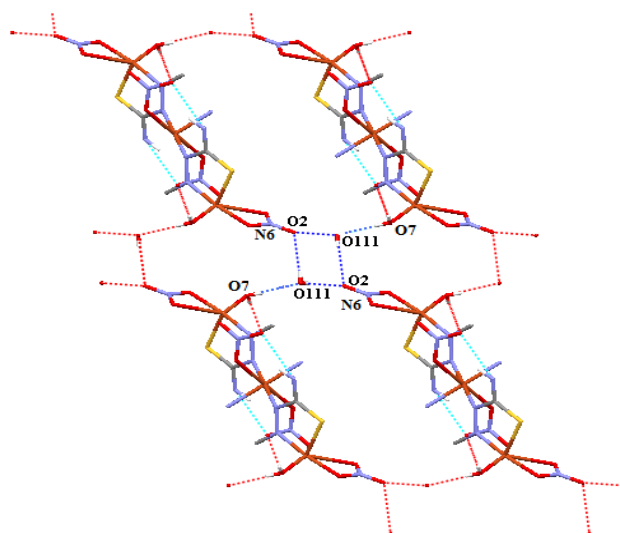
Fig. 6.49. A view of the hydrogen bonding interactions in compound **17**, dipyridyl portions omitted for clarity

The ring puckering analysis show that the ring Cg(3) consisting of atoms Cu(2)–N(1)–C(5)–C(6)–N(3) adopts an envelope on N(3) [Q(2) = 0.147(7)] [48]. The packing diagram along *c* axis shows the diverse π–π stacking and CH–π and N–O–π interactions giving rise to a supramolecular three-dimensional net work. When viewed along the *b* axis, units are arranged in superimposing layers as in Fig. 6.50.

Table 6.7. H-bonding, π–π, CH–π and N–O–π interaction parameters of **17**

Hydrogen bonding

D—H···A (Å)	D—H (Å)	H···A (Å)	D···A (Å)	D—H···A (°)
N(5)—H(5)···O(6)*ᵃ*	0.88	2.12	2.895	147
O(7)—H(101)···O(111)*ᵇ*	0.71	2.07	2.779	172
O(7)—H(102)···O(6)*ᶜ*	0.56	2.26	2.813	169
O(111)—H(111)···O(2)*ᵈ*	0.68	2.21	2.847	158
O(111)—H(222)···O(2)*ᵉ*	0.57	2.26	2.818	167

π–π interactions

Cg(I)···Cg(J)	Cg—Cg (Å)	α (°)	β (°)
Cg(2)···Cg(7)*ᵃ*	4.795(5)	45.51	44.00
Cg(6)···Cg(6)*ᵍ*	4.701(6)	0.00	45.24

CH–π interactions

X—H(I)···Cg(J)	H···Cg (Å)	X—H···Cg (°)	X···Cg(Å)
C(11)—H(11)···Cg(2)*ᵃ*	2.94	132	3.638(10)

N-O–π interaction

Y···X(I)	Cg(J)*ᶠ*	X···Cg (Å)	Y—X···Cg (°)	Y···Cg(Å)
N(7)—O(5)	Cg(3)	3.123(8)	85.0(5)	3.251(8)

Equivalent position code *a* =-x, 2-y, 1-z; *b* = 1-x, 2-y, 1-z; *c* = 1+x, y, z;

   d = 1-x, 1-y, 1-z; *e* = x, y, 1+z; *f* = x, y, z; *g* = -x, 2-y, -z

Cg(2) = Cu(2), S(1), C(12), N(4), N(3)

Cg(3) = Cu(2), N(1), C(5), C(6), N(3)

Cg(6) = N(1), C(1), C(2), C(3), C(4), C(5)

D = donor; A = acceptor

α (°) = Dihedral angle between planes I and J

β (°) = Angle between Cg(I)-Cg(J) vector and normal to plane I
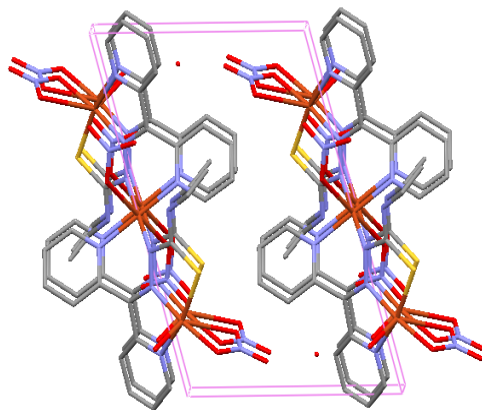
Fig. 6.50. Packing diagram along b axis of compound **17**

A very interesting aspect observed is the pentadentate coordination shown by the ligand which is usually tridentate. The usual coordinating sites (NNS) are coordinated to Cu(2) while the unusual sites ie, N(2) (second pyridine N) and N(4) to the central Cu(1). This type of Cu(1)–N(4) coordination is first observed according to the best of our knowledge.

References

[1] P. Akilan, M. Thirumavalavan, M. Kandaswamy, Polyhedron 22 (2003) 3483.

[2] C. Lodeiro, R. Bastida, E. Bertolo, A. Macías, A. Rodríguez, Polyhedron 22 (2003) 1701.

[3] R. Senthil Kumar, S. Arunachalam, Polyhedron 26 (2007) 3255.

[4] B. Le Guennic, S. Petit, G. Chastanet, G. Pilet, D. Luneau, N. Ben Amor, V. Robert, Inorg. Chem. 47 (2008) 572.

[5] T. Mallah, M. L. Boillot, O. Kahn, J. Gouteron, S. Jeannin, Y. Jeannin, Inorg. Chem. 25 (1986) 3058.

[6] T. Mallah, O. Kahn, J. Gouteron, S. Jeannin, Y. Jeannin, C. J. O'Connor, Inorg. Chem. 26 (1987) 1375.

[7] O. Kahn, T. Mallah, J. Gouteron, S. Jeannin, Y. Jeannin, J. Chem. Soc., Dalton Trans. (1989) 1117.

[8] A. Benzekri, P. Dubourdeaux, J. M. Latour, J. Laugier, P. Rey,Inorg. Chem. 27 (1988) 3710.

[9] T. Chattopadhyay, K. S. Banu, A. Banerjee, J. Ribas, A. Majee, M. Nethaji, D. Das, J. Mol. Struct. 833 (2007) 13.

[10] P. Chaudhuri, R. Wagner, T. Weyhermuller, Inorg. Chem. 46 (2007) 5134.

[11] J. Yoon, E. I. Solomon, Coord. Chem. Rev. 251 (2007) 379.

[12] T. Glaser, M. Heidemeier, J. B. H. Strautmann, H. Bogge, A. Stammler, E. Krickemeyer, R. Huenerbein, S. Grimme, E. Bothe, E. Bill, Chem. Eur. J. 13 (2007) 9191.

[13] B. Sarkar, M. S. Ray, Y. -Z. Li, Y. Song, A. Figuerola, E. Ruiz, J. Cirera, J. Cano, A. Ghosh, Chem. Eur. J. 13 (2007) 9297.

[14] M.A. Ali, D.A. Chowdhury, M. Nazimuddin, Polyhedron 3 (1984) 595.

[15] D.X. West, A.E. Liberta, S.B. Padhye, R.C. Chikate, P.B. Sonawane, A.S. Kumbhar, R.G. Yerande, Coord. Chem. Rev. 123 (1993) 49.

[16] 16. D.X. West, J.S. Ives, G.A. Bain, A.E. Liberta, J. Valdes-Martinez, K.H. Ebert, S. H-Ortega, Polyhedron 16 (1997) 1895.

[17] P.F. Rapheal, E. Manoj, M.R.P. Kurup, Polyhedron 26 (2007) 818.

[18] R.C. Chikate, A.R. Belapure, S.B. Padhye, D.X. West, Polyhedron 24 (2005) 889.

[19] Z. Afrasiabi, E. Sinn, J. Chen, Y. Ma, A.L. Rheingold, L.N. Zakharov, N. Rath, S. Padhye, Inorg. Chim. Acta 357 (2004) 271.

[20] E.C. Alyea, G. Fergusen, R.J. Restivo, Inorg. Chem. 14 (1975) 2491.

[21] K. Nakamoto, Infrared and Raman Spectra of Inorganic and Coordination Compounds, Part B, 5th edition, Wiley, New York, 1997.

[22] M. Morshedi, M. Amirnasr, A.M.Z. Slawin, J.D. Woollins, A.D. Khalaji, Polyhedron 28 (2009) 167.

[23] S.D. Robinson, M.F. Uttley, J. Chem. Soc. (1973) 1912.

[24] R.A. Bailey, S.L. Kozak, T.W. Michelson, W.N. Mills, Coord. Chem. Rev. 6 (1971) 407.

[25] J.R. Wasson, C. Trapp, J. Phys. Chem. 73 (1969) 3763.

[26] M.J. Bew, B.J. Hathaway, R.R. Faraday, J. Chem. Soc., Dalton Trans. (1972) 1229.

[27] B.J. Hathaway, R.J. Dudley, P. Nicholls, J. Chem. Soc. (A) (1969) 1845.

[28] B.J. Hathaway, I.M. Procter, R.S. Slade, A.A. Tomlinson, J. Chem. Soc. (A) (1969) 2219.

[29] R. J. Dudley, B. J. Hathaway, J. Chem. Soc. (A), (1970) 1725.

[30] A.B.P. Lever, Inorganic Electronic Spectroscopy, 2nd ed., Elsevier Science, Netherlands, 1986.

[31] R.P. John, A. Sreekanth, M.R.P. Kurup, S.M. Mobin, Polyhedron 21 (2002) 2515.

[32] D. Kivelson, R. Neiman, J. Chem. Phys. 35 (1961) 149.

[33] V. Philip, V. Suni, M.R.P. Kurup, M. Nethaji, Polyhedron 25 (2006) 1931.

[34] I.M. Procter, B.J. Hathaway, P. Nicholis, J. Chem. Soc. (1968) 1678.

[35] B.J. Hathaway, D.E. Billing, Coord. Chem. Rev. 5 (1970) 1949.

[36] E.B. Seena, M.R.P. Kurup, Polyhedron 26 (2007) 829.

[37] D. Reinen, C. Friebel, Inorg. Chem. 23 (1984) 791.

[38] A.H. Maki, B.R. McGarvey, J. Chem. Phys. 29 (1958) 35.

[39] M. Antosik, N.M.D. Brown, A.A. McConnell, A.L. Porte, J. Chem. Soc. A (1969) 545.

[40] B.J. Hathaway, G. Wilkinson, R.D. Gillard, J.A. McCleverty (Eds.), Comprehensive Coordination Chemistry, Pergamon, Oxford, 1987.

[41] M. Joseph, M. Kuriakose, M.R.P. Kurup, E. Suresh, A. Kishore, S.G. Bhat, Polyhedron 25 (2006) 61.

[42] P. Bindu, M.R.P. Kurup, T.R. Satyakeerty, Polyhedron 18 (1999) 321.

[43] R.P. John, A. Sreekanth, V. Rajakannan, T.A. Ajith, M.R.P. Kurup, Polyhedron 23 (2004) 2549.

[44] G.M. Sheldrick SHELXL-97 and SHELXS-97, Program for the Solution of Crystal Structures, University of Göttingen, Germany, 1997.

[45] K. Brandenburg, Diamond Version 3.1f, Crystal Impact GbR, Bonn, Germany, 2008.

[46] C.F. Macrae, P.R. Edgington, P. McCabe, E. Pidcock, G.P. Shields, R. Taylor, M. Towler, J. Van de Streek, J. Appl. Cryst. 39 (2006) 453.

[47] D. Natale, J.C. Mareque-Rivas, Chem. Commun. (2008) 425.

[48] D. Cremer, J.A. Pople, J. Amer. Chem. Soc. 97 (1975) 1354.

........................෨෨෨........................

SYNTHESES, SPECTRAL AND STRUCTURAL CHARACTERIZATION OF Zn(II) AND Cd(II) COMPLEXES OF KETONE BASED N(4)-SUBSTITUTED THIOSEMICARBAZONES

7.1. Introduction

Zinc and cadmium have the electronic configuration $d^{10}s^2$ and typically form Zn^{2+} and Cd^{2+} ions. In view of the stability of the filled d sublevel, the element shows few of the characteristics of transition metals despite its position in the d-block of the periodic table. Zn^{2+} and Cd^{2+} occur largely in four coordination spheres as tetrahedral complexes. They also form octahedral complexes. The octahedral complexes of zinc are not very stable. But cadmium forms octahedral complexes readily and they are more stable than zinc complexes because of its larger size [1].

The chemical similarity of Zn(II) and Cd(II) suggest that the latter may displace the former active site in enzyme containing Zn(II). Zinc atom has either a structural or analytical role in several proteins. It has been recognized as an important cofactor in biological molecules, either as a structural template in protein folding or as a Lewis acid catalyst that can readily adopt 4, 5 or 6 coordination [2]. Zinc is able to play a catalytic role in the activation of thiols as nucleophiles at physiological pH. Mononuclear zinc complexes may serve as model compounds for zinc enzymes such as phospholipase C, bovine lens

leucine aminopeptidase, ATPases, carbonic anhydrases and peptide deformylase. Binuclear cores are versatile at active sites of many metalloenzymes and play essential role in biological systems [3]. Zinc is an essential element, necessary for sustaining all life. In the human body, generally, 2-3 g of zinc is present and about 15 mg per day is necessary for the maintenance of healthy condition. It is estimated that about 3000 proteins in the human body contain zinc.

The zinc(II) ion is known to have a high affinity towards nitrogen and sulfur donor ligands. Zinc(II) - sulfur interactions are of great interest in biochemical systems, due to the presence of sulfur at the active sites of several enzymes, vitamins and proteins. Biologically it is the second most important transition metal. It resembles other transition metals in the formation of stable complexes with O, N and S - donor ligands and with ions like cyanide, halide etc. The d^{10} configuration affords no crystal field stabilization, which implies that the stereochemistry of a Zn^{2+} complex depends on the size and polarizing power of this ion. Because of this versatility towards different kinds of ligands and its flexibility towards coordination number ranging from two to six, the zinc(II) ion provides various types of chelate complexes. Among these complexes, some have attracted special attention as model compounds for the active sites of zinc-containing enzymes [4,5] and their functions strongly depend upon the coordination environment around the zinc ion. Therefore, for understanding or creating functional zinc complexes, it is important to consider the relationship of the coordination characteristics peculiar to the zinc ion.

Cadmium is an extremely toxic element that is naturally present in the environment and also as a result of human activities. There is substantial interest in the coordination chemistry of cadmium complexes because of the toxic environmental impact of cadmium. The mobilization and immobilization

of cadmium in the environment, in organisms and in some technical processes (such as in ligand exchange chromatography) have been shown to depend significantly on the complexation of the metal center by chelating nitrogen donor ligands [6]. Complexes of Cd(II) with different molecular architectures with the same trimesate ligands showing strong fluorescence have been reported [7]. Though cadmium has been known as a toxic metal and is often associated with mercury and lead as one of the biologically harmful metal ions, the cadmium(II) ion has recently been found to serve as the catalytic center in a newly discovered carbonic anhydrase [8].

Thiosemicarbazones and their metal complexes have been subject of interest in numerous studies because of their chemical and biological activities, in as much as possess a wide range of beneficial medicinal properties that are often attributed to their chelating ability with metal ions. Really, an important number of thiosemicarbazones being NNS tridentate donors possess carcinostatic efficacy and substantial *in vivo* activity against various human tumor lines but structural variations in some thiosemicarbazones with regard to the chelating ability may be destroy or reduce its medicinal value. Complexes of Group 12 metals, zinc and cadmium, can provide an interesting range of stoichiometries depending on the preparative salts [9]. In this chapter we report the syntheses, spectral and structural characterization of zinc(II) and cadmium(II) complexes of the ligand di-2-pyridyl ketone-*N*(4)-methyl thiosemicarbazone (HDpyMeTsc).

7.2. Experimental

7.2.1. Materials

All the chemicals and solvents used for the syntheses were of analytical grade. Di-2-pyridyl ketone (Aldrich), *N*(4)-methyl thiosemicarbazide (Aldrich),

zinc(II) acetate dihydrate (Aldrich), zinc(II) nitrate hexahydrate (E-Merk), zinc(II) chloride (E-Merk), cadmium(II) acetate dihydrate (E-Merk), sodium azide (Reidel-De Haen), ethanol and methanol were used as supplied.

7.2.2. Synthesis of the ligand

The synthesis of the thiosemicarbazone ligand, HDpyMeTsc has been described already in Chapter 2.

7.2.3. Syntheses of zinc(II) complexes of di-2-pyridyl ketone-*N*(4)-methyl thiosemicarbazone

7.2.3a. Synthesis of [Zn(DpyMeTsc)₂] (23)

To a solution of HDpyMeTsc (0.542 g, 2 mmol) in hot ethanol was added a methanolic solution of $Zn(CH_3COO)_2 \cdot 2H_2O$ (0.219 g, 1 mmol). The mixture was heated under reflux for 2 hours and cooled. The yellow colored complex obtained was filtered, washed with ethanol, ether and dried over P_4O_{10} *in vacuo*.

λ_m (DMF): 21 ohm⁻¹ cm² mol⁻¹, Elemental Anal. Found (Calcd.) (%): C: 51.14 (51.52); H: 3.59 (3.99); N: 23.14 (23.11).

7.2.3b. Synthesis of [Zn(DpyMeTsc)(CH₃COO)] (24)

To a solution of the ligand, HDpyMeTsc (0.271 g, 1 mmol) in hot ethanol, was added a methanolic solution of $Zn(CH_3COO)_2 \cdot 2H_2O$ (0.219 g, 1 mmol). The mixture was heated under reflux for 2 hours and cooled. Yellow solid obtained soon after refluxing was filtered, washed with ethanol and then with ether and dried over P_4O_{10} *in vacuo*.

λ_m (DMF): 2 ohm⁻¹ cm² mol⁻¹, Elemental Anal. Found (Calcd.) (%): C: 45.67 (45.63); H: 3.64 (3.83); N: 17.96 (17.74).

7.2.3c. Synthesis of [Zn(DpyMeTsc)N₃] (25)

HDpyMeTsc (0.271 g, 1 mmol) was dissolved in ethanol by heating. To this solution, NaN_3 (0.065 g, 1 mmol) in water and $Zn(CH_3COO)_2 \cdot 2H_2O$ (0.219 g, 1 mmol) in hot methanol were added and stirred the mixture for 4 hours. Yellow precipitate obtained was filtered, washed with ethanol followed by ether and dried over P_4O_{10} *in vacuo*.

λ_m (DMF): 4 ohm^{-1} cm^2 mol^{-1}, Elemental Anal. Found (Calcd.) (%): C: 41.29 (41.33); H: 2.95 (3.20); N: 29.44 (29.66).

7.2.3d. Synthesis of [Zn(HDpyMeTsc)Cl₂] (26)

To a solution of HDpyMeTsc (0.271 g, 1 mmol) in hot ethanol was added a methanolic solution of $ZnCl_2$ (0.136, 1 mmol). The mixture was heated under reflux for two hours and cooled. The yellow colored complex obtained was filtered, washed with ethanol and ether and dried over P_4O_{10} *in vacuo*.

λ_m (DMF): 12 ohm^{-1} cm^2 mol^{-1}, Elemental Anal. Found (Calcd.) (%): C: 38.50 (38.30); H: 3.37 (3.21); N: 17.21 (17.18).

7.2.3e. Synthesis of [Zn(DpyMeTsc)(NO₃)] (27)

To a solution of the ligand, HDpyMeTsc (0.271 g, 1 mmol) in hot ethanol, was added a solution of $Zn(NO_3)_2 \cdot 6H_2O$ (0.297 g, 1 mmol) in methanol. The mixture was refluxed for 2 hours and allowed to stand at room temperature. The yellow crystalline precipitate obtained was filtered, washed with ethanol followed by ether and dried over P_4O_{10} *in vacuo*.

λ_m (DMF): 21 ohm^{-1} cm^2 mol^{-1}, Elemental Anal. Found (Calcd.) (%): C: 39.27 (39.26); H: 2.97 (3.04); N: 21.26 (21.13).

7.2.4. Syntheses of cadmium(II) complexes of di-2-pyridyl ketone-*N*(4)-methyl thiosemicarbazone

7.2.4a. Synthesis of [Cd(DpyMeTsc)₂] (28)

To a solution of HDpyMeTsc (0.542 g, 2 mmol) in hot ethanol was added a methanolic solution of $Cd(CH_3COO)_2 \cdot 2H_2O$ (0.266 g, 1 mmol). The mixture was heated under reflux for two hours and cooled. The yellow colored complex obtained was filtered, washed with ethanol and ether and dried over P_4O_{10} *in vacuo*.

λ_m (DMF): 2 ohm⁻¹ cm² mol⁻¹, Elemental Anal. Found (Calcd.) (%): C: 47.30 (47.82); H: 3.57 (3.70); N: 21.56 (21.45).

7.2.4b. Synthesis of [Cd(DpyMeTsc)(CH₃COO)] (29)

To a solution of the ligand, HDpyMeTsc (0.271 g, 1 mmol) in hot ethanol, was added a methanolic solution of $Cd(CH_3COO)_2 \cdot 2H_2O$ (0.266 g, 1 mmol). The mixture was heated under reflux for two hours and cooled. Yellow solid obtained soon after refluxing was filtered, washed with ethanol and then with ether and dried over P_4O_{10} *in vacuo*.

λ_m (DMF): 2 ohm⁻¹ cm² mol⁻¹, Elemental Anal. Found (Calcd.) (%): C: 41.08 (40.78); H: 3.38 (3.42); N: 15.85 (15.85).

7.2.4c. Synthesis of [Cd(DpyMeTsc)N₃] (30)

HDpyMeTsc (0.271 g, 1 mmol) was dissolved in ethanol by heating. To this solution, NaN₃ (0.065 g, 1 mmol) in water and $Cd(CH_3COO)_2 \cdot 2H_2O$ (0.266 g, 1 mmol) in hot methanol were added and stirred the mixture for 4 hours.

Yellow precipitate obtained was filtered, washed with ethanol followed by ether and dried over P_4O_{10} *in vacuo*.

λ_m (DMF): 11 ohm^{-1} cm^2 mol^{-1}, Elemental Anal. Found (Calcd.) (%): C: 36.20 (36.76); H: 2.76 (2.85); N: 25.83 (26.38).

Caution: Although no problems were encountered during this research, azido complexes of metal ions with organic ligands are potentially explosive. So they should be prepared in small quantities and handled with care.

7.3. Results and discussion

Five Zn(II) complexes and three Cd(II) complexes of thiosemicarbazone were prepared and they are found to be yellow in color. The molar conductivities of the complexes in DMF (10^{-3} M) solution were measured at 298 K with a Systronic model 303 direct-reading conductivity bridge, which suggest that these complexes are non-electrolytic in nature [10]. In the complex **26**, the thiosemicarbazone moiety is in the thioamido form, while in all other complexes, the thiosemicarbazones deprotonate and chelate in thiolate form as evidenced by the IR spectral data. The complexes are found to be diamagnetic as expected for a d^{10} Zn(II) system.

7.3.1. Infrared spectra

The IR spectrum of the free ligand when compared with those of complexes confirm the coordination of the thiosemicarbazone to the metal. The significant bands observed in the IR spectrum of the ligand and its complexes with the tentative assignments are summarized in Table 7.1.

The v(C=N) band of thiosemicarbazone is found to be shifted to lower frequencies in all complexes representing the coordination *via* the azomethine nitrogen [11,12]. Strong band found at 1110 cm⁻¹ in the ligand is assigned to the v(N–N) band of the thiosemicarbazone. The increase in the frequency of this band in the spectra of complexes is due to the increase in the bond strength, again confirming the coordination *via* the azomethine nitrogen. In the spectrum of complex **26**, the band corresponding to the newly formed C=N bond due to the enolization of the ligand is absent, while this band is present in the spectra of all other complexes. This observation supports the enolization of the ligand into the thiolate form during coordination with the metal to form these complexes. Coordination *via* thiolate sulfur is also indicated by the downward shift of frequencies of v/δ(CS) bands found at 1431 and 800 cm⁻¹ [13]. The in-plane bending vibrations of the pyridine ring in uncomplexed ligand shift to higher frequencies on complexation, confirming the coordination of the ligands to the metal *via* the pyridine nitrogen [14]. The IR spectra of complexes are given in Figs. 7.1–7.8.

Table 7.1. IR spectral data (cm⁻¹) of Zn(II)/Cd(II) complexes

Compound	v(C=N)	v(C=N)[a]	v/δ(C–S)	v(N–N)	py(ip)
HDpyMeTsc	1588	...	1431, 800	1110	618
[Zn(DpyMeTsc)₂] (**23**)	1512	1589	1384, 786	1152	658
[Zn(DpyMeTsc)(CH₃COO)] (**24**)	1484	1593	1374,779	1169	657
[Zn(DpyMeTsc)N₃] (**25**)	1517	1594	1384, 781	1181	635
[Zn(HDpyMeTsc)Cl₂] (**26**)	1541	...	1438, 799	1174	650
[Zn(DpyMeTsc)(NO₃)] (**27**)	1516	1600	1383, 787	1172	657
[Cd(DpyMeTsc)₂] (**28**)	1545	1588	1361, 784	1175	626
[Cd(DpyMeTsc)(CH₃COO)] (**29**)	1503	1594	1374, 788	1172	670
[Cd(DpyMeTsc) N₃] (**30**)	1557	1593	1383, 781	1172	624

[a] Newly formed C=N
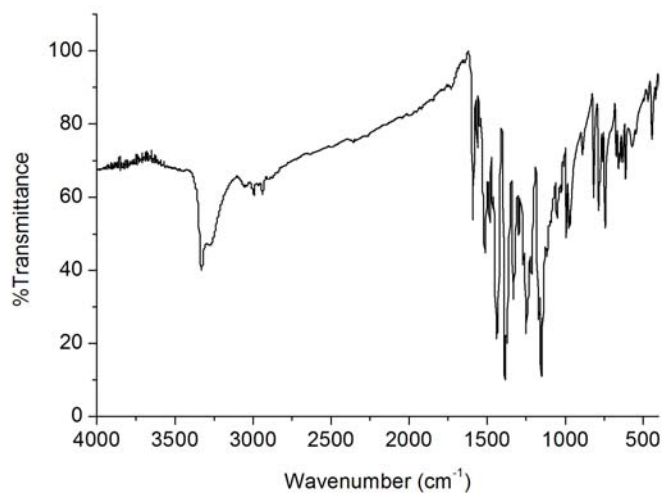
Fig. 7.1. IR spectrum of [Zn(DpyMeTsc)₂] (**23**)
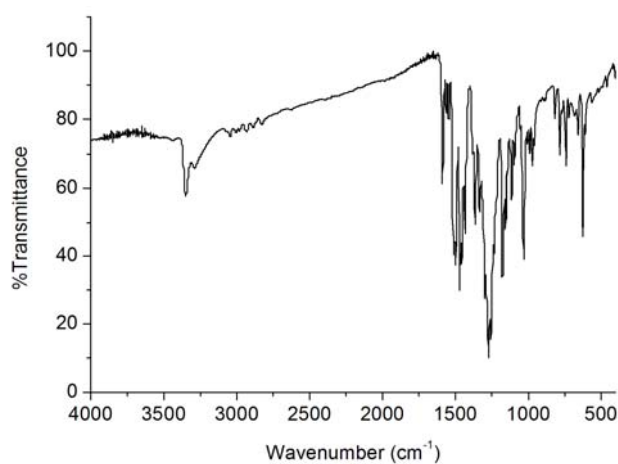
Fig. 7.2. IR spectrum of [Cd(DpyMeTsc)₂] (**28**)

The spectra of acetate-containing complexes **24** and **29** display relatively strong bands at 1513 and 1563 cm^{-1} respectively due to v_{as}(COO) and at 1428 and 1434 cm^{-1} respectively due to v_s(COO) support the unidentate nature of the acetate group in this compounds.
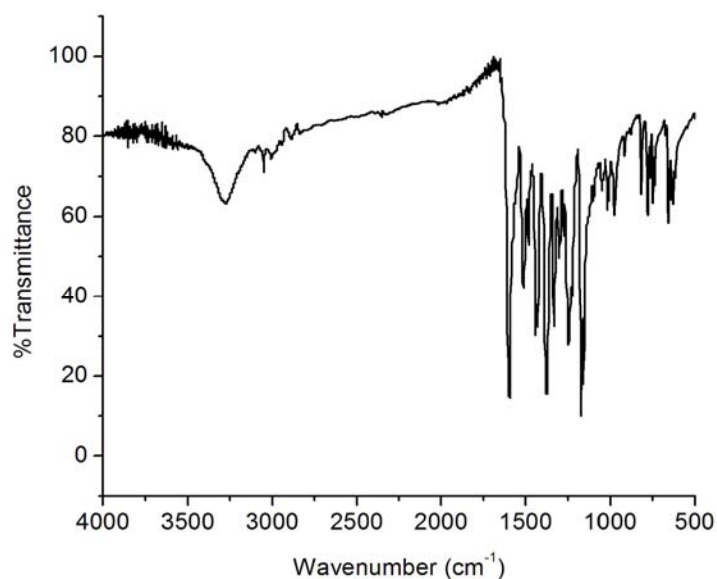
Fig. 7.3. IR spectrum of [Zn(DpyMeTsc)(CH₃COO)] **(24)**
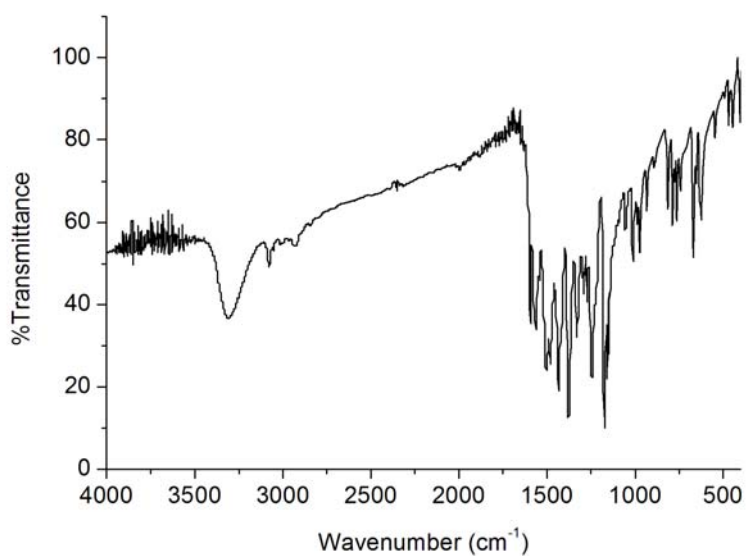
Fig. 7.4. IR spectrum of [Cd(DpyMeTsc)(CH₃COO)] **(29)**

The azido complexes **25** and **30** show strong bands at 2061 and 2040 cm^{-1} respectively due to asymmetric $\nu(N_3)$ mode. The bands associated with the symmetric $\nu(N_3)$ modes are located at 1300 cm^{-1} for **25** and 1275 cm^{-1} for **30**.

The broad bands observed at 676 and 662 cm^{-1} are assigned to δ(N–N–N) vibrations.
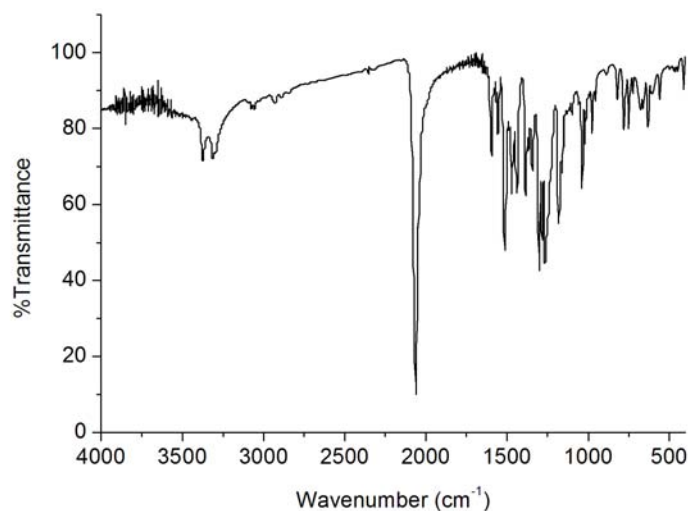
Fig. 7.5. IR spectrum of [Zn(DpyMeTsc)N$_3$] (**25**)
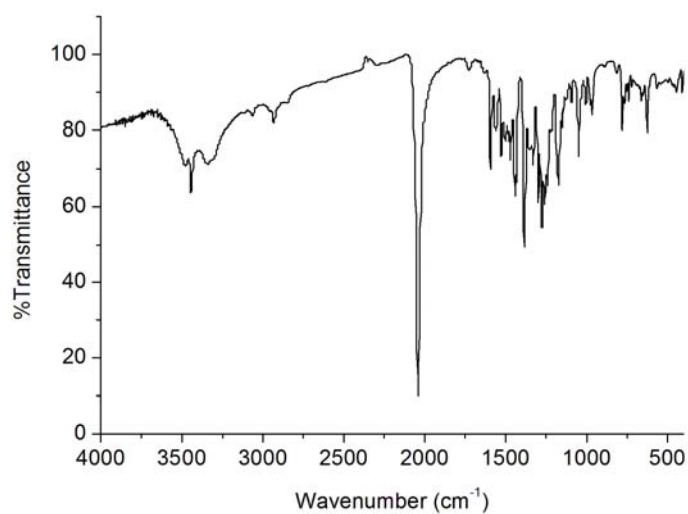
Fig. 7.6. IR spectrum of [Cd(DpyMeTsc) N$_3$] (**30**)

The spectrum of **27** exhibited bands at 1442, 1336 and 1020 cm^{-1} with a separation of 106 cm^{-1} between two highest-frequency bands, indicating the presence of monodentate nitrato ion [15].
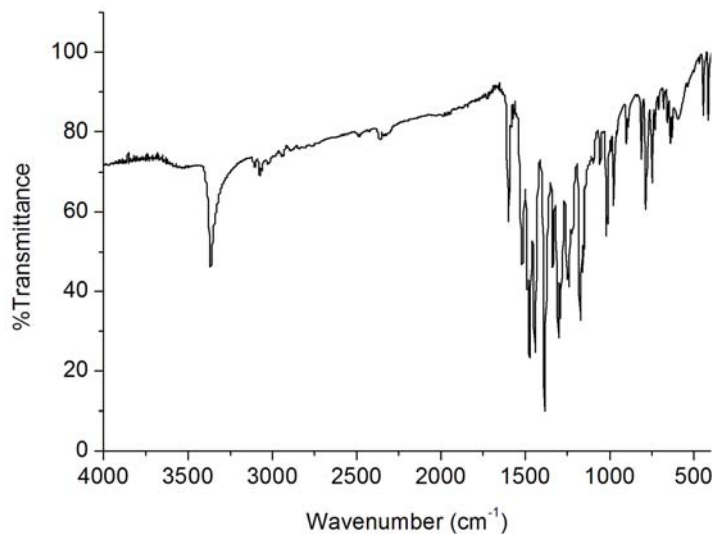
Fig. 7.7. IR spectrum of [Zn(DpyMeTsc)(NO$_3$)] **(27)**

The expected region for zinc-halide stretching frequencies for complex **26** is below 400 cm^{-1} which is beyond the scan range.
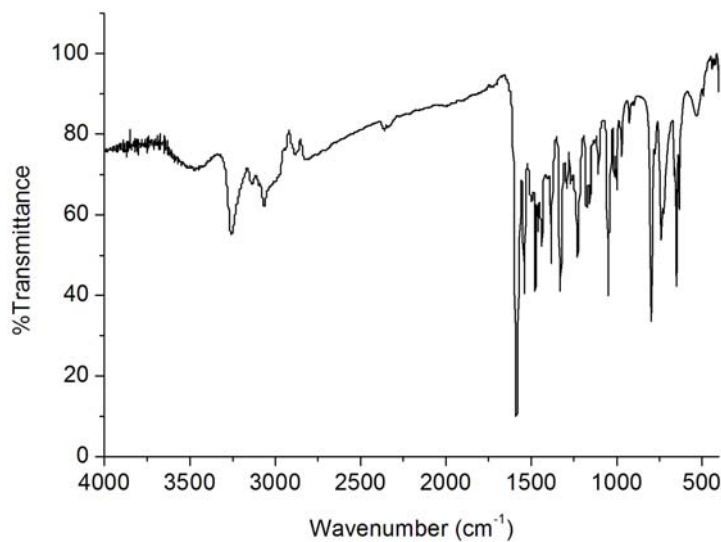
Fig. 7.8. IR spectrum of [Zn(HDpyMeTsc)Cl$_2$] **(26)**

7.3.2. Electronic spectra

The electronic spectral assignments for the free ligand (HDpyMeTsc) and its Zn(II)/Cd(II) complexes recorded in acetonitrile solution are summarized in Table 7.2. The electronic spectrum of HDpyMeTsc recorded in acetonitrile solution showed bands at 35890 and 29280 cm^{-1} assignable to $\pi \rightarrow \pi^*$ transitions of the pyridyl ring and thiosemicarbazone moiety [16]. The energy of these bands are slightly shifted on complexation. In addition to these intra-ligand bands, new bands around 23500-25100 cm^{-1} range are observed in the spectra of complexes. This bands can safely be assigned to metal$\rightarrow$ligand charge-transfer bands. No appreciable absorptions occurred below 20000 cm^{-1}, indicating the absence of *d-d* bands, which is in accordance with the d^{10} configuration of the Zn(II) and Cd(II) ion [17]. The electronic spectra of complexes are given in Figs. 7.9–7.12.

Table 7.2. Electronic spectral data (cm^{-1}) of Zn(II)/Cd(II) complexes

Compound	UV absorption bands (cm^{-1})			
HDpyMeTsc	35890	29280		
[Zn(DpyMeTsc)$_2$] **(23)**	34450	29020	23980	
[Zn(DpyMeTsc)(CH$_3$COO)] **(24)**	33260	29810	24570	
[Zn(DpyMeTsc)N$_3$] **(25)**	34400	29130	24160	
[Zn(HDpyMeTsc)Cl$_2$] **(26)**	43830	35700	29250	24240
[Zn(DpyMeTsc)(NO$_3$)] **(27)**	38820	33030	25010	
[Cd(DpyMeTsc)$_2$] **(28)**	37670	32620	24750	
[Cd(DpyMeTsc)(CH$_3$COO)] **(29)**	37680	33520	24700	
[Cd(DpyMeTsc)N$_3$] **(30)**	32700	24750		

[Zn(DpyMeTsc)$_2$] **(23)**

[Zn(DpyMeTsc)(CH$_3$COO)] **(24)**
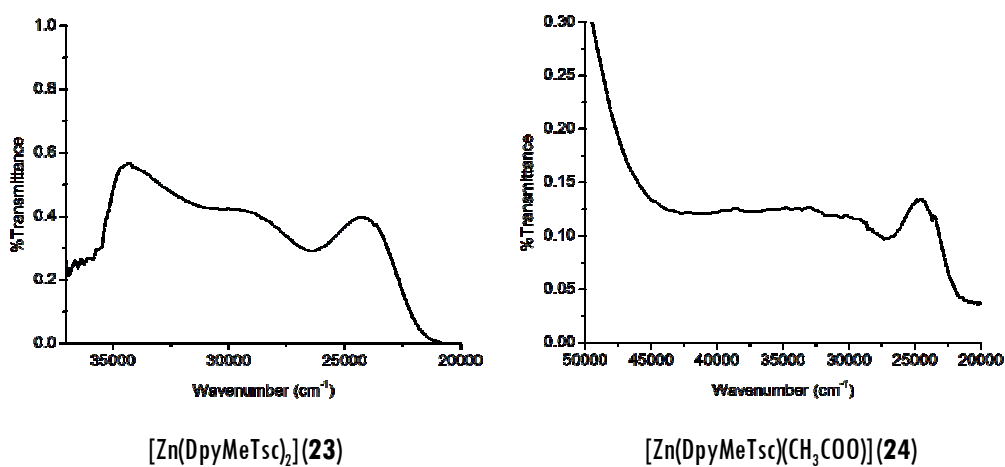
Fig. 7.9. Electronic spectra of **23** and **24**

[Zn(DpyMeTsc)N$_3$] **(25)**

[Zn(HDpyMeTsc)Cl$_2$] **(26)**
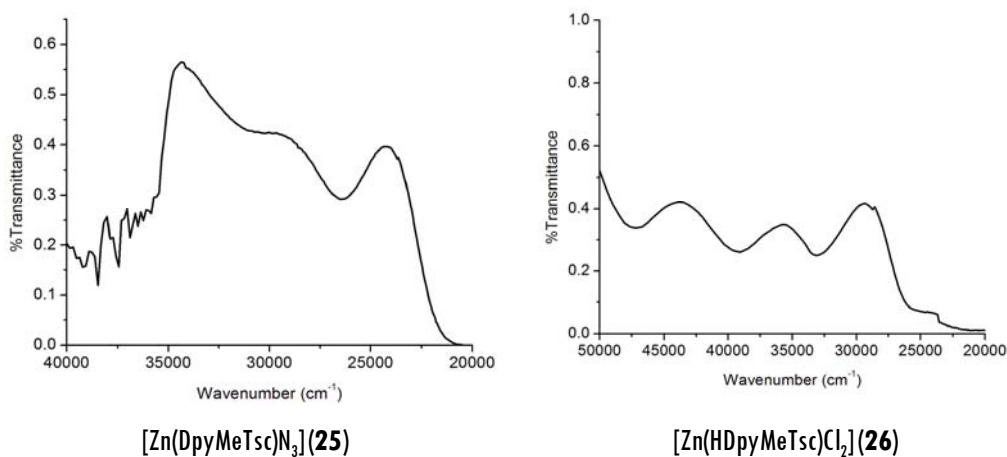
Fig. 7.10. Electronic spectra of **25** and **26**

[Zn(DpyMeTsc)(NO$_3$)] **(27)**

[Cd(DpyMeTsc)$_2$] **(28)**
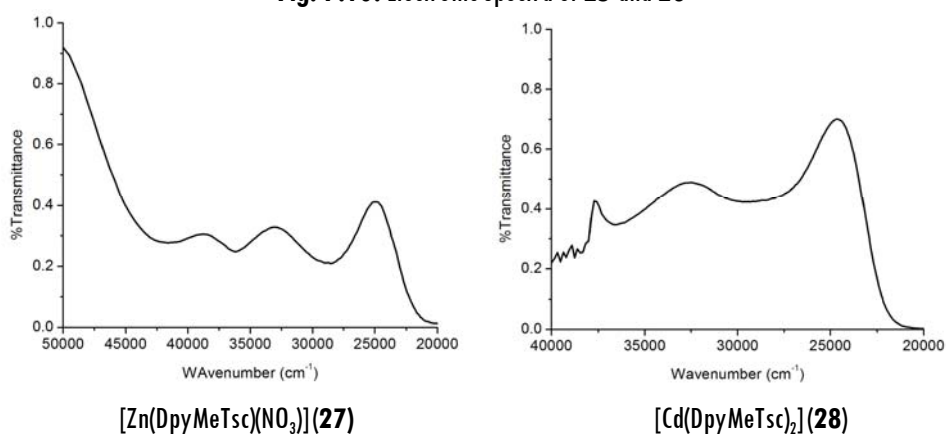
Fig. 7.11. Electronic spectra of **27** and **28**

[Cd(DpyMeTsc)(CH₃COO)] **(29)**   [Cd(DpyMeTsc) N₃] **(30)**
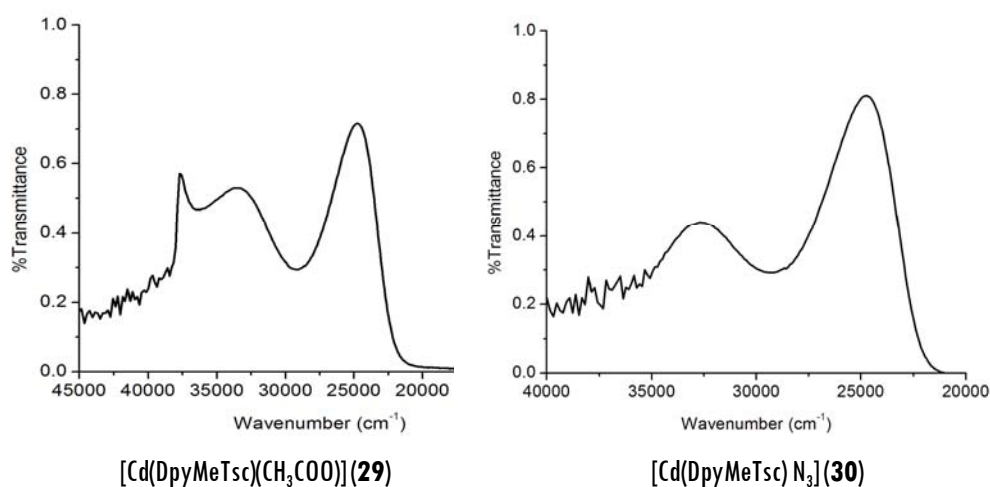
Fig. 7.12. Electronic spectra of **29** and **30**

7.3.3. Crystal structure of [Zn(DpyMeTsc)(NO₃)]₂ (27)

X-ray quality light yellow single crystals of compound **27** were obtained by slow evaporation from its ethanol solution at room temperature in air and the data were collected on a Bruker SMART APEX diffractometer equipped with graphite monochromated radiation (λ = 0.71073 Å) at room temperature. The structure was solved using SHELXTL-97 [18] program and refined by full-matrix least-squares on F^2 with anisotropic displacement parameters for non-hydrogen atoms. The Bruker SAINT software was used for data reduction and Bruker SMART for cell refinement. The crystallographic data and structure refinement parameters for the compound **27** are given in Table 7.3.

Molecular graphics employed was DIAMOND [19]. Molecular structure of the compound along with atom labeling scheme is shown in Fig. 7.13.
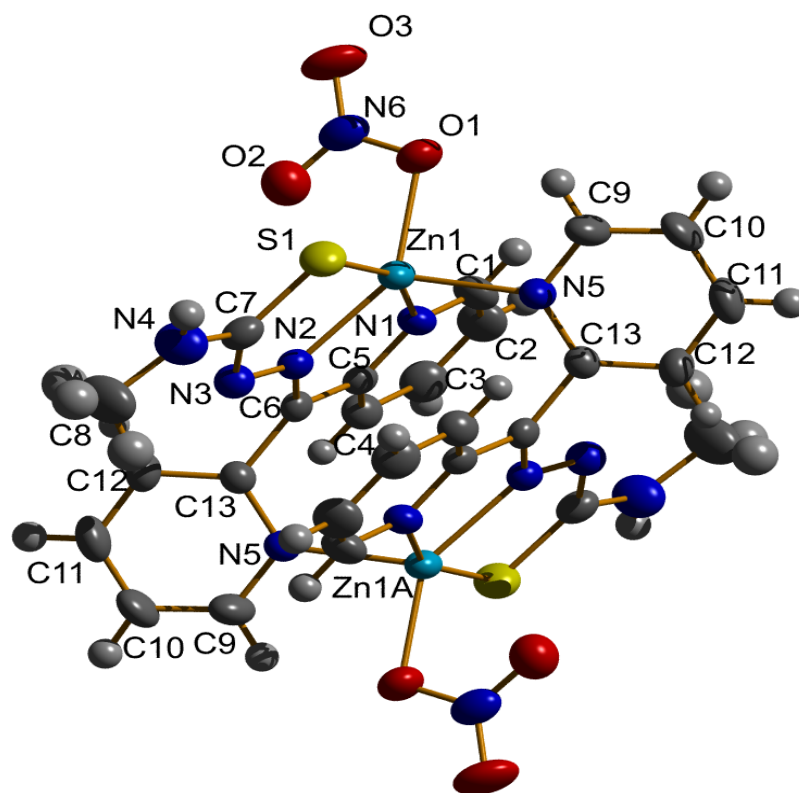
Fig. 7.13. Molecular structure of [Zn(DpyMeTsc)(NO₃)]₂ (**27**) along with atom numbering scheme.

The structure consists of two units of [Zn(DpyMeTsc)(NO$_3$)]. The lattice nature is monoclinic with space group *P*2$_1$/n. The structure contains two zinc centers where each center is pentacoordinate with pyridyl nitrogen, azomethine nitrogen, thiolate sulfur, one oxygen of nitrate anion and pyridyl nitrogen N(5) of the second thiosemicarbazone moiety. The trigonality index τ is calculated using the equation $\tau = (\beta-\alpha)/60$ [20] (for perfect square pyramidal and trigonal bipyramidal geometries the values of τ are zero and unity, respectively). The value of τ for the molecule is 0.268, which shows the coordination polyhedron around each zinc atom is a distorted square pyramid.

Table7.3 Crystal refinement parameters of [Zn(DpyMeTsc)(NO$_3$)]$_2$ **(27)**

Empirical formula	C$_{26}$H$_{24}$Zn$_2$ N$_{12}$O$_6$S$_2$
Formula weight	795.49
Temperature (T) K	298(2) K
Wavelength (Mo Kα) (Å)	0.71073
Crystal system	monoclinic
Space group	$P2_1$/n
Lattice constants	
a(Å)	9.3364(10)
b(Å)	15.8438(17)
c(Å)	10.9903(12)
α (°)	90.00
β (°)	100.520(2)
γ(°)	90.00
Volume V (Å^3)	1598.4(3)
Z	2
Calculated density (ρ) (Mg m^{-3})	1.653
Absorption coefficient, μ (mm^{-1})	1.693
F(000)	808.0
θ range for data collection	2.28 to 26.13
Limiting indices	-11≤h≤11, -19≤k≤19, -13≤l3
Reflections collected	16441
Unique Reflections (R$_{int}$)	3190 [R$_{(int)}$ = 0.0371]
Refinement method	Full-matrix least-squares on F^2
Data / restraints / parameters	3190 / 0 / 218
Goodness-of-fit on F^2	1.085
Final R indices [I > 2σ (I)]	R$_1$ = 0.0380 , wR$_2$ = 0.0821
R indices (all data)	R$_1$ = 0.0468, wR$_2$ = 0.0860

R$_1$ = Σ||F$_o$| - |F$_c$|| / Σ|F$_o$|

wR$_2$ = [Σw(F$_o^2$-F$_c^2$)^2 / Σw(F$_o^2$)^2]$^{1/2}$

The base of each distorted square pyramidal unit is occupied by the thiosemicarbazone ligand and the unidentate nitrate group. The pyridyl nitrogen of the second thiosemicarbazone moiety plugs in to the axial position resulting in a dimer with a Zn-Zn separation of approximately 5.072 Å. There is not much differences between the bond distance of Zn–N$_{azomethine}$ and Zn–N$_{py}$ bonds; this may be attributed to the fact that the the two bonds are equally strong. But, the Zn–S bond is longer than Zn–N bonds, suggest that nitrogen coordination is stronger than sulfur coordination. The relevant bond lengths and bond angles are given in Table 7.4.

The distortion from the regular square geometry is evident from the departure of the bond angles around Zn(II) [N(1)–Zn(1)–N(2) (75.96(8)), N(2)–Zn(1)–S(1) (81.03(6)), S(1)–Zn(1)–O(1) (99.29(6)), O(1)–Zn(1)–N(1) (96.55(8))] from 90º. The found distortion may be due to the rigidity of the chelate rings formed.

Table 7.4. Selected bond lengths (Å) and bond angles (°) for [Zn(DpyMeTsc)(NO$_3$)]$_2$ (**27**)

Bond lengths (Å)		Bond angles (°)	
Zn(1)—N(1)	2.127(2)	N(1)—Zn(1)—N(2)	75.96(8)
Zn(1)—N(2)	2.121(2)	N(2)— Zn(1)—S(1)	81.03(6)
Zn(1)—S(1)	2.353(9)	S(1)— Zn(1)—O(1)	99.29(6)
Zn(1)—N(5)	2.132(2)	N(1)—Zn(1)—O(1)	96.55(8)
Zn(1)—O(1)	2.104(2)	N(2)— Zn(1)—O(1)	140.66(8)
N(2)—C(6)	1.294(3)	N(1)— Zn(1)—S(1)	156.78(6)
N(2)—N(3)	1.358(3)	N(5)— Zn(1)—N(1)	91.12(9)
N(3)—C(7)	1.327(3)	N(5)— Zn(1)—O(1)	92.35(8)
N(4)—C(7)	1.344(4)		
S(1)—C(7)	1.734(3)		

The crystal structure is stabilized by π-π, ring-metal and hydrogen bonding interactions which are shown in Table 7.5. Additional Y–X···π ring interactions are found between N(6)–O(3) [1] and Cg(5) with $d_{O(3)—Cg}$ = 3.253 Å [sym. code: ½ + x, ½ - y, -½ + z]. Ring-metal interactions Cg(3)--Zn(1) [sym. code: -x, -y, −z] is observed at a distance of 3.795 Å. There are no C–H···π interactions seen in the crystal structure.

Table 7.5. Interaction parameters of [Zn(DpyMeTsc)(NO₃)]₂ **(27)**

Hydrogen bonding

D—H···A (Å)	D—H (Å)	H···A (Å)	D···A (Å)	D—H···A(°)
N4(H) ···O(1)	0.86	2.51	3.274	149

D = donor; A = acceptor

π-π interactions

Cg(I)···Cg(J)	Cg···Cg (Å)	α (°)	β (°)
Cg(1)···Cg(4)ᵃ	3.863	78.82	32.43
Cg(2)···Cg(1)ᵃ	2.951	85.90	57.40
Cg(2)···Cg(3)ᵇ	3.884	3.18	38.86
Cg(2)···Cg(4)ᵇ	3.372	7.10	15.86
Cg(3)···Cg(1)ᵃ	2.795	82.86	56.16
Cg(3)···Cg(2)ᵇ	3.884	3.18	36.13
Cg(3)···Cg(3)ᵇ	3.110	0	10.03
Cg(4)···Cg(2)ᵇ	3.372	7.10	16.96

Equivalent position codes: a = x, y, z; b = - x, - y, - z

Cg(1) = Zn(1), O(1),N(6), O(2);
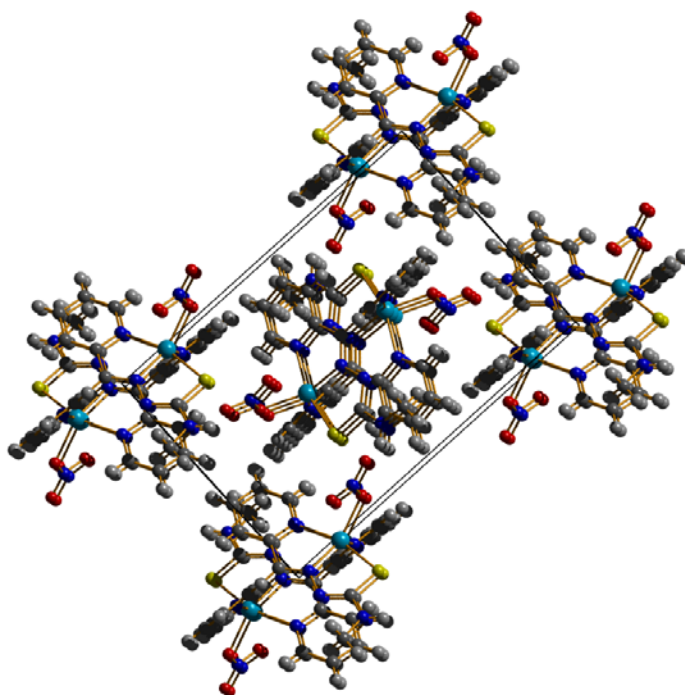
Cg(2) = Zn(1), S(1), C(7), N(3), N(2);

Cg(3) = Zn(1), N(1), C(5), C(6), N(2);
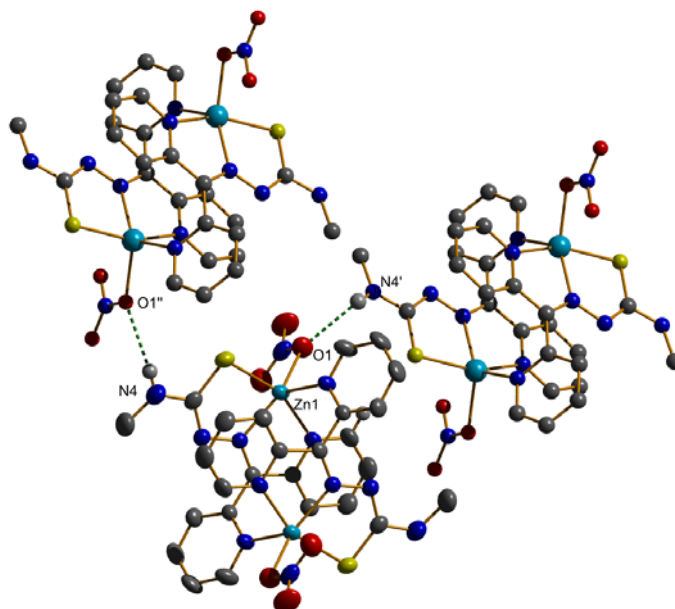
Cg(4) = N(1), C(1), C(2), C(3), C(4), C(5)

α (°) = Dihedral angle between planes I and J;

β (°) = Angle between Cg(I)-Cg(J) vector and normal to plane I.

Fig. 7.14. The unit cell packing diagram of the compound 27 viewed along a-axis

Fig. 7.15. Packing diagram of compound **27** showing H-bonding

References

[1] J.E. Huheey, E.A. Keiter, R.A. Keiter, Inorganic Chemistry, 4th Ed, Harper Collin College Publishers, New York (1993).

[2] K. Peariso, C.W. Goulding, S. Huang, R.G. Matthews, J.E. Penner-Hahn, J. Am. Chem. Soc. 120 (1998) 8410.

[3] E.B. Seena, M.R.P. Kurup, Spectrochim. Acta A 69 (2008) 726.

[4] G. Parkin, Chem. Commun. 1971 (2000).

[5] M. Doring, M. Ciesielski, O. Walterand, H. Gorls, Eur. J. Inorg. Chem. (2002) 1615.

[6] L. Pag, J.N. Lindner, G. Davies, D.E. Seitz, B.L. Karger, Anal. Chem. 51 (1979) 433.

[7] J.-C. Dai, X.-T. Wu, Z.-Y. Fu, C.-P. Cui, S.-M. Hu, W.-X. Du, L.-M. Wu, H.-H. Zhang, R.-Q. Sun, Inorg. Chem. 41 (2002) 1391.

[8] T.W. Lane, F.M.M. Morel, Proc. Natl. Acad. Sci. USA 97 (2000) 4627.

[9] E. Bermejo, A. Castineiras, L.M. Fostiak, I.G. Santos, J.K. Swearingen, D.X. West, Polyhedron 23 (2004) 2303.

[10] W.J. Geary, Coord. Chem. Rev. 7 (1971) 81.

[11] Y.-P. Tian, W.-T. Yu, C.-Y. Zhao, M.-H. Jiang, Z.-G. Cai, H.-K. Fun, Polyhedron 21 (2002) 1217.

[12] R.P. John, A. Sreekanth, V. Rajakannan, T.A. Ajith, M.R.P. Kurup, Polyhedron 23 (2004) 2549.

[13] L. Letheef, E. Manoj, M.R.P. Kurup, Polyhedron 26 (2007) 607.

[14] P.F. Rapheal, E. Manoj, M.R.P. Kurup, Polyhedron 26 (2007) 607.

[15] K. Nakamoto, Infrared and Raman Spectra of Inorganic and Coordination Compounds, Part B, 5th edition, Wiley, New York, 1997.

[16] A. Castineiras, E. Bermejo, D.X. West, L.J. Ackerman, J.V. Martinez, S.H. Ortega, Polyhedron 18 (1999) 1469.

[17] V. Philip, V. Suni, M.R.P. Kurup, Polyhedron 25 (2006) 1931.

[18] G.M. Sheldrick, SHELXTL98, Version 5.1, Bruker AXS, Inc., Madison, Wiisconsin, USA (1999).

[19] K. Brandenburg, Diamond Version 3.1f, Crystal Impact GbR, Bonn, Germany, 2008.

[20] A.W. Addison, T.N. Rao, J. Reedijk, J. van Rijin, G.C. Verschoor, J. Chem. Soc., Dalton Trans. (1984) 1349.

........................ઇઇઇ........................

SUMMARY AND CONCLUSION

Coordination compounds have been known for well over a century and the scientific interest in these compounds increased dramatically. Coordination chemistry was pioneered by Nobel prize winner Alfred Werner. The recent surge in the popularity of coordination compounds is their perceived applications in many areas such as catalysis, analytical chemistry and medicine. The importance of coordination complexes in our day to day life is increasing due to their complex structures and interesting magnetic, electronic and optical properties. The stereochemistry of coordination compounds is one of the major interests of the coordination chemists. Coordination complexes show diversity in structures depending on the metal ion, its coordination number and the denticity of the ligands used.

For the past three decades, thiosemicarbazones with the general formula $(R^1)NH-C(S)-NH-N(R^2R^3)$ has remained an important ligand construction unit in both the neutral and anionic forms. These organic molecules with potential donor atoms in their structural skeleton fascinate coordination chemists with their versatile chelating behavior. Heterocyclic thiosemicarbazones have aroused considerable interest in chemistry due to their remarkable coordination properties and in biology owing to a wide spectrum of potential biological activities. Really, an important number of thiosemicarbazones being NNS tridentate donors possess carcinostatic efficacy and substantial *in vivo* activity against various human tumor lines. An attractive aspect of the thiosemicarbazones is that they are capable of exhibiting tautomerism. In the solid state, the compound predominantly exists in the thioamido form, whereas in the solution state the thiol form predominates. Upon complexation, the ligand can bind to the central metal ion in thioamido form or in thiolate form depending on the reaction conditions and nature of the ligand.

To explore the coordination properties of thiosemicarbazones, in this work we have synthesized two different thiosemicarbazones by the condensation of di-2-pyridyl ketone with N(4)-substituted thiosemicarbazides. The thesis is divided into seven chapters.

Chapter 1, entitled 'a brief introduction to thiosemicarbazones and their metal complexes' gives an introduction to thiosemicarbazones, importance of thiosemicarbazones and their mode of bonding in complexes. The objectives of the present work and the details of different analytical techniques used for the characterization are also presented in this chapter.

Chapter 2 deals with the syntheses and characterization of two different thiosemicarbazones. The ligand systems of our interest include

1. Di-2-pyridyl ketone-*N*(4)-methyl thiosemicarbazone (HDpyMeTsc)

2. Di-2-pyridyl ketone-*N*(4)-ethyl thiosemicarbazone (HDpyETsc)

They were characterized by elemental analyses, FTIR, ^{1}H NMR and electronic spectral studies. The ^{1}H NMR studies indicate the enolization of these compounds in solution state.

Chapter 3 describes the syntheses and characterization of two oxovanadium complexes of thiosemicarbazones. Both the compounds were characterized by various spectroscopic techniques such as IR, electronic and EPR. Magnetic susceptibility measurements clearly indicate that, all the compounds are paramagnetic compounds with vanadium is in +4 oxidation state. The molar conductivity values for the complexes in 10^{-3} M DMF solution indicate that both the complexes are non-electrolytic in nature. The thiosemicarbazones are found to coordinate in the thioamido form in one complex and in thiolate form in the other one. EPR spectra of the compounds in DMF at 77 K displayed axial features with eight hyperfine splitting.

Chapter 4 deals with the syntheses and characterization of four manganese(II) complexes. The complexes were characterized by elemental analyses, IR, UV-Vis, EPR spectral studies, thermogravimetric analyses, conductance and magnetic susceptibility measurements. The molar conductivity measurements in DMF (10^{-3} M) solution indicate that three complexes are non-electrolytes and one complex is probably a 2:1 electrolyte. Magnetic susceptibility measurements suggest that all the compounds are paramagnetic with central metal atom has a d^5 high spin configuration. The EPR spectrum of most of the complexes in the polycrystalline state were very broad and it is a characteristic feature of Mn(II) complexes in the polycrystalline state, which arises due to dipolar interactions and enhanced spin lattice relaxation. The spectra in DMF revealed six lines hyperfine splittings for two complexes. In addition to the hyperfine pattern, a pair of low intensity lines is found in between each of the two main hyperfine lines. These are the forbidden lines corresponding to the mixing of the nuclear hyperfine levels with the zero field splitting factor. Single crystals of one of the Mn(II) complexes were isolated from ethanol/methanol mixture and it is found that in this compound Mn(II) is in a distorted octahedral environment.

Chapter 5 explains the syntheses and characterization five Ni(II) complexes. The IR and electronic spectral studies, thermogravimetric analyses, conductance and magnetic susceptibility measurements of all the complexes were done. Magnetic susceptibility measurements suggest that two of the complexes are diamagnetic while all others are found to be paramagnetic. The thiosemicarbazones are found to coordinate in the neutral form in two complexes and in anionic form in other complexes as evidenced by the IR spectral data.

Chapter 6 deals with the syntheses of eleven Cu(II) complexes and their characterization by different physicochemical techniques. The molar conductivity values indicate that the perchlorate complexes are found to be 2:1 electrolytes while all other complexes are non-electrolytic in nature. The magnetic susceptibility measurements suggest that the compounds are paramagnetic and in close agreement with the spin only value for a d^9 copper system. Some complexes show substantial low magnetic moment may be due to the coupling of metal centers. EPR spectra of the complexes were taken in polycrystalline state at 298 K and in frozen DMF at 77 K. The g value obtained from EPR spectral assignments are consistent with the single unpaired electron is in the $d_{x^2-y^2}$ orbital. Some of the complexes were found to be dimeric and was evident from the half field signal and in some complexes half field signal with seven hyperfine splittings were observed due to the coupling of the electron spin with nuclear spin of two copper atoms. We could isolate X-ray quality single crystals for one of the complexes from its ethanol solution and it was found to be a trinuclear complex. A very interesting aspect observed in this crystal is the pentadentate coordination shown by the ligand which is usually tridentate. Packing of the compound is stabilized by strong $\pi - \pi$ stacking interactions. In addition to the $\pi - \pi$ stacking interactions significant C–H···π interactions and hydrogen bonding are also present.

Chapter 7 describes the syntheses and characterization of five Zn(II) complexes and three Cd(II) complexes. The characterization techniques include elemental analyses, FTIR, electronic spectral studies, thermogravimetric analyses and conductance measurements. All the complexes are non-electrolytic as well as diamagnetic compounds. Single crystals of one zinc complex could be isolated. Single crystal X-ray diffraction studies of the complex revealed that the structure contains two zinc centers where each center

is pentacoordinate with pyridyl nitrogen, azomethine nitrogen, thiolate sulfur, nitrate anion and pyridyl nitrogen of the second thiosemicarbazone moiety. The coordination polyhedron around each zinc atom is a distorted square pyramid.

.........................�✧.........................